Doctoral Thesis

Optogenetic analyses of inhibitory neurotransmission in the mouse spinal dorsal horn

Author(s):
Tudeau, Laetitia

Publication Date:
2017

Permanent Link:

https://doi.org/10.3929/ethz-b-000176837 →

DISS. ETH NO. 24206

Optogenetic analyses of inhibitory neurotransmission in the mouse spinal dorsal horn

A thesis submitted to attain the degree of

DOCTOR OF SCIENCES of ETH ZURICH

(Dr.sc. ETH Zurich)

presented by

LAETITIA TUDEAU

MSc Neuroscience, ETH Zurich

Born on 15.02.1988

citizen of Geneva, Switzerland

Accepted on the recommendation of

Prof. Dr. Hanns Ulrich Zeilhofer, examiner

Prof. Dr. David P. Wolfer, co-examiner

Prof. Dr. Martin Müller, co-examiner

2017

Post tenebras lux

Summary

In all higher organisms, the experience of pain is associated with an unpleasant feeling. Nevertheless, our ability to perceive pain warns us of harmful threats that originate either from the inside of our body or from the environment. Perceiving pain relies on a well-functioning nociceptive system, which starts with nociceptive fibers conveying noxious inputs from the periphery to the first relay platform in the central nervous system (CNS), namely the spinal dorsal horn. At this site, inputs are modulated and filtered by a network of excitatory and inhibitory interneurons. The final output is relayed via projection neurons to higher cortical areas in the brain where pain becomes a conscious experience. However, in some cases nociception becomes dysfunctional and eventually leads to persistent and chronic pain. Underlying symptoms of chronic pain are allodynia, where innocuous stimuli such as light-touch become painful and hyperalgesia defined as an enhanced sensitivity to noxious stimuli. Studies have shown that reduced GABAergic or glycinergic neurotransmission in the dorsal horn leads to increased nociceptive signaling to the brain. This indicates that a functional inhibitory network in the dorsal horn is important for avoiding uncontrolled transmission of nociceptive stimuli to higher levels of the central nervous system. Several studies in rodent models of neuropathic or inflammatory pain have demonstrated that $GABA_A$ receptors containing the α2 subunit (α2-$GABA_A$ receptors) in addition to certain glycine receptors play a key role in the inhibitory control of nociceptive signaling at the spinal cord level.

In the three experimental studies of this thesis, I used optogenetics and whole-cell patch-clamp recordings to provide a detailed analysis of inhibitory neurotransmission in the spinal dorsal horn of mice. In the first chapter, I focused on a genetic mouse model of diminished GABAergic inhibition at the spinal cord level. The mice used in this study were hoxb8α2$^{-/-}$ mice which lack α2-$GABA_A$ receptors in the spinal cord up to the cervical segment C4. Although these mice lacked a $GABA_A$ receptor subtype (α2-$GABA_A$ receptors) that is critically involved in spinal nociceptive control and although GABAergic inhibitory postsynaptic currents (GABA-IPSCs) recorded from excitatory superficial dorsal horn neurons were reduced, these mice did not show exaggerated pain responses indicating that some compensatory mechanisms were active in these mice. Several potential compensatory mechanisms were investigated. No significant differences were found for the decay kinetics

of GABA-IPSCs. No changes were found in the amplitude of glycinergic IPSCs or of membrane currents evoked by extracellular application of GABA. I also did not find significant changes in the amplitudes of sensory afferent evoked excitatory postsynaptic currents (EPSCs), which are known to be under control by presynaptic $GABA_A$ receptors. By contrast, I found increased bicuculline-sensitive (GABAergic) tonic membrane currents in hoxb8$\alpha 2^{-/-}$ mice. Furthermore, in immunohistochemical experiments, I found a significant increase in serotonin immunoreactivity and in the expression of the serotonin producing enzyme tryptophan hydroxylase (TPH2). Both the increases in tonic GABAergic currents and in serotonergic input to the spinal cord may on a behavioral level compensate for the loss of synaptic GABAergic inhibition and may explain why hoxb8$\alpha 2^{-/-}$ mice lack a pronociceptive phenotype.

In the second chapter, Part A, I aimed at identifying the origin of inhibitory inputs onto excitatory lamina II (LII) neurons. To this end, I used laser scanning photostimulation (LSPS) in combination with whole-cell patch-clamp recordings in spinal cord slices of BAC transgenic vGAT::ChR2 mice. These mice express the blue light-activated ion channel channelrhodopsin 2 in all inhibitory neurons of the CNS including the spinal cord. About half (46%) of the sites triggering inhibitory input to the recorded neurons were located in the superficial dorsal horn, one third was located in the deep dorsal horn, and 21% were in the white matter. These results indicate that inhibitory input to LII neurons does not only originate from inhibitory neurons of the same lamina but also from deep dorsal horn interneurons and very likely from inhibitory fiber tracts descending from higher CNS areas. This interpretation is consistent with results described in Part B, where I characterized inhibitory neurotransmission in GlyT2::Cre;vGAT::ChR2 mice in which dorsal horn glycinergic neurons were locally ablated by virus-mediated cre-dependent diphtheria toxin expression. In these experiments, I found a reduction of inhibitory neurotransmission to excitatory LII neurons by 55%. Because most of the glycinergic neurons are located in the deep dorsal horn, these results also support a strong contribution of deep dorsal horn neurons to inhibition of neurons and circuits of LII.

Taken together, this thesis provides new insights on the organization of inhibitory neurotransmission in the spinal dorsal horn and on potential mechanisms contributing to a compensation of compromised synaptic inhibition in spinal dorsal horn nociceptive circuits.

Resumé

La douleur est une sensation désagréable perçue lorsqu'un danger réel ou potentiel menace l'intégrité de l'organisme. La perception de la douleur témoigne du bon fonctionnement de notre système nociceptif. Ce dernier est composé de fibres périphériques qui transmettent les influx nociceptifs de la périphérie au premier relais du système nerveux central, la corne dorsale. Celle-ci module et filtre les informations par un réseau d'interneurones excitateurs et inhibiteurs. L'information est ensuite relayée par un neurone de projection au cerveau où le signal nociceptif active des mécanismes complexes aboutissant à la perception de la douleur par l'individu. Dans certains cas, le dysfonctionnement du système nociceptif conduit à une douleur persistante qui, à long terme, peut devenir chronique. Les symptômes sous-jacents de la douleur chronique sont l'allodynie, par laquelle des stimuli indolores tels qu'une légère pression, deviennent douloureux, et l'hyperalgésie qui est définie comme une sensibilité accrue aux stimuli douloureux. Des recherches ont démontré qu'une diminution de neurotransmission GABAergique ou glycinergique dans la corne dorsale provoquait une augmentation des informations douloureuses transmises au cerveau. Ceci indique qu'un réseau inhibiteur fonctionnel dans la corne dorsale permet d'éviter la transmission incontrôlée de stimuli douloureux aux niveaux supérieurs du système nerveux central. Jusqu'ici, les études ont démontré que des benzodiazépines spécifiques à un sous-type de récepteur $GABA_A$, à savoir les récepteurs α2-$GABA_A$, soulagent la douleur chez les rongeurs souffrant de douleur neuropathique ou inflammatoire. Ceci indique que si l'on rétablit la neurotransmission inhibitrice de la moelle épinière en facilitant la neurotransmission GABAergique, par exemple, l'on approcherait de manière rationnelle le traitement des symptômes de la douleur chronique.

Dans les trois études expérimentales de cette thèse, j'ai combiné l'optogénétique et les enregistrements électrophysiologiques, afin de fournir une analyse détaillée de la neurotransmission inhibitrice au niveau de la corne dorsale de la moelle épinière chez la souris. Dans le premier chapitre, j'ai focalisé mon travail sur un modèle de souris qui présente une diminution de l'inhibition GABAergique au niveau de la moelle épinière. Les souris utilisées dans cette étude étaient hoxb8α$2^{-/-}$, qui sont dépourvues de récepteurs α2-

$GABA_A$ dans la moelle épinière jusqu'au segment cervical C4. Bien que ces souris ne possèdent pas un sous-type de récepteur $GABA_A$ (α2-$GABA_A$), crucialement impliqué dans le control nociceptif au niveau de la moelle épinière, et qu'elles aient une diminution des courants postsynaptiques GABAergiques inhibiteurs (CPSI-GABA) enregistrés depuis des neurones excitateurs de la corne dorsale superficielle, ces souris n'ont pas manifesté de réponses exagérées à la douleur, indiquant ainsi la possible présence de mécanismes compensatoires actifs. Plusieurs de ces mécanismes compensatoires ont été étudiés. Aucune différence significative n'a été trouvée au niveau de la décroissance cinétique des CPSI-GABA. Par ailleurs, je n'ai pas trouvé de changements significatifs au niveau de l'amplitude des courants postsynaptiques excitateurs évoqués par les fibres sensorielles afférentes, connues pour être sous contrôle de récepteurs $GABA_A$ présynaptiques. En revanche, j'ai trouvé que les courants membranaires toniques (GABAergiques) chez les souris hoxb8$\alpha 2^{-/-}$ avaient un accroissement de sensibilité à la bicuculline. De plus, dans les expériences d'immunohistochimie, j'ai trouvé un accroissement significatif de l'immunoréactivité à la sérotonine ainsi qu'à l'enzyme produisant la sérotonine, la tryptophane hydroxylase (TPH2). L'accroissement de courants toniques GABAergiques ainsi que la contribution sérotoninergique au niveau de la moelle épinière peuvent, à l'échelle comportementale, compenser la perte d'inhibition GABAergique synaptique et ainsi expliquer pourquoi les souris hoxb8$\alpha 2^{-/-}$ ne présentent pas de phénotype pronociceptif.

Dans le second chapitre, Partie A, j'ai tenté d'identifier les sources d'influx inhibiteurs s'exerçant sur les neurones excitateurs de la lamina II (LII). Pour ce faire, j'ai employé la technique de laser scanning photostimulation (LSPS) sur des tranches de moelle épinière de souris vGAT::ChR2 BAC transgéniques. Ces souris expriment dans tous les neurones inhibiteurs du système nerveux central (SNC), le canal ionique channelrhodopsin 2, un canal qui s'active à la lumière bleue. Environ la moitié (46 %) des sites provoquant des influx inhibiteurs aux neurones enregistrés proviennent de la corne dorsale superficielle, un tiers est localisé dans la corne dorsale profonde et 21 % proviennent de la substance blanche. Ces résultats indiquent que les influx inhibiteurs s'exerçant sur les neurones de la LII ne proviennent pas entièrement de neurones inhibiteurs de la même lamina, mais aussi d'interneurones de la corne dorsale profonde ainsi que très certainement de faisceaux de fibres inhibitrices descendant du SNC. Cette interprétation est très cohérente avec les

résultats décrits dans la partie B, où j'ai caractérisé la neurotransmission inhibitrice chez les souris GlyT2::Cre;vGAT::ChR2 chez lesquelles les neurones glycinergiques de la corne dorsale ont été localement éliminées par l'expression de la toxine de la diphtérie transmise par le virus AAV-flex-DTA. Dans ces expériences, j'ai trouvé une réduction d'environ 55% de la neurotransmission inhibitrice chez les neurones excitateurs de la LII. Parce que la plupart des neurones glycinergiques sont localisés dans la corne dorsale profonde, ces résultats soutiennent l'idée d'une forte contribution des neurones de la corne dorsale profonde à l'inhibition des neurones et circuits de la LII.

Cette thèse, dans son ensemble, apporte un nouvel aperçu sur l'organisation de la neurotransmission inhibitrice dans la corne dorsale de la moelle épinière ainsi que sur des potentiels mécanismes contribuant à compenser l'inhibition synaptique qui serait compromise dans la corne dorsale de la moelle épinière au niveau des circuits nociceptifs.

Abbreviations

2-AG: 2-arachidonyl-glycerol

AEA: anandamide

AMPA: α-amino-3-hydroxy-5-methyl-4-isoxazolepropionic acid

AAV1: Adeno-Associated virus serotype 2

BAC: bacterial artificial chromosome

BDNF: brain-derived neuroptrophic factor

Bic: bicuculline

CGRP: calcitonin gene-related peptide

ChR: channelrhodopsin

CCI: chronic constriction injury

CNS: central nervous system

Ctrl: control

Ddh: deep dorsal horn

DZP: diazepam

DAB: diaminobenzidine (DAB) hydrochloride

eCB: endocannabinoids

EPSC: excitatory postsynaptic current

GABA: γ-Aminobutyric acid

GlyR: glycine receptor

5-HT: 5-hydroxytryptamin (Serotonin)

IPSC: inhibitory postsynaptic current

IR: infra-red

KO: knock-out

Lat: lateral

Med: medial

NGF: nerve growth factor

NMDA: N-Methyl-D-aspartic acid or N-Methyl-D-aspartate

PSF: primary sensory fibers

PG: prostaglandin

RVM: rostral ventromedial medulla

Sdh: superficial dorsal horn

SNI: spared nerve injury

Stry: strychnine

Substance P: SP

SG: substantia gelatinosa

TPH2: tryptophan hydroxylase 2

TTL: transistor-transistor logic

TTX: tetrodotoxin

VgluT: vesicular GABAergic transporter

Veh: vehicle

WM: white matter

GM: grey matter

Table of contents

General introduction

I. Pain

Pain is a conscious perception generated in the brain as a consequence of nociception. Nociception refers to the processing and encoding of the noxious stimuli taking place in the peripheral and central nervous system (Loeser and Treede, 2008). Our ability to sense impending damage to the organism has a direct impact on our life span and well-being since it makes us take the appropriate measures to avoid further damage. Recurrent trauma and infections are responsible for reduced life expectancy among humans suffering from congenital insensitivity to pain (Cox et al., 2006). As pain is a subjective experience, it has been defined according to the International Association for the Study of Pain (IASP) as "an unpleasant sensory and emotional experience associated with actual or potential tissue damage, or described in terms of such damage". Physiological pain, also known as acute pain, is potentially triggered by noxious stimuli, such as cold or heat, irritant chemicals and mechanical pressure (Blondell et al., 2013). Pain, however, can also persist beyond the acute threats, and sustain pain far beyond the initial cause (Luo et al., 2014).

II. Physiology of acute pain

Anatomy of the nociceptive pathway

i. Dorsal horn inputs: Primary sensory fibers

Primary sensory fibers have a peripheral axon terminal that responds to sensory stimuli. Noxious or innocuous stimuli depolarize primary sensory fibers at their peripheral terminals and elicit a generator potential through the activation of voltage-gated sodium channels (e.g. Na_v 1.8) (Waxman and Zamponi, 2014). The signals propagate along the peripheral nerve until they reach the spinal dorsal horn. At this site, the nociceptors make synapses with local excitatory and inhibitory interneurons or projection neurons, which ultimately convey nociceptive information to higher levels of the CNS (Figure 1). Sensory fibers respond either to noxious (heat, pressure, cold) or innocuous inputs (i.e., pleasant touch). Accordingly,

primary sensory fibers can be classified as either low-threshold mechanoreceptors (LTMRs, Aβ-fibers) that respond to light touch and tactile inputs, or high-threshold, slowly conducting afferents, which require noxious stimuli to be activated. Aβ-fibers are thickly myelinated, which endows them with high conduction velocities (Leem et al., 1993; Abraira and Ginty, 2013). Nociceptive Aδ-fibers are only thinly myelinated and C-fibers are devoid of myelination. Conduction velocities of nerve fibers depend on the degree of myelination. Typically, C-fibers have conduction velocities of 0.5-2 m/s; Aδ 12-30 m/s and Aβ 30-70 m/s (Kakigi et al., 2003; Djouhri and Lawson, 2004). Aδ-fibers usually mediate sharp and localized pain sensations, whereas C-fibers elicit slower and more diffuse sensations. C-fibers can be sub-classified into two groups depending on their responsiveness to neurotrophic factors: peptidergic or non-peptidergic (Snider and McMahon, 1998b). Most peptidergic C-fibers express the capsaicin receptor TRPV1, involved in mediating heat pain (Caterina and Julius, 2001; McCoy et al., 2013) and in addition to glutamate, release calcitonin gene-related peptide (CGRP) or substance P (SP). Non-peptidergic C-fibers are characterized by the binding of isolectin B4 ($IB4^+$) and are implicated in mechanical (Bogen et al., 2008) and possibly thermal nociception (Malin et al., 2006). Recently, a population of low-threshold C-fibers, characterized by the expression of tyrosine hydroxylase and of the vesicular glutamate transporter subtype 3 (VgluT3), was shown to play a major role in mechanical allodynia following inflammation, nerve injury or trauma (Seal et al., 2009). The broad distribution of primary sensory fibers terminating within different dorsal horn laminae suggests functional distinctions in their contribution to the activity of dorsal horn neurons.

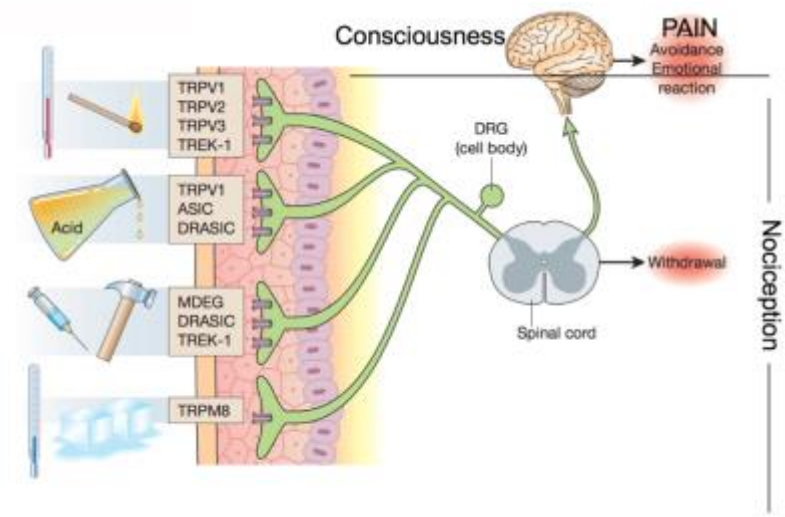

Figure 1. Nociceptive pathway. Noxious stimuli are sensed by specific receptors or ion channels located on the terminals of nociceptors which are sensitive to heat, mechanical stimuli, protons and cold. Thinly myelinated Aδ fibers or unmyelinated C-fibers convey these signals to the spinal dorsal horn, where they are modulated, processed, and ultimately transmitted to the brain, where the sensation of pain is experienced and becomes conscious. Modified from Scholz and Woolf (2002).

ii. Laminar organization

Rexed (1952) divided the grey matter of the cat spinal dorsal horn into a series of parallel layers. This scheme has in the meantime been applied to other species. The spinal cord can be broadly subdivided into a dorsal horn (DH), the sensory part, and a ventral horn (VH), involved in motor control. The dorsal horn harbors a plethora of neuronal subpopulations that are targeted by primary afferent terminals (Figure 2) and terminals from supraspinal sites. In total, the spinal cord is subdivided in ten different laminae.

Lamina I (LI) is the most superficial layer of the dorsal horn, and not thicker than two cell body diameters. It contains projection neurons (discussed in *Ascending pathways*) that receive direct monosynaptic and polysynaptic inputs from peptidergic C-fiber and Aδ-fibers but also a wide range of excitatory and inhibitory interneurons. Central terminals of Aδ and peptidergic C-fibers can be found in this layer.

Lamina II (LII), also known as Substantia gelatinosa (SG) due to its translucid appearance, is located below LI. This translucency reflects the lack of axon myelination from C-fibers, which terminate in the area. Very often, LI and LII are named the superficial dorsal horn (sdh). LII is densely innervated by peptidergic and nonpeptidergic C-fibers. Peptidergic C-fibers

terminate in LII_{outer} (LII_o), while non-peptidergic terminate at the inner LII (LII_i), close to the border with LIII (Snider and McMahon, 1998a; Braz et al., 2014). In addition, LII harbors a network of inhibitory (GABAergic and glycinergic) and excitatory (glutamatergic) interneurons that modulate the incoming nociceptive inputs. The most ventral part of LII_i is characterized by excitatory glutamatergic neurons expressing protein kinase C isoform γ (PKCγ), which are innervated by non-nociceptive primary afferents (Neumann et al., 2008). The inhibitory population accounts for approximately one-third of the total amount of interneurons. The majority of inhibitory neurons of LI/LII are purely GABAergic (Popratiloff et al., 1996; Todd et al., 1996b).

The deeper dorsal horn laminae (LIII-LVI) are mainly innervated by Aβ and Aδ-fibers (Naim et al., 1997). They nevertheless also receive inputs from nociceptive C-fibers (Basbaum et al., 2009; Foster et al., 2015). Like LI, LIII and LV also contain projection neurons. LIII projection neurons receive inputs from peptidergic C-fibers, and LV. Projection neurons are innervated by non-nociceptive Aβ and Aδ fibers, and indirect (polysynaptic) C-fiber inputs. Neurons in LV are termed wide dynamic-range neurons (WDRs) because they respond to noxious and innocuous stimuli (i.e., noxious and innocuous). Inhibitory neurons in this region co-release both GABA and glycine.

Rexed's anatomical organization of the laminae is well defined and highlights the different projection patterns and circuits of primary afferents and dorsal horn neurons. However, the functional neuronal circuits within the laminae (interlaminae) and between laminae (translaminar) are still poorly understood.

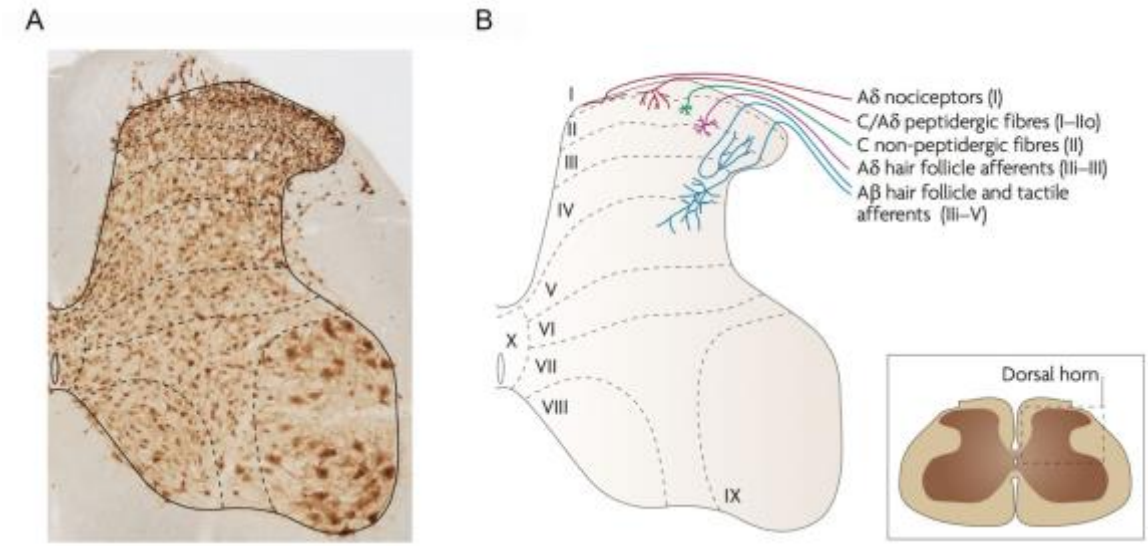

Figure 2. Laminar organization of the spinal cord and primary afferent inputs. A, Rat spinal cord hemisection immunostained for NeuN that specifically labels neurons. Dotted lines indicate boundaries of the different laminae. B, Scheme representing the preferred termination sites of primary afferent fibers onto the different laminae (Todd, 2010).

iii. Biochemical markers of dorsal horn interneurons

Identifying markers for interneurons is important to gain a better understanding of their physiological and morphological properties. Many neurochemical markers have been identified so far to label excitatory and inhibitory interneurons. For example, different subpopulations of excitatory interneurons were shown to express the calcium-binding proteins calbindin-D 28k (Antal et al., 1991) and calretinin, PKCγ (Polgar et al., 1999), c-Maf, a transcription factor (Hu et al., 2012), neurokinin B (Polgar et al., 2006), and neurotensin (Todd et al., 1992). Gastrin-releasing peptide (GRP) labels a subpopulation of excitatory neurons involved in itch (Mishra and Hoon, 2013). We recently investigated cholecystokinin (CCK)-expressing cells, which appear to be an additional subpopulation of excitatory neurons (Dr. S. Haueter, V. Jamarillo, unpublished data). Markers of inhibitory neurons have also been extensively studied (Ross et al., 2010; Polgar et al., 2013; Wildner et al., 2013). So far, galanin, neuronal nitric oxide synthase (nNOS), parvalbumin (PV), and neuropeptide Y (NPY) were identified as different markers of inhibitory interneurons responding differently to painful stimulation and targeting different cell types (Polgar et al., 2013).

The generation of eGFP reporter mouse lines facilitated the morphological and electrophysiological analysis of the different types of neuron in the dorsal horn (Tamamaki et al., 2003; Zeilhofer et al., 2005). Although there is no reliable immunocytochemical marker for glutamatergic cell bodies, it is generally accepted that neurons not immunoreactive for GABA or glycine are glutamatergic, and release L-glutamate (Todd et al. 2010). Glutamatergic axons can be identified in VgluT2::eGFP mice in which the vesicular glutamate transporter (VgluT) is tagged by an eGFP reporter (Todd et al., 2003). VgluT1 has been shown to be expressed by Aβ-fibers, and VgluT2 by C-fibers and Aδ-fibers (Scherrer et al., 2010). Finally, VglutT3 was found to be exclusively expressed by C-LTMRs (Seal et al., 2009; Seal, 2016). Although the expression of VgluTs in spinal dorsal horn neurons during development is not well characterized, it was nevertheless demonstrated that deep dorsal horn neurons transiently expressed VgluT3 to convey normal mechanical pain sensation (Peirs et al., 2015).

Visualizing GABAergic or glycinergic neurons is possible with GAD67^{eGFP}, GAD65::eGFP or GlyT2::eGFP mouse lines, where GAD, the GABA synthesizing-enzymes (Tamamaki et al., 2003; Heinke et al., 2004) or GlyT2, the neuronal glycine transporter are marked with eGFP (Zeilhofer et al., 2005).

iv. Morphological and biophysical hallmarks of dorsal horn interneurons

Studies have used dendritic tree reconstruction and electrophysiological recordings to distinguish four morphological classes of cells (Grudt and Perl, 2002; Prescott and De Koninck, 2002; Hantman et al., 2004; Heinke et al., 2004; Yasaka et al., 2010; Punnakkal et al., 2014). These cell types are known as islet, central, radial and vertical neurons. Islet cells are mostly found in LII_i. Their dendritic tree predominantly extends into a rostrocaudal direction. Activation of islet cells triggers the release of GABA, defining them as inhibitory neurons (Lu and Perl, 2003; Maxwell et al., 2007). Islet cells receive monosynaptic inputs from C-fibers, and display tonic firing patterns, a good indicator of inhibitory GABAergic or glycinergic phenotype (Zeilhofer et al., 2012). Central cells are found in both LII_i and LII_o. Although their dendritic tree extends with the same orientation as islet cells, they remain shorter. A particularity of central cells is that they can be either excitatory or inhibitory, and can fire either transiently or tonically. Like islet cells, central cells are monosynaptically targeted by C-fibers, and Aδ-fibers (Grudt and Perl, 2002). Radial cells expand their dendrites in

rostrocaudal and dorsoventral orientations. Most radial cells are excitatory (Yasaka et al., 2010) although some inhibitory cells were reported (Maxwell et al., 2007). Finally, vertical cells are nested in LII_o, and their dendritic tree extends dorsoventrally. Although vertical cells are associated with excitatory neurons, some exceptions have been reported (Heinke et al., 2004; Maxwell et al., 2007) (Figure 3). Despite this extensive morphological characterization of dorsal horn interneurons, a substantial 30 % of cells remain unclassified.

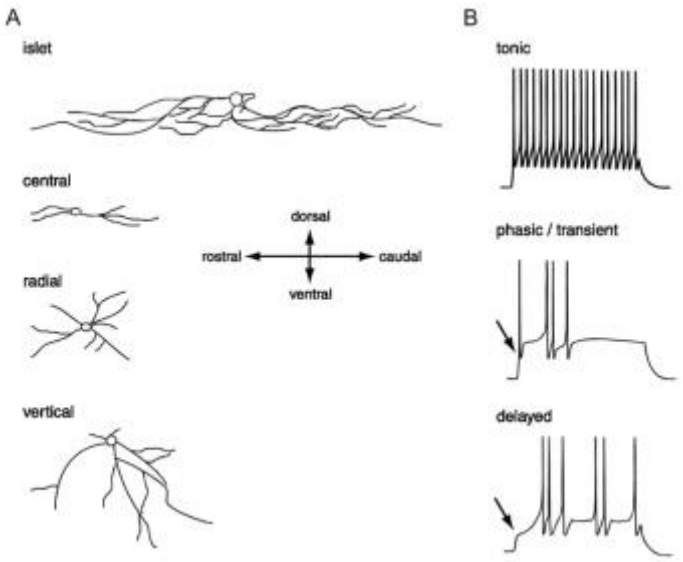

Figure 3. Morphology and action potential firing pattern of dorsal horn interneurons. A, The dendritic tree of Islet and central cells mainly spreads in a rostrocaudal orientation. Dendrites from radial cells extend in all directions, and vertical cells have a dominant ventral arborization of their dendrites. B, Tonic cells fire action potentials (AP) at high frequency with constant intervals throughout the duration of the stimulus. Phasic/transient cells show an immediate onset of APs separated by silent periods. Delayed cells fire the first action potential with a certain delay (Zeilhofer et al., 2012).

v. Ascending pathways and brain centers for pain perception

Projection neurons provide the major output from the dorsal horn to higher levels of the CNS. However, in LI they account for only 5 to 10 % of all LI neurons (Spike et al., 2003). Although most projection neurons are clustered in LI, scattered expression is also observed throughout LIII-LV. LI projection neurons receive direct inputs from LII inhibitory and excitatory interneurons as well as from C-fibers (Gobel et al., 1980). The neurokinin 1 receptor (NK1R) is expressed by projection neurons and becomes active upon binding of

substance P (Todd et al., 2002). In addition, LI projection neurons were shown to receive indirect inputs from Aβ-fibers via a polysynaptic connection with LII vertical cells (Kato et al., 2009; Kosugi et al., 2013). Before reaching supraspinal territories, projection neurons target their axon to the contralateral side and project rostrally towards higher areas in the brainstem through the white matter until terminating in various brainstem and thalamic nuclei. These pathways constitute the spinoreticulothalamic and spinothalamic tracts, respectively. Anterograde and retrograde tracing have revealed the different termination sites of LI projection neurons (Gauriau and Bernard, 2004). These results led to the conclusion that the main targets of LI projection neurons were the caudal ventrolateral medulla (CVLM), the nucleus of the solitary tract (NTS), the lateral parabrachial area (LPb), the periaqueductal grey matter (PAG) and the thalamus (Gauriau and Bernard, 2004). From the brainstem and thalamus nuclei, relay neurons then project their axons onto different cortical areas of the brain, leaving the "unconscious" nociceptive pathway for conscious perception of pain in the cortex. Several cortical areas are involved in representing pain (Apkarian, 2013; Lee and Tracey, 2013) such as the somatosensory cortex, the cingulate cortex, and the insular cortex (Basbaum et al., 2009).

vi. Descending pathways

Dorsal horn neurons also receive either negative or positive control from supraspinal descending fibers that influence the transmission of pain messages (Gebhart, 2004). Important descending pathways include the serotonergic system, originating from the nucleus raphe magnus (of the rostral ventromedial medulla, RVM) (Belin et al., 1983; Antal et al., 1996), the noradrenergic pathway from the locus coeruleus (Moore and Bloom, 1979), and GABAergic/glycinergic inputs, originating from the RVM (Kato et al., 2006). The RVM sends projections to LI, LII and LV dorsal horn neurons (Hylden et al., 1985). As mentioned earlier, neurons in these laminae are also engaged by nociceptors, which suggest a critical contribution of these descending pathways to the modulation of nociceptive signaling. It has been shown that activating certain neurons in the RVM could promote either pronociception or antinociception in nociceptive signaling of the dorsal horn (Basbaum and Fields, 1984; Heinricher and McGaraughty, 1998; Neubert et al., 2004; Lau and Vaughan, 2014). For example, the pro- or antinociceptive effects elicited by serotonin (5-HT) rely on the type of 5-HT receptors expressed by the postsynaptic neurons in the spinal cord. Although it is clear

that postsynaptic 5-HT1a receptors inhibit spinal dorsal horn neurons, divergent results were reported with 5-HT_3 (Ali et al., 1996; Rahman et al., 2004; Suzuki et al., 2004; Fukushima et al., 2009; Bardin, 2011; Gu et al., 2011). However, it was shown in a study that 5-HT_3 was expressed on presynaptic terminals of GABAergic neurons, facilitating GABAergic inhibitory synaptic transmission in the sdh (Fukushima et al., 2009).

Fast inhibitory neurotransmission

Inhibitory neurons play a critical role in modulating nociceptive pathways (Lu and Perl, 2010). In the spinal dorsal horn, inhibition is mediated by GABA and glycine, two fast inhibitory neurotransmitters (Zeilhofer et al., 2012). Ionotropic $GABA_A$ and glycine receptors belong to the Cys-loop superfamily of ligand-gated ion channels, which includes also nicotinic acetylcholine receptors and ionotropic serotonin (5-HT_3) receptors (Olsen and Sieghart, 2008, 2009). $GABA_AR$ and GlyR are permeable to chloride ions and, to a lesser extent, to bicarbonate (Blaesse et al., 2009; Passlick et al., 2013) and thus upon activation of their pore hyperpolarize the cell.

i. $GABA_A$ receptors

Mammalian $GABA_A$ receptors are heteropentameric ligand-gated ion channels composed from a repertoire of 19 different subunits: α1-α6, β1-β3, γ1-γ3, δ, ε, π, τ, and ρ1-ρ3. The subunit composition of most $GABA_A$ receptor subtypes is well established and there is general agreement that the most likely subunit stoichiometry in the CNS is 2α/2β/1γ (Boileau et al., 2005) (Figure 4). However, $GABA_A$ receptors may display different stoichiometries or express only α and β subunits (Jones and Henderson, 2007).

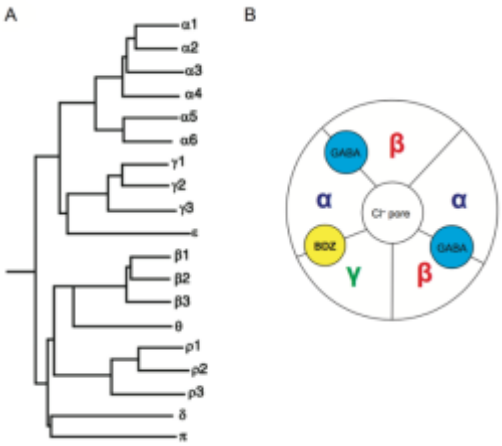

Figure 4. $GABA_A$ receptor subunits and structure. A, Dendogram of mammalian $GABA_A$ receptor showing the subunit repertoire. B, In the CNS, heteropentameric $GABA_A$ receptors are mainly composed by 2α/2β/1γ subunits. The GABA neurotransmitters bind on two α/β interfaces, and allow the channel to open, allowing Cl^- ions to flow through the pore. Benzodiazepines (BDZ) bind on the α/γ interface and increase the Cl^- conductance. Modified from Zeilhofer et al. (2012).

In the spinal cord, the most abundant configuration is α2-α3/β3/γ2, as opposed to the brain where it is mainly α1/β2/γ2 (Wisden et al., 1991; Laurie et al., 1992; Bohlhalter et al., 1996). $GABA_A$ receptor subunit arrangement can influence the affinity of the receptor to GABA, the channel conductance, pharmacological properties, and the location of $GABA_A$ receptor on the cell membrane. For instance, α1, α2, α3 subunits as well as β2 and β3 subunits can interact directly with gephyrin, a cytoplasmic scaffolding protein believed to anchor postsynaptic $GABA_A$ receptors as well as glycine receptors to the postsynaptic membrane (Tretter et al., 2008; Mukherjee et al., 2011; Kowalczyk et al., 2013). In addition, the γ2 subunit was shown to be required for synaptic clustering of most $GABA_A$ receptor subtypes (Essrich et al., 1998). Synaptic $GABA_A$ receptors mediate phasic inhibition in the CNS. Conversely, extrasynaptic $GABA_A$ receptors are generally associated with a δ subunit which substitutes the γ subunit and either α4 or α5 subunits. This composition renders extrasynaptic $GABA_A$ receptors more sensitive to GABA, and makes them mediators of tonic inhibition (Belelli et al., 2009). The $GABA_A$ receptors α subunits display a differential distribution across the spinal cord. The α1 subunit is mainly expressed in LIII, the deep dorsal horn and the central canal. The α2 subunit is strongly expressed in the sdh and ventral horn, as well as around the central canal. α3 has a similar expression pattern as α2, although its expression in the ventral horn is lower. The α4

subunit displays a very sparse expression in the spinal cord and finally the α5 subunit is mostly expressed in the sdh (Paul et al., 2012) (Figure 5).

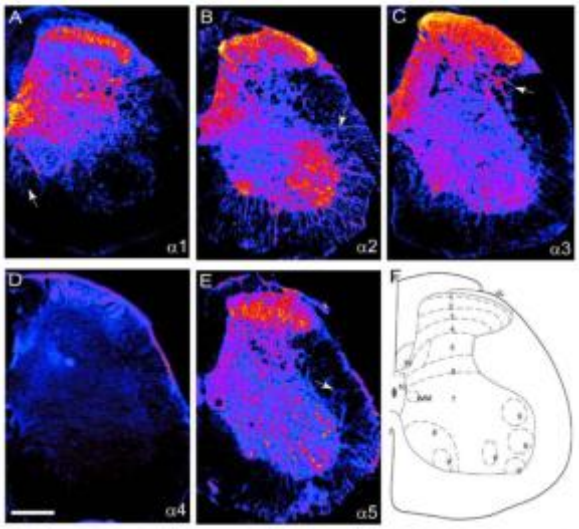

Figure 5. Differential distribution of the $GABA_AR$ α subunits in the spinal cord. Color-coded images revealing the wide-spread distribution of α (1-5) subunits on a coronal hemisection of the spinal cord. The tissue was processed for immunoperoxidase stainings with α subunit-specific antibodies. The α1, α2, α3 and α5 subunits are strongly expressed in the superficial and deep dorsal horn as well as around the central canal. α2, α3 and α5 are also expressed in the ventral horn. However, expression of the α4 subunit in the spinal cord remains quite sparse. Scale bar: 100 µm. (Paul et al., 2012).

After release from the presynaptic terminals, GABA binds to an interface formed by α and β subunits, which occurs twice in $GABA_A$ receptors. $GABA_A$ receptors can be modulated by endogenous neuromodulators (neurosteroids) or exogenous compounds, including benzodiazepines (BDZ), barbiturates, alcohol, and anesthetics (Johnston, 1996; Rudolph and Mohler, 2006). BDZ typically bind between γ2 and one α subunit (Mohler et al., 2001). BZD site-agonists can also bind to $GABA_A$ receptors containing either γ1 or γ3 subunits but with reduced affinity (Benke et al., 1996). Only $GABA_A$ receptors containing at least one α1, α2, α3 or α5 subunit are potentiated by BDZs. α4 and α6 do not respond to BZDs (Mohler et al., 2001). $GABA_A$ receptors can be antagonized by bicuculline through competitive inhibition with GABA, which ultimately blocks Cl^- conductance (Akaike et al., 1985).

ii. Glycine receptors

Glycine is another inhibitory neurotransmitter, mostly used in the spinal cord, brainstem, and retina (Araki et al., 1988). Glycine receptors are more limited in terms of subunit

heterogeneity than $GABA_A$ receptors. Their repertoire is restricted to four α subunits and one β subunit (Figure 6). Although all five genes encode functional glycine receptors in rodents, in humans the glycine receptor α4 subunit (GlyRα4) is not functional due to several mutations including a premature stop codon (Laube et al., 2002). Glycine receptors composed solely of α subunits remain functional homopentameric glycine-sensitive ion channels, which is not the case with homopentameric β glycine receptors. Recent evidence has suggested that, in general, functional glycine receptors are heteropentameric and composed of two α subunits and three β subunits (Grudzinska et al., 2005) (Figure 6). The interaction between the β subunit and the postsynaptic anchoring protein gephyrin targets glycine receptors to the synaptic sites (Fritschy et al., 2008). In the immature CNS, it is believed that glycine receptors are first expressed as α2 homomeric receptors, which in the mature CNS become either α1β or α3β heteromeric receptors, with α1β being the most prevalent configuration (Malosio et al., 1991; Takahashi et al., 1992). In the spinal cord, glycine receptors α3 subunit (GlyRα3) are restricted to the sdh, which suggests these receptors play a crucial role in spinal inhibitory nociceptive processing (Harvey et al., 2004).

Glycine receptors are selectively antagonized by strychnine, an alkaloid from the Indian plant *Strychnos nux vomica*. This drug distinguishes glycine receptors from $GABA_A$ receptors, but also from the excitatory N-methyl D-aspartate receptors (NMDARs), on which glycine also has a binding site (Johnson and Ascher, 1987; Berger et al., 1998).

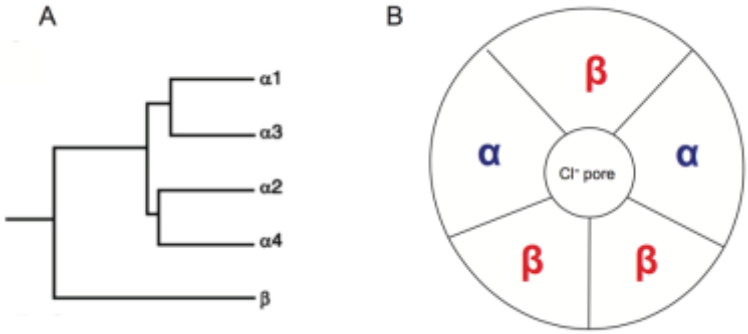

Figure 6. Glycine receptor subunits and structure. A, Repertoire of the glycine receptor subunits. B, Heteropentameric glycine receptors composed of 2α and 3β subunits. Upon activation, glycine receptors open and allow Cl^- to flow through the pore. Modified from Zeilhofer et al. (2012)

III. Chronic pain

Chronic pain is a social and economic burden, affecting about 19 % of the adult European population of which 40 % claim not being satisfied with their pain therapy (Breivik et al., 2006). Two main types of chronic pain may be distinguished, namely inflammatory pain, which follows tissue injury, and neuropathic pain, induced by nerve injury (Jensen et al., 2011). Underlying symptoms of these two conditions include hyperalgesia, defined as enhanced pain sensitivity, and allodynia, pain sensitivity to innocuous stimuli (Basbaum et al., 2009). A major class of analgesic drugs used today are the nonsteroidal anti-inflammatory drugs (NSAIDs). Although they relieve patients from inflammatory pain, on the long term, these drugs are often associated with gastrointestinal harm (Moore et al., 2014). Similarly, opioids, although effective against neuropathic pain in the short term, over time may cause addiction. Therefore, despite major advances in pharmacological research, no drug has to this day led to a successful treatment against chronic pain without mediating secondary effects such as sedation, addiction or tolerance, to cite just a few.

Mechanism of diminished spinal inhibition

i. Peripheral sensitization

During inflammation or after tissue damage, primary afferent fibers develop lower excitation thresholds in reaction to mechanical and thermal stimuli, and fire action potentials at higher frequencies (Schaible and Richter, 2004). This peripheral sensitization is mainly due to the exposure of nociceptor terminals to inflammatory mediators released at the site of injury by the so-called “inflammatory soup”. These compounds include extracellular protons (involved in acidosis), arachidonic acid and other lipid metabolites, serotonin, bradykinin, nucleotides and nerve growth factor (NGF), all of which modulate the properties of receptors and ion channels located on the nociceptor terminals (Julius and Basbaum, 2001). The abnormal activation of nociceptors facilitates the release of the inflammatory mediators from other resident cells, namely the keratinocytes and mast cells, which in addition release prostaglandins (PGE), protons (H^+), and ATP. This process is known as neurogenic inflammation (Gold and Gebhart, 2010). An important player in the maintenance of the nociceptors’ sensitivity are the NGF activated TrkA receptors (receptor tyrosine kinase A). NGF triggers several signaling cascades aimed at increasing the expression levels of receptors

(TRPV1r) and ion channels (Na^+ channels) on nociceptors, leading to hypersensitivity (Woolf, 1996) (Sandkuhler, 2009). A consequence of peripheral sensitization is the development of primary hyperalgesia, a localized sensitization in the area of the tissue damage. Therefore, increased sensitization of nociceptors in the periphery may increase the excitability of spinal dorsal horn neurons (Woolf, 1983).

ii. Central sensitization

Central sensitization refers to pain originating from enhanced excitability of CNS neurons. It is typically associated with allodynia, spontaneous pain and primary and secondary hyperalgesia (Latremoliere and Woolf, 2009; Sandkuhler, 2009; Kuner, 2010). Primary and secondary hyperalgesia respectively describe increases in pain sensitivity either at the site of an injury or in the area surrounding this site.

ii.1 Alteration in glutamatergic neurotransmission

Long-term potentiation (LTP) has been shown to be important in the hippocampus for reinforcing memory. This activity-dependent sensitization relies on the stimulation of presynaptic fibers at high frequency (Bliss and Lomo, 1973). LTP also takes place in the spinal cord and involves high or low frequency activity of C-fibers and spinal projection neurons (Liu and Sandkuhler, 1997; Ikeda et al., 2006). This mechanism of synaptic potentiation depends on NMDARs and T-type voltage-gated calcium channels (Ikeda et al., 2003). In addition, it includes also the insertion of α-amino-3-hydroxy-5-methyl-4-isoxazolepropionic acid receptors (AMPARs) at glutamatergic synapses (Randic et al., 1993). *In vivo* injection of capsaicin (agonist of TRPV1 receptors) or formalin as well as nerve injury can contribute to strengthening synaptic transmission between C-fibers and dorsal horn neurons and lead to secondary hyperalgesia and allodynia (Ikeda et al., 2003).

ii.2 Disinhibition of dorsal horn neurons

Inhibitory neurons are densely distributed in the sdh and, as postulated in the gate control theory, a loss of function of these inhibitory interneurons (disinhibition) would lead to increased pain (Melzack and Wall, 1965). Further evidence for the importance of these inhibitory neurons in regulating pain signals was shown after spinal administration of bicuculline and strychnine, whereby rodents developed spontaneous pain (Yaksh, 1989;

Sivilotti and Woolf, 1994). A recent publication from our group also demonstrated the importance of dorsal horn glycinergic neurotransmission in pain signaling (Foster et al., 2015). The following paragraphs will introduce different mechanisms involved in compromising spinal GABAergic and glycinergic inhibition in neuropathic and inflammatory pain.

It has been demonstrated that injury to peripheral nerves induces a depolarizing shift in the chloride equilibrium potential of dorsal horn neurons (Coull et al., 2003). Microglia activated by the release of cytokine CCL2 from damaged nerves (Thacker et al., 2009) release brain-derived neurotrophic factor (BDNF). BDNF binds to trkB receptors on dorsal horn neurons, ultimately leading to the down-regulation of KCC2, required for maintaining low levels of intracellular chloride (Coull et al., 2005). Consequently, increased intracellular chloride concentrations reverse the hyperpolarizing effect of GABA and glycine on dorsal horn neurons due to a depolarizing shift in the chloride reversal potential (Coull et al., 2003; Coull et al., 2005).

Partial nerve injury was shown to decrease spinal dorsal horn levels of the GABA synthesizing enzyme, glutamic acid decarboxylase (GAD65) (Moore et al., 2002). This leads to reduced GABAergic synaptic transmission, possibly explained by apoptosis of GABAergic inhibitory neurons (Moore et al., 2002).

Peripheral inflammation is also a trigger to diminished synaptic inhibition (Harvey et al., 2004; Reinold et al., 2005). During peripheral inflammation, the expression of specific enzymes such as COX2 or mPGES-1 is up-regulated leading to the production of pronociceptive and proinflammatory prostaglandin E2 (PGE_2) in the spinal cord. Upon binding to its receptor (EP2), PGE_2 activates protein kinase A (PKA) which induces phosphorylation of the α3 subunit-containing glycine receptors (Ahmadi et al., 2002). This reduction in spinal glycinergic inhibition leads to mechanical and thermal hyperalgesia in mice.

Diminished synaptic inhibition may also indirectly originate from a mechanism involving endocannabinoids (eCB). Work from our group has demonstrated that upon strong stimulation of nociceptive C-fibers, excitatory interneurons from the sdh received less GABAergic/glycinergic neurotransmission due to disinhibition of inhibitory presynaptic neurons connected to these excitatory neurons (Pernia-Andrade et al., 2009).

The common denominator of all these above-mentioned mechanisms is a diminished inhibition originating from GABAergic or glycinergic neurons in the dorsal horn leading to persistent pain. Therefore, a rational approach for restoring inhibition, and thereby reestablish normal pain signaling in the dorsal horn could be to pharmacologically target either GABAergic or glycinergic neurons (Figure 7).

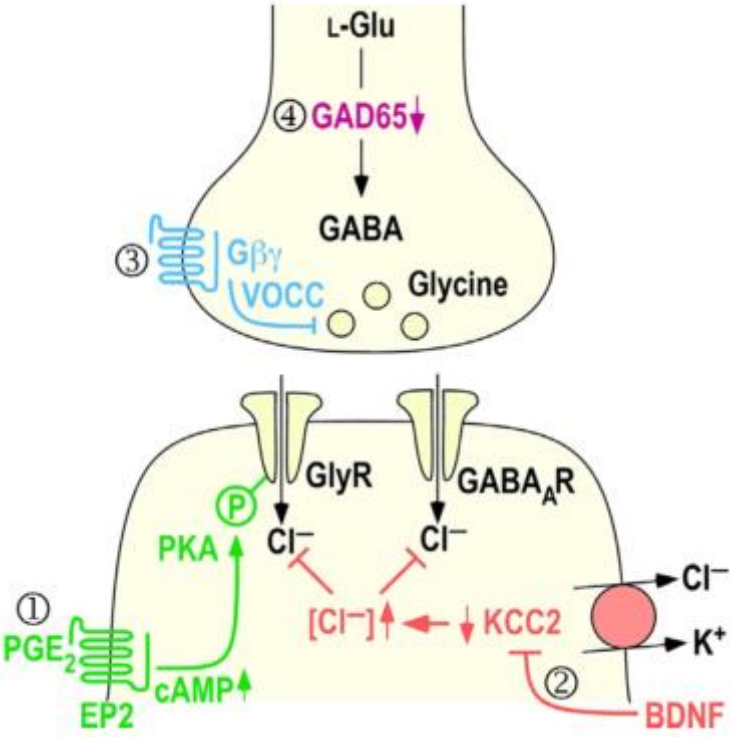

Figure 7. Four signaling pathways causing disinhibition in pathological pain states. (1) PGE_2 produced in the spinal cord in response to peripheral nerve inflammation increases cAMP, which ultimately phosphorylates and inhibits GlyRs of dorsal horn neurons. (2) BDNF released by microglia down-regulates the potassium-chloride transporter (KCC2), important for maintaining low chloride gradients in dorsal horn neurons. As a consequence, GABAergic and glycinergic neurons become depolarized upon activation of their receptors and their inputs become less inhibitory (more excitatory). (3) Neuromodulators such as eCB inhibit voltage operated calcium channels (VOCC) via $G_{\beta\gamma}$ protein-coupled CB1 receptors. This leads to a decrease in calcium influx and ultimately to a reduction in neurotransmitter release. (4) Down-regulation of the GABA synthesizing enzyme GAD65, which possibly reduces the GABA content in inhibitory dorsal horn neurons (Zeilhofer et al., 2015).

Strategies for restoring spinal inhibitory neurotransmission

i. $GABA_A$ receptor subunit-specific benzodiazepines

$GABA_A$ receptors have been the center of attention for pharmacological drug targeting mainly because many spinal dorsal horn inhibitory neurons release both GABA and glycine from their terminals, but also because most neurons receive inputs form GABAergic and glycinergic neurons (Todd and Sullivan, 1990; Yoshimura and Nishi, 1995; Todd et al., 1996a).

Following this logic, GABAergic facilitation should also permit to compensate for a reduction in glycinergic inhibition (Ahmadi et al., 2002). Classical BDZs enhance inhibitory neurotransmission by binding to four subunits (α1, α2, α3, α5) of $GABA_A$ receptors. When applied to the spinal cord intraspinally, these classical BDZs can alleviate pathological pain (Enna and McCarson, 2006; Knabl et al., 2009). Since $GABA_A$ receptors display an array of different subunit configurations, which provide them with channel properties and cellular localizations, it was important to develop $GABA_A$ receptor subtype-selective drugs to separate the antihyperalgesic effects from the unwanted ones (i.e., sedation, tolerance, addiction). To attribute the different actions of diazepam to single $GABA_A$ receptor subtypes, point-mutated knock-in mice were generated in which one or several α subunits of $GABA_A$ receptors were rendered insensitive to diazepam (DZP) (Rudolph and Mohler, 2006; Knabl et al., 2008; Knabl et al., 2009; Ralvenius et al., 2015). Through this approach, it was demonstrated by some studies that $GABA_A$ receptor α subunits contributed to different effects of BDZ (Figure 8).

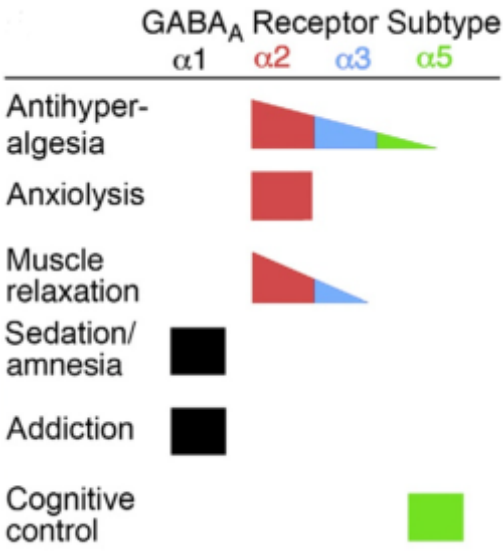

Figure 8. Contribution of the four α-$GABA_A$ receptor subtypes to antihyperalgesia and comparison with other behavioral effects of BDZs. Spinal antihyperalgesia is mainly mediated by α2-$GABA_A$Rs and to a lesser extent by α3 and α5-$GABA_A$Rs. The α2-$GABA_A$Rs also mediate anxiolysis and muscle relaxation. The α1-$GABA_A$Rs mediate sedation and addiction. Modified from Zeilhofer et al.(2015).

It was evidenced using an inflammatory and neuropathic pain model that α1-$GABA_A$R subtypes were involved in mediating sedation, whereas α2 and α3-containing $GABA_A$Rs mediated anxiolysis and pronounced analgesia (Low et al., 2000; Knabl et al., 2008). Further

work investigated the roles of α2, α3, and α5-$GABA_AR$ subunits to DZP-induced antinociception (in an α1 point-mutated background) and found that α2 and α3 $GABA_AR$ subunits were most relevant to DZP-mediated antihyperalgesia after systemic and intrathecal injection of DZP in a model of inflammatory and neuropathic pain (Knabl et al., 2008; Ralvenius et al., 2015). These results provided evidence that the spinal cord was a major site for benzodiazepine-induced antihyperalgesia. A study from our lab made use of a mouse line in which the α2-$GABA_AR$ subtype was specifically ablated from the spinal cord and primary sensory neurons up to the segment C4 (Witschi et al., 2010; Paul et al., 2014). Using this mouse, it was demonstrated that the antihyperalgesic effects of systemically administered BDZ originated exclusively from the spinal cord and mediated spinal antihyperalgesia (Rivas et al., 2009; Di Lio et al., 2011).

In addition, it is now clear that developing BDZs devoid of activity at α1-$GABA_ARs$ is crucial for avoiding unwanted effects. Such drugs (e.g. L838417) have already been used in inflammatory and neuropathic pain models and have elicited antinociceptive effects without sedation (Munro et al., 2009). Altogether, we may conclude that developing compounds with increased specificity to α2-$GABA_ARs$ as well as insensitivity to α1-$GABA_ARs$, might offer new therapeutic opportunities to restore disinhibition and ultimately mediate spinal antihyperalgesia.

IV. Approaches to studying the connectivity and functionality of spinal neurons

Progress towards a better understanding of the organization and function of neural circuits involved in pain signaling relies on the development of useful and novel tools that I shall describe in the following section.

Optogenetics

i. Channelrhodopsins (ChRs)

In the last decade, exploiting light has become one of the most widely used strategies to study neural connectivity, functionality and dysfunction not only in the brain but also in the spinal cord (Zhao et al., 2011; Kato et al., 2013; Foster et al., 2015).

ChRs are light-gated cation-selective channels located in the cell membrane, and used as photoreceptors in algae during photosynthesis (Nagel et al., 2002). Upon photon absorption, ChRs mediate a fast depolarizing inward current due to the channels' permeability to sodium (Na^+) and calcium (Ca^{2+}) ions as well as protons (H^+) (Nagel et al., 2003). The engineering of ChRs has permitted the development of hybrids with improved spectral and kinetics properties as well as improved expression on cellular membranes (Lin, 2011). ChRs are therefore used to depolarize neuronal membranes with light and therefore control their excitability (Boyden et al., 2005; Li et al., 2005; Nagel et al., 2005; Zhang et al., 2006).

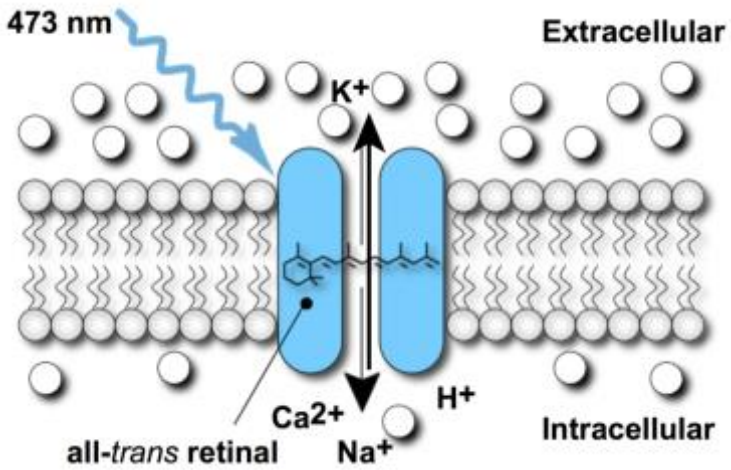

Channelrhodopsin (ChR2). Light absorption (λ=473 nm) by the chromophore (all-trans-retinal) causes a conformational change from all-*trans* to 13-*cis*-retinal. These changes introduce an additional conformational change in the channel that leads to the opening of the pore and allows the flow of sodium (Na^+), calcium (Ca^{2+}), protons (H^+) and potassium (K^+) ion, involved in depolarizing the cell. Modified from Wong et al.(2012).

The most commonly used ChR is ChR2, which upon activation can drive spiking with millisecond precision. The advantage of selectively activating individual cell populations is that it improves our understanding of the role of a specific cell type in a given circuit. For example, a study expressed ChR2 in spinal astrocytes to determine the effects of *in-situ* astrocyte activation on pain sensitization (Nam et al., 2016). In this study as in many others (Depuy et al., 2011; Yang et al., 2015), viral vectors were used to target ChR2 to a defined cell population. In addition to inevitable tissue damage, this approach could lead to gradients of transgene expression levels in the infected tissue and variable spreads of the virus in the tissue. To circumvent these potential limitations, new technologies allowed the development of cell-type specific ChR2-YFP BAC transgenic mouse lines (Zhao et al., 2011). BAC transgenic

mice expressing ChR2 are used to specifically activate a wide range of cell types such as cholinergic cells (Chat-ChR2) to study the function of these cells in motor circuits (Caggiano et al., 2016), or inhibitory cells (vGAT::ChR2-YFP) to investigate the importance of inhibitory neurotransmission in spinal pain signaling (Foster et al., 2015).

Inhibition of neural activity allows assessing the functional role of individual circuit components. A widely used inhibitory opsin is the NpHR (halorhodopsin) (Han et al., 2015). As opposed to ChR2, NpHR pumps chloride ions into the cell upon light activation and leads to hyperpolarization of the cell membrane. An alternative to NpHRs are the proton pumps (ArCh), which also lead to cell hyperpolarization upon light stimulation (Hedrick et al., 2016).

ii. Laser scanning photostimulation (LSPS)

Lu and Perl were pioneers in dissecting interneuronal connectivity in the spinal dorsal horn. To achieve this they performed paired recordings, which can be very tedious and time consuming (Lu and Perl, 2003, 2005) given that one must record from connected pairs of neurons. Data obtained from paired recordings is useful for examining interneuronal connectivity (Lu and Perl, 2003; Schneider, 2008; Zhang and Schneider, 2011). This technique makes it nevertheless difficult to get an overview of patterns of connectivity across neuronal populations throughout the dorsal horn. The LSPS technique, instead, circumvents this limitation and provides population-wide spatial information on the connectivity between cell types. Moreover, it allows rapid sampling across multiple sites in a stimulus pattern. LSPS can either be combined with glutamate uncaging (Kato et al., 2007; Kato et al., 2013; Kosugi et al., 2013) or with light-sensitive ligand-gated channels (ChR2) (Petreanu et al., 2007). Through both methods, the locations of neurons forming functional synaptic connections to single neurons can be revealed and mapped onto the spinal dorsal horn or the brain. LSPS combined with glutamate uncaging selectively activates neurons perisomatically, and spares axons de passage or distal dendrites. This ensures a sub-laminar mapping resolution.

iii. Contactless activation of pain pathways

A milestone in the application of optogenetics to pain research was the design of a mouse line expressing ChR2 on the terminals of its nociceptors (Nav1.8) (Daou et al., 2013). There are two main advantages to this strategy, namely: 1) the selective activation of nociceptors

by shining light through the skin; and 2) the isolation of the nociceptive input with reduced risk of activating touch-pathways upon handling of the animal. However, one caveat to this technique is that mice are generally moving, making it harder to attempt stimulating the nociceptors and produce sensitization by repeated stimulations to the nociceptors (Bonin and De Koninck, 2014).

Viruses to assess the function of spinal neuronal populations

Specific cell-ablation is another useful method to analyze the function of cells in a circuit. In addition to characterizing the electrophysiological changes in synaptic transmission, the phenotype provides a supplementary readout on the importance or not of such cell population in the circuit.

i. Diphtheria toxin (DT)

In experimental biology, DT is frequently used to ablate cells. Two mechanisms can lead to cell death with DT. Either the human DT receptor is expressed in the target cell population, so that upon DT injection only cells expressing the receptor are ablated (Saito et al., 2001) or, the expression of DT fragment A (DTA) is triggered by Cre recombinase, expressed in a specific cell type (and thus leads to conditional induction of cytotoxicity). This method of conditional ablation with DTA has been exploited in several studies where the injection of DT ablated specifically Cre^{+} cells upon expression of the toxin (Brockschnieder et al., 2006; Duan et al., 2014; Bourane et al., 2015). Such loss-of-function experiments revealed the contribution of a subpopulation of inhibitory and excitatory neurons to the regulation of pain (Duan et al., 2014; Foster et al., 2015) or itch circuits (Bourane et al., 2015).

References

Abraira VE, Ginty DD (2013) The Sensory Neurons of Touch. Neuron 79:618-639.

Ahmadi S, Lippross S, Neuhuber WL, Zeilhofer HU (2002) PGE(2) selectively blocks inhibitory glycinergic neurotransmission onto rat superficial dorsal horn neurons. Nature neuroscience 5:34-40.

Akaike N, Hattori K, Oomura Y, Carpenter DO (1985) Bicuculline and picrotoxin block gamma-aminobutyric acid-gated Cl- conductance by different mechanisms. Experientia 41:70-71.

Ali Z, Wu G, Kozlov A, Barasi S (1996) The role of 5HT3 in nociceptive processing in the rat spinal cord: results from behavioural and electrophysiological studies. Neuroscience letters 208:203-207.

Antal M, Petko M, Polgar E, Heizmann CW, Storm-Mathisen J (1996) Direct evidence of an extensive GABAergic innervation of the spinal dorsal horn by fibres descending from the rostral ventromedial medulla. Neuroscience 73:509-518.

Apkarian AV (2013) A brain signature for acute pain. Trends in cognitive sciences 17:309-310.

Araki T, Yamano M, Murakami T, Wanaka A, Betz H, Tohyama M (1988) Localization of glycine receptors in the rat central nervous system: an immunocytochemical analysis using monoclonal antibody. Neuroscience 25:613-624.

Bardin L (2011) The complex role of serotonin and 5-HT receptors in chronic pain. Behavioural pharmacology 22:390-404.

Basbaum AI, Fields HL (1984) Endogenous pain control systems: brainstem spinal pathways and endorphin circuitry. Annual review of neuroscience 7:309-338.

Basbaum AI, Bautista DM, Scherrer G, Julius D (2009) Cellular and molecular mechanisms of pain. Cell 139:267-284.

Belelli D, Harrison NL, Maguire J, Macdonald RL, Walker MC, Cope DW (2009) Extrasynaptic GABAA receptors: form, pharmacology, and function. The Journal of neuroscience : the official journal of the Society for Neuroscience 29:12757-12763.

Belin M.F, Nanopoulos D, Didier M, Aguera M, Steinbusch H, Verhofstad A, Maitre M, Pujol J.F (1983)Immunohistochemical evidence for the presence of gamma-aminobutyric acid and serotonin in one nerve cell. A study of the raphe nuclei of the rat using antibodies to glutamate decarboxylase and serotonin. Brain research 2:329-339.

Benke D, Honer M, Michel C, Mohler H (1996) GABAA receptor subtypes differentiated by their gamma-subunit variants: prevalence, pharmacology and subunit architecture. Neuropharmacology 35:1413-1423.

Berger AJ, Dieudonne S, Ascher P (1998) Glycine uptake governs glycine site occupancy at NMDA receptors of excitatory synapses. Journal of neurophysiology 80:3336-3340.

Blaesse P, Airaksinen MS, Rivera C, Kaila K (2009) Cation-chloride cotransporters and neuronal function. Neuron 61:820-838.

Bliss TV, Lomo T (1973) Long-lasting potentiation of synaptic transmission in the dentate area of the anaesthetized rabbit following stimulation of the perforant path. The Journal of physiology 232:331-356.

Blondell RD, Azadfard M, Wisniewski AM (2013) Pharmacologic therapy for acute pain. American family physician 87:766-772.

Bogen O, Joseph EK, Chen X, Levine JD (2008) GDNF hyperalgesia is mediated by PLCgamma, MAPK/ERK, PI3K, CDK5 and Src family kinase signaling and dependent on the IB4-binding protein versican. The European journal of neuroscience 28:12-19.

Bohlhalter S, Weinmann O, Mohler H, Fritschy JM (1996) Laminar compartmentalization of GABAA-receptor subtypes in the spinal cord: an immunohistochemical study. The Journal of neuroscience : the official journal of the Society for Neuroscience 16:283-297.

Boileau AJ, Pearce RA, Czajkowski C (2005) Tandem subunits effectively constrain GABAA receptor stoichiometry and recapitulate receptor kinetics but are insensitive to GABAA receptor-associated protein. The Journal of neuroscience : the official journal of the Society for Neuroscience 25:11219-11230.

Bonin R.P, De Koninck Y (2014) A spinal analog of memory reconsolidation enables reversal of hyperalgesia. Nature neuroscience 17:1043-1045.

Bourane S, Duan B, Koch SC, Dalet A, Britz O, Garcia-Campmany L, Kim E, Cheng L, Ghosh A, Ma Q, Goulding M (2015) Gate control of mechanical itch by a subpopulation of spinal cord interneurons. Science 350:550-554.

Boyden ES, Zhang F, Bamberg E, Nagel G, Deisseroth K (2005) Millisecond-timescale, genetically targeted optical control of neural activity. Nature neuroscience 8:1263-1268.

Braz J, Solorzano C, Wang X, Basbaum AI (2014) Transmitting pain and itch messages: a contemporary view of the spinal cord circuits that generate gate control. Neuron 82:522-536.

Breivik H, Collett B, Ventafridda V, Cohen R, Gallacher D (2006) Survey of chronic pain in Europe: prevalence, impact on daily life, and treatment. Eur J Pain 10:287-333.

Brockschnieder D, Pechmann Y, Sonnenberg-Riethmacher E, Riethmacher D (2006) An improved mouse line for Cre-induced cell ablation due to diphtheria toxin A, expressed from the Rosa26 locus. Genesis 44:322-327.

Caggiano V, Cheung VC, Bizzi E (2016) An Optogenetic Demonstration of Motor Modularity in the Mammalian Spinal Cord. Scientific reports 6:35185.

Caterina MJ, Julius D (2001) The vanilloid receptor: a molecular gateway to the pain pathway. Annual review of neuroscience 24:487-517.

Coull JA, Boudreau D, Bachand K, Prescott SA, Nault F, Sik A, De Koninck P, De Koninck Y (2003) Trans-synaptic shift in anion gradient in spinal lamina I neurons as a mechanism of neuropathic pain. Nature 424:938-942.

Coull JA, Beggs S, Boudreau D, Boivin D, Tsuda M, Inoue K, Gravel C, Salter MW, De Koninck Y (2005) BDNF from microglia causes the shift in neuronal anion gradient underlying neuropathic pain. Nature 438:1017-1021.

Cox JJ, Reimann F, Nicholas AK, Thornton G, Roberts E, Springell K, Karbani G, Jafri H, Mannan J, Raashid Y, Al-Gazali L, Hamamy H, Valente EM, Gorman S, Williams R, McHale DP, Wood JN, Gribble FM, Woods CG (2006) An SCN9A channelopathy causes congenital inability to experience pain. Nature 444:894-898.

Daou I, Tuttle AH, Longo G, Wieskopf JS, Bonin RP, Ase AR, Wood JN, De Koninck Y, Ribeiro-da-Silva A, Mogil JS, Seguela P (2013) Remote optogenetic activation and sensitization of pain pathways in freely moving mice. The Journal of neuroscience : the official journal of the Society for Neuroscience 33:18631-18640.

Depuy SD, Kanbar R, Coates MB, Stornetta RL, Guyenet PG (2011) Control of breathing by raphe obscurus serotonergic neurons in mice. The Journal of neuroscience : the official journal of the Society for Neuroscience 31:1981-1990.

Di Lio A, Benke D, Besson M, Desmeules J, Daali Y, Wang ZJ, Edwankar R, Cook JM, Zeilhofer HU (2011) HZ166, a novel GABAA receptor subtype-selective benzodiazepine site ligand, is antihyperalgesic in mouse models of inflammatory and neuropathic pain. Neuropharmacology 60:626-632.

Djouhri L, Lawson SN (2004) Abeta-fiber nociceptive primary afferent neurons: a review of incidence and properties in relation to other afferent A-fiber neurons in mammals. Brain research Brain research reviews 46:131-145.

Duan B, Cheng L, Bourane S, Britz O, Padilla C, Garcia-Campmany L, Krashes M, Knowlton W, Velasquez T, Ren X, Ross SE, Lowell BB, Wang Y, Goulding M, Ma Q (2014) Identification of spinal circuits transmitting and gating mechanical pain. Cell 159:1417-1432.

Enna SJ, McCarson KE (2006) The role of GABA in the mediation and perception of pain. Adv Pharmacol 54:1-27.

Essrich C, Lorez M, Benson JA, Fritschy JM, Luscher B (1998) Postsynaptic clustering of major GABAA receptor subtypes requires the gamma 2 subunit and gephyrin. Nature neuroscience 1:563-571.

Foster E, Wildner H, Tudeau L, Haueter S, Ralvenius WT, Jegen M, Johannssen H, Hosli L, Haenraets K, Ghanem A, Conzelmann KK, Bosl M, Zeilhofer HU (2015) Targeted ablation, silencing, and activation establish glycinergic dorsal horn neurons as key components of a spinal gate for pain and itch. Neuron 85:1289-1304.

Fritschy JM, Harvey RJ, Schwarz G (2008) Gephyrin: where do we stand, where do we go? Trends in neurosciences 31:257-264.

Fukushima T, Ohtsubo T, Tsuda M, Yanagawa Y, Hori Y (2009) Facilitatory actions of serotonin type 3 receptors on GABAergic inhibitory synaptic transmission in the spinal superficial dorsal horn. Journal of neurophysiology 102:1459-1471.

Gauriau C, Bernard JF (2004) A comparative reappraisal of projections from the superficial laminae of the dorsal horn in the rat: the forebrain. The Journal of comparative neurology 468:24-56.

Gebhart GF (2004) Descending modulation of pain. Neuroscience and biobehavioral reviews 27:729-737.

Gobel S, Falls WM, Bennett GJ, Abdelmoumene M, Hayashi H, Humphrey E (1980) An EM analysis of the synaptic connections of horseradish peroxidase-filled stalked cells and islet cells in the substantia gelatinosa of adult cat spinal cord. The Journal of comparative neurology 194:781-807.

Gold MS, Gebhart GF (2010) Nociceptor sensitization in pain pathogenesis. Nature medicine 16:1248-1257.

Grudt TJ, Perl ER (2002) Correlations between neuronal morphology and electrophysiological features in the rodent superficial dorsal horn. The Journal of physiology 540:189-207.

Grudzinska J, Schemm R, Haeger S, Nicke A, Schmalzing G, Betz H, Laube B (2005) The beta subunit determines the ligand binding properties of synaptic glycine receptors. Neuron 45:727-739.

Gu M, Miyoshi K, Dubner R, Guo W, Zou S, Ren K, Noguchi K, Wei F (2011) Spinal 5-HT(3) receptor activation induces behavioral hypersensitivity via a neuronal-glial-neuronal signaling cascade. The Journal of neuroscience : the official journal of the Society for Neuroscience 31:12823-12836.

Han Y, Ma F, Li H, Wang Y, Xu K (2015) Optogenetic control of thalamus as a tool for interrupting penicillin induced seizures. Conference proceedings : Annual International Conference of the IEEE Engineering in Medicine and Biology Society IEEE Engineering in Medicine and Biology Society Annual Conference 2015:6606-6609.

Hantman AW, van den Pol AN, Perl ER (2004) Morphological and physiological features of a set of spinal substantia gelatinosa neurons defined by green fluorescent protein expression. The Journal of neuroscience : the official journal of the Society for Neuroscience 24:836-842.

Harvey RJ, Depner UB, Wassle H, Ahmadi S, Heindl C, Reinold H, Smart TG, Harvey K, Schutz B, Abo-Salem OM, Zimmer A, Poisbeau P, Welzl H, Wolfer DP, Betz H, Zeilhofer HU, Muller U (2004) GlyR alpha3: an essential target for spinal PGE2-mediated inflammatory pain sensitization. Science 304:884-887.

Hedrick T, Danskin B, Larsen RS, Ollerenshaw D, Groblewski P, Valley M, Olsen S, Waters J (2016) Characterization of Channelrhodopsin and Archaerhodopsin in Cholinergic Neurons of Cre-Lox Transgenic Mice. PloS one 11:e0156596.

Heinke B, Ruscheweyh R, Forsthuber L, Wunderbaldinger G, Sandkuhler J (2004) Physiological, neurochemical and morphological properties of a subgroup of GABAergic spinal lamina II neurones identified by expression of green fluorescent

protein in mice. The Journal of physiology 560:249-266.

Heinricher MM, McGaraughty S (1998) Analysis of excitatory amino acid transmission within the rostral ventromedial medulla: implications for circuitry. Pain 75:247-255.

Hu J, Huang T, Li T, Guo Z, Cheng L (2012) c-Maf is required for the development of dorsal horn laminae III/IV neurons and mechanoreceptive DRG axon projections. The Journal of neuroscience : the official journal of the Society for Neuroscience 32:5362-5373.

Hylden JL, Ruda MA, Hayashi H, Dubner R (1985) Descending serotonergic fibers in the dorsolateral and ventral funiculi of cat spinal cord. Neuroscience letters 62:299-304.

Ikeda H, Heinke B, Ruscheweyh R, Sandkuhler J (2003) Synaptic plasticity in spinal lamina I projection neurons that mediate hyperalgesia. Science 299:1237-1240.

Ikeda H, Stark J, Fischer H, Wagner M, Drdla R, Jager T, Sandkuhler J (2006) Synaptic amplifier of inflammatory pain in the spinal dorsal horn. Science 312:1659-1662.

Jensen TS, Baron R, Haanpaa M, Kalso E, Loeser JD, Rice AS, Treede RD (2011) A new definition of neuropathic pain. Pain 152:2204-2205.

Johnson JW, Ascher P (1987) Glycine potentiates the NMDA response in cultured mouse brain neurons. Nature 325:529-531.

Johnston GA (1996) GABAA receptor pharmacology. Pharmacology & therapeutics 69:173-198.

Jones BL, Henderson LP (2007) Trafficking and potential assembly patterns of epsilon-containing GABAA receptors. Journal of neurochemistry 103:1258-1271.

Julius D, Basbaum AI (2001) Molecular mechanisms of nociception. Nature 413:203-210.

Kakigi R, Tran TD, Qiu Y, Wang X, Nguyen TB, Inui K, Watanabe S, Hoshiyama M (2003) Cerebral responses following stimulation of unmyelinated C-fibers in humans: electro- and magneto-encephalographic study. Neuroscience research 45:255-275.

Kato G, Kawasaki Y, Ji RR, Strassman AM (2007) Differential wiring of local excitatory and inhibitory synaptic inputs to islet cells in rat spinal lamina II demonstrated by laser scanning photostimulation. The Journal of physiology 580:815-833.

Kato G, Kosugi M, Mizuno M, Strassman AM (2013) Three-dimensional organization of local excitatory and inhibitory inputs to neurons in laminae III-IV of the spinal dorsal horn. The Journal of physiology 591:5645-5660.

Kato G, Yasaka T, Katafuchi T, Furue H, Mizuno M, Iwamoto Y, Yoshimura M (2006) Direct GABAergic and glycinergic inhibition of the substantia gelatinosa from the rostral ventromedial medulla revealed by in vivo patch-clamp analysis in rats. The Journal of neuroscience : the official journal of the Society for Neuroscience 26:1787-1794.

Kato G, Kawasaki Y, Koga K, Uta D, Kosugi M, Yasaka T, Yoshimura M, Ji RR, Strassman AM (2009) Organization of intralaminar and translaminar neuronal connectivity in the superficial spinal dorsal horn. The Journal of neuroscience : the official journal of the Society for Neuroscience 29:5088-5099.

Knabl J, Zeilhofer UB, Crestani F, Rudolph U, Zeilhofer HU (2009) Genuine antihyperalgesia by systemic diazepam revealed by experiments in GABAA receptor point-mutated mice. Pain 141:233-238.

Knabl J, Witschi R, Hosl K, Reinold H, Zeilhofer UB, Ahmadi S, Brockhaus J, Sergejeva M, Hess A, Brune K, Fritschy JM, Rudolph U, Mohler H, Zeilhofer HU (2008) Reversal of pathological pain through specific spinal GABAA receptor subtypes. Nature 451:330-334.

Kosugi M, Kato G, Lukashov S, Pendse G, Puskar Z, Kozsurek M, Strassman AM (2013) Subpopulation-specific patterns of intrinsic connectivity in mouse superficial dorsal horn as revealed by laser scanning photostimulation. The Journal of physiology 591:1935-1949.

Kowalczyk S, Winkelmann A, Smolinsky B, Forstera B, Neundorf I, Schwarz G, Meier JC (2013) Direct binding of GABAA receptor beta2 and beta3 subunits to gephyrin. The European journal of neuroscience 37:544-554.

Kuner R (2010) Central mechanisms of pathological pain. Nature medicine 16:1258-1266.

Latremoliere A, Woolf CJ (2009) Central sensitization: a generator of pain hypersensitivity by central neural plasticity. The journal of pain : official journal of the American Pain Society 10:895-926.

Lau BK, Vaughan CW (2014) Descending modulation of pain: the GABA disinhibition hypothesis of analgesia. Current opinion in neurobiology 29:159-164.

Laube B, Maksay G, Schemm R, Betz H (2002) Modulation of glycine receptor function: a novel approach for therapeutic intervention at inhibitory synapses? Trends in pharmacological sciences 23:519-527.

Laurie DJ, Wisden W, Seeburg PH (1992) The distribution of thirteen GABAA receptor subunit mRNAs in the rat brain. III. Embryonic and postnatal development. The Journal of neuroscience : the official journal of the Society for Neuroscience 12:4151-4172.

Lee MC, Tracey I (2013) Imaging pain: a potent means for investigating pain mechanisms in patients. British journal of anaesthesia 111:64-72.

Leem JW, Willis WD, Chung JM (1993) Cutaneous Sensory Receptors in the Rat Foot. Journal of neurophysiology 69:1684-1699.

Li X, Gutierrez DV, Hanson MG, Han J, Mark MD, Chiel H, Hegemann P, Landmesser LT, Herlitze S (2005) Fast noninvasive activation and inhibition of neural and network activity by vertebrate rhodopsin and green algae channelrhodopsin. Proceedings of the National Academy of Sciences of the United States of America 102:17816-17821.

Lin JY (2011) A user's guide to channelrhodopsin variants: features, limitations and future developments. Experimental physiology 96:19-25.

Liu X, Sandkuhler J (1997) Characterization of long-term potentiation of C-fiber-evoked potentials in spinal dorsal horn of adult rat: essential role of NK1 and NK2 receptors. Journal of neurophysiology 78:1973-1982.

Loeser JD, Treede RD (2008) The Kyoto protocol of IASP Basic Pain Terminology. Pain 137:473-477.

Low K, Crestani F, Keist R, Benke D, Brunig I, Benson JA, Fritschy JM, Rulicke T, Bluethmann H, Mohler H, Rudolph U (2000) Molecular and neuronal substrate for the selective attenuation of anxiety. Science 290:131-134.

Lu Y, Perl ER (2003) A specific inhibitory pathway between substantia gelatinosa neurons receiving direct C-fiber input. The Journal of neuroscience : the official journal of the Society for Neuroscience 23:8752-8758.

Lu Y, Perl ER (2005) Modular organization of excitatory circuits between neurons of the spinal superficial dorsal horn (laminae I and II). The Journal of neuroscience : the official journal of the Society for Neuroscience 25:3900-3907.

Luo C, Kuner T, Kuner R (2014) Synaptic plasticity in pathological pain. Trends in neurosciences 37:343-355.

Malin SA, Molliver DC, Koerber HR, Cornuet P, Frye R, Albers KM, Davis BM (2006) Glial cell line-derived neurotrophic factor family members sensitize nociceptors in vitro and produce thermal hyperalgesia in vivo. The Journal of neuroscience : the official journal of the Society for Neuroscience 26:8588-8599.

Malosio ML, Marqueze-Pouey B, Kuhse J, Betz H (1991) Widespread expression of glycine receptor subunit mRNAs in the adult and developing rat brain. The EMBO journal 10:2401-2409.

Maxwell DJ, Belle MD, Cheunsuang O, Stewart A, Morris R (2007) Morphology of inhibitory and excitatory interneurons in superficial

laminae of the rat dorsal horn. The Journal of physiology 584:521-533.

McCoy ES, Taylor-Blake B, Street SE, Pribisko AL, Zheng J, Zylka MJ (2013) Peptidergic CGRPalpha primary sensory neurons encode heat and itch and tonically suppress sensitivity to cold. Neuron 78:138-151.

Melzack R, Wall PD (1965) Pain mechanisms: a new theory. Science 150:971-979.

Mishra SK, Hoon MA (2013) The cells and circuitry for itch responses in mice. Science 340:968-971.

Mohler H, Crestani F, Rudolph U (2001) GABA(A)-receptor subtypes: a new pharmacology. Current opinion in pharmacology 1:22-25.

Moore R.Y, Bloom F.E (1979) Central catecholamine neuron systems: anatomy and physiology of the norepinephrine and epinephrine systems. Annual review of neuroscience 2:113-168.

Moore KA, Kohno T, Karchewski LA, Scholz J, Baba H, Woolf CJ (2002) Partial peripheral nerve injury promotes a selective loss of GABAergic inhibition in the superficial dorsal horn of the spinal cord. The Journal of neuroscience : the official journal of the Society for Neuroscience 22:6724-6731.

Moore RA, Derry S, Simon LS, Emery P (2014) Nonsteroidal anti-inflammatory drugs, gastroprotection, and benefit-risk. Pain practice : the official journal of World Institute of Pain 14:378-395.

Mukherjee J, Kretschmannova K, Gouzer G, Maric HM, Ramsden S, Tretter V, Harvey K, Davies PA, Triller A, Schindelin H, Moss SJ (2011) The residence time of GABA(A)Rs at inhibitory synapses is determined by direct binding of the receptor alpha1 subunit to gephyrin. The Journal of neuroscience : the official journal of the Society for Neuroscience 31:14677-14687.

Munro G, Ahring PK, Mirza NR, Mirza R (2009) Developing analgesics by enhancing spinal inhibition after injury: GABA(A) receptor subtypes as novel targets. Trends in pharmacological sciences 30:453-459.

Nagel G, Brauner M, Liewald JF, Adeishvili N, Bamberg E, Gottschalk A (2005) Light activation of channelrhodopsin-2 in excitable cells of Caenorhabditis elegans triggers rapid behavioral responses. Current biology : CB 15:2279-2284.

Nagel G, Ollig D, Fuhrmann M, Kateriya S, Musti AM, Bamberg E, Hegemann P (2002) Channelrhodopsin-1: a light-gated proton channel in green algae. Science 296:2395-2398.

Nagel G, Szellas T, Huhn W, Kateriya S, Adeishvili N, Berthold P, Ollig D, Hegemann P, Bamberg E (2003) Channelrhodopsin-2, a directly light-gated cation-selective membrane channel. Proceedings of the National Academy of Sciences of the United States of America 100:13940-13945.

Naim M, Spike RC, Watt C, Shehab SA, Todd AJ (1997) Cells in laminae III and IV of the rat spinal cord that possess the neurokinin-1 receptor and have dorsally directed dendrites receive a major synaptic input from tachykinin-containing primary afferents. The Journal of neuroscience : the official journal of the Society for Neuroscience 17:5536-5548.

Nam Y, Kim JH, Jha MK, Jung JY, Lee MG, Choi IS, Jang IS, Lim DG, Hwang SH, Cho HJ, Suk K (2016) Reversible Induction of Pain Hypersensitivity following Optogenetic Stimulation of Spinal Astrocytes. Cell reports 17:3049-3061.

Neubert MJ, Kincaid W, Heinricher MM (2004) Nociceptive facilitating neurons in the rostral ventromedial medulla. Pain 110:158-165.

Neumann S, Braz JM, Skinner K, Llewellyn-Smith IJ, Basbaum AI (2008) Innocuous, not noxious, input activates PKCgamma interneurons of the spinal dorsal horn via myelinated afferent fibers. The Journal of neuroscience : the official journal of the Society for Neuroscience 28:7936-7944.

Olsen RW, Sieghart W (2008) International Union of Pharmacology. LXX. Subtypes of gamma-aminobutyric acid(A) receptors: classification on the basis of subunit composition, pharmacology, and function.

Update. Pharmacological reviews 60:243-260.

Olsen RW, Sieghart W (2009) GABA A receptors: subtypes provide diversity of function and pharmacology. Neuropharmacology 56:141-148.

Passlick S, Grauer M, Schafer C, Jabs R, Seifert G, Steinhauser C (2013) Expression of the gamma2-subunit distinguishes synaptic and extrasynaptic GABA(A) receptors in NG2 cells of the hippocampus. The Journal of neuroscience : the official journal of the Society for Neuroscience 33:12030-12040.

Paul J, Zeilhofer HU, Fritschy JM (2012) Selective distribution of GABA(A) receptor subtypes in mouse spinal dorsal horn neurons and primary afferents. The Journal of comparative neurology 520:3895-3911.

Paul J, Yévenes GE, Benke D, Di Lio A, Ralvenius WT, Witschi R, Scheurer L, Cook JM, Rudolph U, Fritschy JM, Zeilhofer HU (2014) Antihyperalgesia by alpha2-GABAA receptors occurs via a genuine spinal action and does not involve supraspinal sites. Neuropsychopharmacology : official publication of the American College of Neuropsychopharmacology 39:477-487.

Peirs C, Williams SP, Zhao X, Walsh CE, Gedeon JY, Cagle NE, Goldring AC, Hioki H, Liu Z, Marell PS, Seal RP (2015) Dorsal Horn Circuits for Persistent Mechanical Pain. Neuron 87:797-812.

Pernia-Andrade AJ, Kato A, Witschi R, Nyilas R, Katona I, Freund TF, Watanabe M, Filitz J, Koppert W, Schuttler J, Ji G, Neugebauer V, Marsicano G, Lutz B, Vanegas H, Zeilhofer HU (2009) Spinal endocannabinoids and CB1 receptors mediate C-fiber-induced heterosynaptic pain sensitization. Science 325:760-764.

Petreanu L, Huber D, Sobczyk A, Svoboda K (2007) Channelrhodopsin-2-assisted circuit mapping of long-range callosal projections. Nature neuroscience 10:663-668.

Polgar E, Fowler JH, McGill MM, Todd AJ (1999) The types of neuron which contain protein kinase C gamma in rat spinal cord. Brain research 833:71-80.

Polgar E, Furuta T, Kaneko T, Todd A (2006) Characterization of neurons that express preprotachykinin B in the dorsal horn of the rat spinal cord. Neuroscience 139:687-697.

Polgar E, Durrieux C, Hughes DI, Todd AJ (2013) A quantitative study of inhibitory interneurons in laminae I-III of the mouse spinal dorsal horn. PloS one 8:e78309.

Popratiloff A, Valtschanoff JG, Rustioni A, Weinberg RJ (1996) Colocalization of GABA and glycine in the rat dorsal column nuclei. Brain research 706:308-312.

Prescott SA, De Koninck Y (2002) Four cell types with distinctive membrane properties and morphologies in lamina I of the spinal dorsal horn of the adult rat. The Journal of physiology 539:817-836.

Punnakkal P, von Schoultz C, Haenraets K, Wildner H, Zeilhofer HU (2014) Morphological, biophysical and synaptic properties of glutamatergic neurons of the mouse spinal dorsal horn. The Journal of physiology 592:759-776.

Rahman W, Suzuki R, Rygh LJ, Dickenson AH (2004) Descending serotonergic facilitation mediated through rat spinal 5HT3 receptors is unaltered following carrageenan inflammation. Neuroscience letters 361:229-231.

Ralvenius WT, Benke D, Acuña MA, Rudolph U, Zeilhofer HU (2015) Analgesia and unwanted benzodiazepine effects in point-mutated mice expressing only one benzodiazepine-sensitive GABAA receptor subtype. Nature communications 6:6803.

Reinold H, Ahmadi S, Depner UB, Layh B, Heindl C, Hamza M, Pahl A, Brune K, Narumiya S, Muller U, Zeilhofer HU (2005) Spinal inflammatory hyperalgesia is mediated by prostaglandin E receptors of the EP2 subtype. The Journal of clinical investigation 115:673-679.

Rexed B (1952) The cytoarchitectonic organization of the spinal cord in the cat. The Journal of comparative neurology 96:414-495.

Rivas FM, Stables JP, Murphree L, Edwankar RV, Edwankar CR, Huang S, Jain HD, Zhou H,

Majumder S, Sankar S, Roth BL, Ramerstorfer J, Furtmuller R, Sieghart W, Cook JM (2009) Antiseizure activity of novel gamma-aminobutyric acid (A) receptor subtype-selective benzodiazepine analogues in mice and rat models. Journal of medicinal chemistry 52:1795-1798.

Ross SE et al. (2010) Loss of inhibitory interneurons in the dorsal spinal cord and elevated itch in Bhlhb5 mutant mice. Neuron 65:886-898.

Rudolph U, Mohler H (2006) GABA-based therapeutic approaches: GABAA receptor subtype functions. Current opinion in pharmacology 6:18-23.

Saito M, Iwawaki T, Taya C, Yonekawa H, Noda M, Inui Y, Mekada E, Kimata Y, Tsuru A, Kohno K (2001) Diphtheria toxin receptor-mediated conditional and targeted cell ablation in transgenic mice. Nature biotechnology 19:746-750.

Sandkuhler J (2009) Models and mechanisms of hyperalgesia and allodynia. Physiological reviews 89:707-758.

Schaible HG, Richter F (2004) Pathophysiology of pain. Langenbeck's archives of surgery 389:237-243.

Scherrer G, Low SA, Wang X, Zhang J, Yamanaka H, Urban R, Solorzano C, Harper B, Hnasko TS, Edwards RH, Basbaum AI (2010) VGLUT2 expression in primary afferent neurons is essential for normal acute pain and injury-induced heat hypersensitivity. Proceedings of the National Academy of Sciences of the United States of America 107:22296-22301.

Schneider SP (2008) Local circuit connections between hamster laminae III and IV dorsal horn neurons. Journal of neurophysiology 99:1306-1318.

Scholz J, Woolf CJ (2002) Can we conquer pain? Nature neuroscience 5 Suppl:1062-1067.

Seal RP (2016) Do the distinct synaptic properties of VGLUTs shape pain? Neurochemistry international 98:82-88.

Seal RP, Wang X, Guan Y, Raja SN, Woodbury CJ, Basbaum AI, Edwards RH (2009) Injury-induced mechanical hypersensitivity requires C-low threshold mechanoreceptors. Nature 462:651-655.

Sivilotti L, Woolf CJ (1994) The contribution of GABAA and glycine receptors to central sensitization: disinhibition and touch-evoked allodynia in the spinal cord. Journal of neurophysiology 72:169-179.

Snider WD, McMahon SB (1998a) Tackling pain at the source: new ideas about nociceptors. Neuron 20:629-632.

Snider WD, McMahon SB (1998b) Tackling pain at the source: New ideas about nociceptors. Neuron 20:629-632.

Spike RC, Puskar Z, Andrew D, Todd AJ (2003) A quantitative and morphological study of projection neurons in lamina I of the rat lumbar spinal cord. The European journal of neuroscience 18:2433-2448.

Suzuki R, Rygh LJ, Dickenson AH (2004) Bad news from the brain: descending 5-HT pathways that control spinal pain processing. Trends in pharmacological sciences 25:613-617.

Takahashi T, Momiyama A, Hirai K, Hishinuma F, Akagi H (1992) Functional correlation of fetal and adult forms of glycine receptors with developmental changes in inhibitory synaptic receptor channels. Neuron 9:1155-1161.

Tamamaki N, Yanagawa Y, Tomioka R, Miyazaki J, Obata K, Kaneko T (2003) Green fluorescent protein expression and colocalization with calretinin, parvalbumin, and somatostatin in the GAD67-GFP knock-in mouse. The Journal of comparative neurology 467:60-79.

Thacker MA, Clark AK, Bishop T, Grist J, Yip PK, Moon LD, Thompson SW, Marchand F, McMahon SB (2009) CCL2 is a key mediator of microglia activation in neuropathic pain states. Eur J Pain 13:263-272.

Todd AJ (2010) Neuronal circuitry for pain processing in the dorsal horn. Nature reviews Neuroscience 11:823-836.

Todd AJ, Sullivan AC (1990) Light microscope study of the coexistence of GABA-like and glycine-like immunoreactivities in the spinal

cord of the rat. The Journal of comparative neurology 296:496-505.

Todd AJ, Russell G, Spike RC (1992) Immunocytochemical evidence that GABA and neurotensin exist in different neurons in laminae II and III of rat spinal dorsal horn. Neuroscience 47:685-691.

Todd AJ, Watt C, Spike RC, Sieghart W (1996a) Colocalization of GABA, glycine, and their receptors at synapses in the rat spinal cord. The Journal of neuroscience : the official journal of the Society for Neuroscience 16:974-982.

Todd AJ, Watt C, Spike RC, Sieghart W (1996b) Colocalization of GABA, glycine, and their receptors at synapses in the rat spinal cord. Journal of Neuroscience 16:974-982.

Todd AJ, Puskar Z, Spike RC, Hughes C, Watt C, Forrest L (2002) Projection neurons in lamina I of rat spinal cord with the neurokinin 1 receptor are selectively innervated by substance p-containing afferents and respond to noxious stimulation. The Journal of neuroscience : the official journal of the Society for Neuroscience 22:4103-4113.

Todd AJ, Hughes DI, Polgar E, Nagy GG, Mackie M, Ottersen OP, Maxwell DJ (2003) The expression of vesicular glutamate transporters VGLUT1 and VGLUT2 in neurochemically defined axonal populations in the rat spinal cord with emphasis on the dorsal horn. The European journal of neuroscience 17:13-27.

Tretter V, Jacob TC, Mukherjee J, Fritschy JM, Pangalos MN, Moss SJ (2008) The clustering of GABA(A) receptor subtypes at inhibitory synapses is facilitated via the direct binding of receptor alpha 2 subunits to gephyrin. The Journal of neuroscience : the official journal of the Society for Neuroscience 28:1356-1365.

Waxman SG, Zamponi GW (2014) Regulating excitability of peripheral afferents: emerging ion channel targets. Nature neuroscience 17:153-163.

Wildner H, Das Gupta R, Brohl D, Heppenstall PA, Zeilhofer HU, Birchmeier C (2013) Genome-wide expression analysis of Ptf1a- and Ascl1-deficient mice reveals new markers for distinct dorsal horn interneuron populations contributing to nociceptive reflex plasticity. The Journal of neuroscience : the official journal of the Society for Neuroscience 33:7299-7307.

Wisden W, Gundlach AL, Barnard EA, Seeburg PH, Hunt SP (1991) Distribution of GABAA receptor subunit mRNAs in rat lumbar spinal cord. Brain research Molecular brain research 10:179-183.

Witschi R, Johansson T, Morscher G, Scheurer L, Deschamps J, Zeilhofer HU (2010) Hoxb8-Cre mice: A tool for brain-sparing conditional gene deletion. Genesis 48:596-602.

Wong J, Abilez OJ, Kuhl E (2012) Computational Optogenetics: A Novel Continuum Framework for the Photoelectrochemistry of Living Systems. Journal of the mechanics and physics of solids 60:1158-1178.

Woolf CJ (1983) Evidence for a central component of post-injury pain hypersensitivity. Nature 306:686-688.

Woolf CJ (1996) Phenotypic modification of primary sensory neurons: the role of nerve growth factor in the production of persistent pain. Philosophical transactions of the Royal Society of London Series B, Biological sciences 351:441-448.

Yaksh TL (1989) Behavioral and autonomic correlates of the tactile evoked allodynia produced by spinal glycine inhibition: effects of modulatory receptor systems and excitatory amino acid antagonists. Pain 37:111-123.

Yang K, Ma R, Wang Q, Jiang P, Li YQ (2015) Optoactivation of parvalbumin neurons in the spinal dorsal horn evokes GABA release that is regulated by presynaptic GABAB receptors. Neuroscience letters 594:55-59.

Yasaka T, Tiong SY, Hughes DI, Riddell JS, Todd AJ (2010) Populations of inhibitory and excitatory interneurons in lamina II of the adult rat spinal dorsal horn revealed by a combined electrophysiological and anatomical approach. Pain 151:475-488.

Yoshimura M, Nishi S (1995) Primary afferent-evoked glycine- and GABA-mediated IPSPs in

substantia gelatinosa neurones in the rat spinal cord in vitro. The Journal of physiology 482 (Pt 1):29-38.

Zeilhofer HU, Wildner H, Yévenes GE (2012) Fast synaptic inhibition in spinal sensory processing and pain control. Physiological reviews 92:193-235.

Zeilhofer HU, Studler B, Arabadzisz D, Schweizer C, Ahmadi S, Layh B, Bosl MR, Fritschy JM (2005) Glycinergic neurons expressing enhanced green fluorescent protein in bacterial artificial chromosome transgenic mice. The Journal of comparative neurology 482:123-141.

Zhang F, Wang LP, Boyden ES, Deisseroth K (2006) Channelrhodopsin-2 and optical control of excitable cells. Nature methods 3:785-792.

Zhang W, Schneider SP (2011) Short-term modulation at synapses between neurons in laminae II-V of the rodent spinal dorsal horn. Journal of neurophysiology 105:2920-2930.

Zhao S, Ting JT, Atallah HE, Qiu L, Tan J, Gloss B, Augustine GJ, Deisseroth K, Luo M, Graybiel AM, Feng G (2011) Cell type-specific channelrhodopsin-2 transgenic mice for optogenetic dissection of neural circuitry function. Nature methods 8:745-752.

Chapter 1

Inhibitory synaptic transmission in the dorsal horn of mice lacking α2-$GABA_A$ receptors from the spinal cord

[1,2]Laetitia Tudeau, [1]William T. Ralvenius, [3]Michael Poe, [3]James C. Cook,

[1]Helge C. Johannssen, [1]Mario A. Acuña [1,2]Hanns Ulrich Zeilhofer

[1] Institute of Pharmacology and Toxicology, University of Zurich, CH-8057 Zurich, Switzerland

[2] Institute of Pharmaceutical Sciences, ETH Zurich, CH-8093 Zurich,

[3] Department of Chemistry and Biochemistry, University of Wisconsin-Milwaukee, 53201, USA

L.T performed the electrophysiological experiments and DAB stainings
W.T.R conducted the behavioral experiments
H.C.J performed the AAV1-ChR2-mCherry virus injections
M.A.A performed the in-vitro electrophysiological experiments in recombinant receptors
M.P and J.C.C synthesized the HZ-166 compound
L.T analyzed and interpreted the experiments with the help of H.C.J and H.U.Z

I Abstract

Diminished synaptic inhibition in the superficial dorsal horn (sdh) is believed to underlie several chronic pain syndromes. Here, we describe electrophysiological and behavioral changes in a genetic mouse model of diminished synaptic inhibition in the spinal cord, i.e. in mice that lack a major $GABA_A$ receptor ($GABA_AR$) α subunit (α2) from the spinal cord and the spinal terminals of peripheral sensory neurons (hoxb8-gabra2$^{-/-}$ or, short, hoxb8α2$^{-/-}$ mice). We first characterized changes in GABAergic inhibition in the sdh where α2-$GABA_A$Rs are abundantly expressed. These experiments were done on a vGAT::ChR2 transgenic background which allowed optogenetic activation of inhibitory neurons in spinal cord slices. In hoxb8α2$^{-/-}$ mice, light-evoked GABA-IPSC amplitudes were reduced by about 50% compared to α2$^{fl/fl}$ mice with no significant change in their decay kinetics. Despite the reduction in GABAergic synaptic inhibition, hoxb8α2$^{-/-}$ mice did not show behavioral sensitization to acute painful stimulation, suggesting the presence of a compensatory plasticity mechanism. No significant changes were found in the amplitudes of glycinergic IPSCs or of membrane currents evoked by extracellular application of GABA. No significant differences were found for the decay kinetics of GABA-IPSCs. We also did not find significant changes in the amplitudes of sensory afferent evoked excitatory postsynaptic currents (EPSCs). By contrast, we found increased bicuculline-sensitive ($GABA_AR$ mediated) tonic membrane currents in hoxb8α2$^{-/-}$ mice. Furthermore, in immunohistochemical experiments, significant increases in serotonin immunoreactivity and in the expression of the serotonin producing enzyme tryptophan hydroxylase (TPH2) were found. Both the increases in tonic GABAergic currents and in serotonergic input to the spinal cord may on a behavioral level compensate for the loss of synaptic GABAergic inhibition and may explain why hoxb8α2$^{-/-}$ mice lack a pronociceptive phenotype. We also used the hoxb8α2$^{-/-}$ mice to investigate the role of α2-$GABA_A$Rs in the analgesic effects of HZ-166, a less sedating benzodiazepine-site agonist with reduced activity at α1-$GABA_A$Rs. In hoxb8α2$^{-/-}$ mice, HZ-166 had almost completely lost its analgesic action, and, in line with this observation, its effects on the kinetics of GABA-IPSCs were significantly reduced. These results confirm the important role of α2-$GABA_A$Rs in spinal nociceptive control. Diminished α2-$GABA_AR$ mediated inhibition may

be compensated by increases in tonic GABAergic inhibition or in the serotonergic input to the spinal cord.

II Introduction

The spinal cord serves as first relay center for incoming sensory and nociceptive signals from the periphery. Nociceptive afferents preferentially terminate in the sdh laminae I and II (LI, LII, respectively) where nociceptive signals undergo extensive processing and modulation by a network of local interneurons and by input from descending excitatory and inhibitory fiber tracks (Snider and McMahon, 1998; Basbaum et al., 2009). It is widely accepted that weakening of synaptic inhibition in the sdh laminae (LI-LII) contributes to chronic pain symptoms, including hyperalgesia and allodynia (De Koninck, 2007; Sandkuhler, 2009; Kuner, 2010; Zeilhofer et al., 2012a). Fast inhibitory neurotransmission in the spinal dorsal horn is mediated by GABA and/or glycine. In the sdh, particularly in LII, most inhibitory neurons are purely GABAergic (Todd and Spike, 1993; Zeilhofer et al., 2012b) whereas most inhibitory neurons of the deep dorsal horn release GABA and glycine. $GABA_A$Rs are heteropentamers, and in the central nervous system (CNS) the most prevalent subunit composition is 2α (α1-5), 2β (β1-3) and 1γ (γ1-3) (Olsen and Sieghart, 2008). In the spinal termination area of nociceptors, $GABA_A$Rs containing the α2 subunit (α2-$GABA_A$Rs) are the most abundant subtype (Bohlhalter et al., 1996). These receptors are expressed presynaptically on the terminals of sensory fibers and postsynaptically on central neurons of the dorsal horn (Persohn et al., 1991; Bohlhalter et al., 1996). A growing body of evidence suggests that α2-$GABA_A$Rs are important contributors to spinal benzodiazepine-mediated antihyperalgesia (Knabl et al., 2008; Knabl et al., 2009; Paul et al., 2014; Ralvenius et al., 2015). In a previous study, our group has shown that hoxb8α2$^{-/-}$ mice, which lack spinal α2-$GABA_A$Rs present no behavioral sensitization in acute pain tests (Paul et al., 2014) suggesting the presence of efficient compensatory mechanisms. In the present study we identified increased tonic GABAergic membrane currents and increased serotonergic innervation of the spinal cord as possible compensatory mechanisms.

III Aim of this chapter

A previous study in our group showed that mice lacking spinal α2-$GABA_AR$ showed no enhanced pain sensitization following acute pain tests when compared to control animals.

In this chapter, I present an electrophysiological characterization of synaptic and extrasynaptic receptors in the $\alpha2^{fl/fl}$hoxb8cre;vGAT::ChR2 mice (referred to as $\alpha2^{fl/fl}$ for control animals and hoxb8$\alpha2^{-/-}$ for conditional knock-out) to reveal potential compensatory mechanisms that may emerge in order to balance the diminished synaptic inhibition in the hoxb8$\alpha2^{-/-}$ mice. In parallel, I addressed the role of α2-$GABA_AR$ in the antihyperalgesic or analgesic effects of HZ-166, a less sedating BDZ with reduced activity on α1-$GABA_ARs$.

IV Material and methods

Animals

Animal procedures were approved by the Cantonal Veterinary Office (licenses 126/2012, 74/2013, 86/2013, 031/2016). Two strains of $GABA_AR$ mutated mice (3-4 weeks old) of either sex were used for the different electrophysiology experiments. $\alpha2^{fl/fl}$;hoxb8cre^{-};vGAT::ChR2-YFP ($\alpha2^{fl/fl}$) and $\alpha2^{fl/fl;}$hoxb8cre^{+};vGAT::ChR2 (hoxb8$\alpha2^{-/-}$) double transgenic mice were obtained by crossing $\alpha2^{fl/fl}$ transgenic mice (Witschi et al., 2011) with double transgenic hoxb8cre^{+};vGAT::ChR2 BAC transgenic mice (Witschi et al., 2010; Zhao et al., 2011). Global α2 knock-out ($\alpha2^{-/-}$) mice were used for control stainings.

Drugs and chemicals

D(-)-2-amino-5-phosphopentanoic acid (APV) was used during spinal cord slicing at a concentration of 50 µM. In electrophysiological experiments GABA, HZ-166 and strychnine hydrochloride were dissolved in extracellular solution to a final concentration of 50 µM, 10 µM and 0.5 µM respectively. (-)-Bicuculline methochloride was used at a concentration of 20 µM. In some cases, 20 µl of 20 mM stock solution NBQX (200 µM) was directly added into the bath at the end of the recording and served as a control to ensure the recorded current was excitatory. For behavioral testing, HZ-166 was suspended in 0.5% methyl cellulose and injected with 16mg kg^{-1} body weight (Paul et al., 2014). All chemicals were purchased from Tocris (Germany).

Electrophysiology and optogenetic stimulation

Light-induced inhibitory post-synaptic currents (IPSCs), exogenous GABA-evoked membrane currents and light-evoked excitatory post-synaptic currents (EPSCs) were recorded using a double patch-clamp EPC 9 amplifier controlled with Patchmaster acquisition software (both HEKA Elektronik Dr. Schulze GmbH, Germany). Activation of the neurons by blue light was applied either directly to the cell soma by the UGA-40 GEO laser system (473 nm, 1 s, spot size 10 µm, 715.9 mW/mm^2, RAPP OptoElectronic, GmbH) to check for the presence of a photocurrent in the recorded cell, or in wide-field mode with a monochromator Polychrome

V (473 nm, 4 ms, Field of illuminations ± 200-300 µm, 2.7 mW, Tillvision, Thermo Fisher Scientific, USA) to evoke IPSCs.

Spinal cord slice preparation and electrophysiological recordings

Transverse 400 µm thick slices of the lumbar spinal cord slices were prepared from 20-30 days old mice of either sex. Slices were cut in ice-cold solution with the following composition in mM (Dugue et al., 2009): 130 K-gluconate, 15 KCl, 0.05 EGTA, 20 HEPES and 25 glucose titrated to pH 7.4 with KOH and supplemented with 50 µM D-APV to prevent glutamate excitotoxicity. Slices were then kept 30 minutes for recovery in a solution containing (in mM) 225 D-Mannitol, 2.5 KCl, 1.25 NaH_2PO_4, 25 $NaHCO_3$, 0.8 $CaCl_2$ and 8 MgCl2 and 25 glucose (37°C, bubbled with 95% O_2, 5% CO_2). In a final step, slices were transferred to an artificial cerebrospinal fluid (aCSF), also known as extracellular solution with the following composition (in mM): 120 NaCl, 2.5 KCl, 1.25 NaH_2PO4, 26 $NaHCO_3$, 5 HEPES, 1 $MgCl_2$, 2 $CaCl_2$ and 14.6 glucose. Slices were transferred to a recording chamber and continuously perfused with aCSF equilibrated with 95% O_2, 5% CO_2 at a flow rate of 1ml min^{-1}. Neurons in the superficial dorsal horn (sdh, LI, II <150 µm from the dorsal margin) were visually identified with an iXON Ultra camera (Andor Technology, Belfast, UK) and using the infrared gradient contrast equipment of the microscope (Zeiss Examiner. A1, Göttingen, Germany). Whole-cell voltage-clamp recordings were performed at room temperature at a holding potential of -60 mV from presumed excitatory neurons. For the recording of inhibitory postsynaptic currents (IPSCs), patch pipettes were prepared from borosilicate glass capillaries and had an open tip resistance of 3-5 MΩ. Recording pipettes were filled with an internal solution containing (in mM): 120 CsCl, 2 $MgCl_2$ + 6 H_20, 10 HEPES, 0.05 EGTA, 2 MgATP, 0.1 NaGTP. CsCl was used to block $GABA_B$ receptor-mediated K^+ currents and Qx-314 (5mM) to block voltage-activated Na^+ channels in the recorded cell. Excitatory postsynaptic currents (EPSCs) were recorded using a K-gluconate based internal solution containing (in mM): 130 K-gluconate, 20 KCl, 0.05 EGTA, 2 $MgCl_2$+6H_20, 2 MgATP, 0.1 NaGTP, 10 Na Hepes, 5 Qx-14.

Access resistance of the cell was continuously monitored by giving short hyperpolarizing steps (-5 mV) between the synaptic light-stimulations or before and after application of the drug in the case of tonic currents. Recordings were discarded if the access resistance changed > 20% or if recovery to baseline currents before GABA application was less than 85-

90% in the case of tonic currents. All recordings were performed on excitatory neurons (excepted where stated) of the sdh (LI/II). To discriminate between excitatory and inhibitory neurons, we applied a one second blue light pulse on the soma of the recorded neuron using laser light-stimulation. Cells showing no photocurrents (i.e. excitatory neurons) were kept for experiments. All electrical signals were sampled either at 20 KHz (light-induced GABAergic currents) or 5 KHz (tonic currents) and filtered at 2.9 kHz. Data was analyzed using IgorPro (WaveMetrics, Inc.,USA).

We elicited light-induced GABAergic currents at a frequency of 4 stimulations per minute using wide-field illumination of the dorsal spinal cord (473 nm, 4ms, 20.4 mW/mm^2). Steady-state GABAergic currents were achieved after 2-3 minutes of continuous strychnine application. After 5 minutes baseline recording, HZ-166 was co-applied for 7-15 minutes. Finally, bicuculline (antagonist of $GABA_A$Rs) was bath-applied in addition to strychnine (antagonist of glycine receptors) to inhibit the $GABA_A$R-mediated current and thus confirm the nature of the current.

Exogenous GABA-evoked membrane currents were also studied. In this approach, we recorded 1 minute baseline. GABA was then bath applied until a steady-state was reached, usually 1 minute after application. Subsequently, HZ-166 was co-applied with GABA until we reached a second steady-state. Finally, bicuculline was added to inhibit the remaining $GABA_A$R-mediated current and thus confirm the recording of a GABAergic current.

Excitatory postsynaptic currents (EPSCs) were recorded from undefined neurons chosen from a region of the sdh with strong mCherry expression (i.e. region where AAV1:ChR2:mCherry infected primary afferent fibers showed strong mcherry fluorescence). We stimulated the terminals using a 4 ms light pulse of blue light every ten seconds and recorded light-evoked EPSCs. In a final step, we injected NBQX (20mM) into the bath to eliminate the excitatory current.

Virus injection

AAV1-ChR2:mCherry virus (approximately 2 µl each side) was bilaterally injected in the sciatic nerve of 15-28 days old $\alpha2^{fl/fl}$ and hoxb8$\alpha2^{-/-}$ mice. One week post-injection, mice were decapitated and acute spinal cord slices were prepared for whole-cell recordings following

the same procedure as described previously with none injected mice (see S*pinal cord slice preparation and electrophysiological recordings).* Infected cells of the dorsal root ganglions (DRGs) at lumbar segment L4 were observed under the two-photon microscope and the soma diameter of the cells (72 cells from 3 animals) was determined after acquiring a z-stack image using the 2-axis average diameter method (Scroggs and Fox, 1992).

Behavioral testing

All behavioral experiments were performed in 8-10-week-old female and male mice. Experiments were conducted by an experimenter blinded either to the genotype of the mice and to their treatment with drug or vehicle.

Formalin (4%, 20 µl) was injected subcutaneously into the dorsal surface of the left hind paw. Licking bouts of the injected paw were counted for 60 minutes in 5 minutes intervals starting immediately after formalin injection (Hösl et al., 2006). HZ-166 (16 mg kg^{-1} body weight) was given intraperitoneally (i.p) 1 hour before formalin (4%, 20 µl) into the hind paw and licking bouts of the injected paw were measured in the same way as previously described.

Mechanical withdrawal thresholds and thermal withdrawal latencies were assessed using an electronic von Frey anesthesiometer and Hargreaves test apparatus with a temperature controlled glass platform (30°C) (both from IITC, Woodland Hills, CA). Responses to noxious cold were determined following the protocol by (Brenner et al., 2012) using a 5 mm thick borosilicate glass platform and applying dry ice below the paw of the animal with a 5 ml syringe. Pin prick technique was performed using a blunt syringe that does not perforate the skin, as described in Foster et al. (2015). Six measurements were made for each time point per animal for both mechanical and heat tests.

Immunohistochemistry

Adult $\alpha2^{fl/fl}$ and hoxb8$\alpha2^{-/-}$ mice were injected i.p with 0.25 ml pentobarbital and perfused through the ascending aorta with 50 ml ice-cold ACSF at RT for 2 minutes (Paul et al., 2012). Spinal cord and brain were then removed and fixed in cold 4% PFA for 90 minutes before being transferred to 30% sucrose in phosphate buffer saline (PBS) at 4°C overnight for cryoprotection (Notter et al., 2014). Tissue was cut coronally at 20 µm from frozen blocks

into cryosections and mounted onto Superfrost Plus microscope slides (Thermo Scientific, Zurich, Switzerland). Immunohistochemistry was performed on tissue

The distribution of the $GABA_AR$ α2 subunit, vesicular glutamate transporter 1-3 (VgluT 1-3), serotonin (5-HT) and tryptophan hydroxylase 2 (TPH2) was visualized on 20 µm-thick lumbar spinal cord cryosections by Diaminobenzidine tetrahydrochloride (DAB, Sigma, St. Louis, MO) staining. In brief, sections were incubated overnight at 4°C in primary antibodies diluted in Tris triton (pH 7.4) containing 4% NGS and 0.2% Triton X-100. The dilutions of antibodies were: α2 subunit, 1:1000 (in house; Paul et al., 2012); VgluT1, 1:12'000 (Synaptic systems); VgluT2 (Synaptic systems), 1:5000; VgluT3 1:3000 (Chemicon); 5HT, 1:500 (Immunostar, France); TPH2, 1:500 (Novus Biologicals). Sections were washed three times with PBS and stained with avidin-biotin complex (ABC) immunoperoxidase method according to specifications of the manufacturer. DAB hydrochloride, diluted 0.05% in Tris saline (pH 7.7) with 0.01% hydrogen peroxide was used as a chromogen. The staining reaction was carried out for 3-5 minutes at room temperature and stopped by transferring the sections to ice-cold buffer. Sections were air-dried, dehydrated with an ascending series of ethanol and xylene and coverslipped with Eukitt (Erne Chemie, Dallikon, Switzerland) (Paul et al., 2012).

Image J was used for quantifying the intensity of the staining. For this ROIs were drawn in the superficial and deep spinal dorsal horn and the intensity mean value was measured. Background mean intensity value was subtracted from the mean intensity values of our ROIs.

Data analysis

For statistical analyses, amplitude and kinetic averages of light-induced IPSCs were calculated from 10 consecutive current traces (2.5 minutes) in control, strychnine, and strychnine with HZ-166 conditions (5.5 minutes after drug application). A weighted tau with a double exponential fit was used to measure the decay kinetics of the light-evoked currents (Labrakakis et al., 2014).

For tonic current measurement, an all-points histogram was plotted for a 30 seconds period immediately preceding drug application (i.e., baseline condition) and finishing drug application (drug was applied for 5-7 minutes), respectively. A Gaussian was fitted to the side of the distribution not skewed by synaptic events, and the peak was used to determine the

mean baseline holding current required to maintain the voltage of the cell at -60 mV. Tonic currents in the presence of bicuculline were determined by repeating the fitting procedure after drug application and measuring the difference in mean baseline holding currents before and after application of bicuculline. Statistical significance between the two genotypes was analyzed using an unpaired Student's t test.

To measure the change in amplitude induced by evoked-GABA, we subtracted a 30 seconds period of GABA-evoked current amplitude from 30 seconds period of baseline current recorded before GABA application. We proceeded similarly with HZ-166-induced potentiation of GABA currents, and subtracted the HZ-166-induced current amplitude to baseline.

V Results

Deletion of α2-GABA$_A$Rs in the spinal cord

We used the hoxb8cre::α2$^{-/-}$ mice (Paul et al., 2014), in which the α2-GABA$_A$R subtype was ablated from dorsal root ganglia (DRGs) and the spinal cord up to cervical segment C4, henceforth known as the hoxb8α2$^{-/-}$ mice. In order to confirm the absence of α2-GABA$_A$R subtypes from the spinal cord in these mice, we performed immunocytochemistry staining on tissue from α2$^{fl/fl}$ and hoxb8α2$^{-/-}$ mice against the α2 subunit and quantified the intensity of the staining by measuring the mean grey values in the superficial and deep dorsal horn (Figure 1A). The staining intensity of the α2 subunit in hoxb8α2$^{-/-}$ mice was significantly reduced as compared to α2$^{fl/fl}$, and was virtually identical to that of global α2 knock-out (α2$^{-/-}$) mice indicating that no α2 subunit expression remained on a spinal level in these mice (Figure 1B).

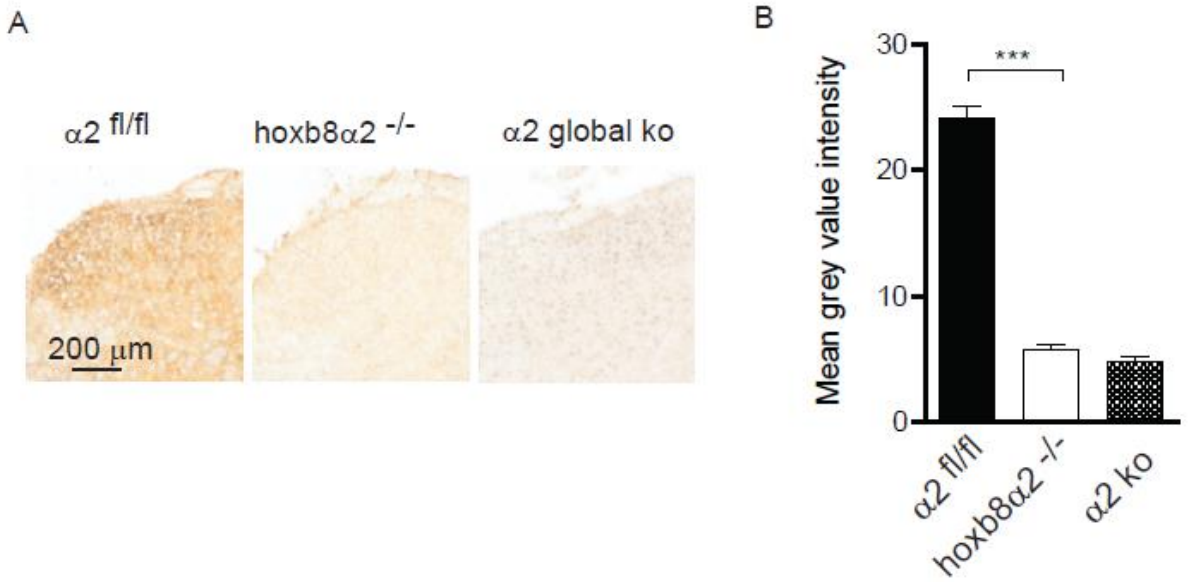

Figure 1. Absence of α2-GABA$_A$R in the spinal cord of hoxb8α2$^{-/-}$ mice. A, Spinal dorsal horn tissue immunocytochemistry against the α2 subunit in α2$^{fl/fl}$ (*left*), hoxb8α2$^{-/-}$ (*middle*) and global α2$^{-/-}$ mice (*right*). B, Quantification of immunoperoxidase intensities in a staining against α2 shows 76% intensity reduction in the hoxb8α2$^{-/-}$ mice compared to α2$^{fl/fl}$ (mean 24.17±0.92 for α2$^{fl/fl}$; mean 5.7±0.5 for hoxb8α2$^{-/-}$, and 4.7±0.5 for α2$^{-/-}$, unpaired Student's t-test *** p<0.0001, N=2 mice, n=8 slices/mouse).

Hoxb8α2$^{-/-}$ mice exhibit normal nociceptive response thresholds

The α2-GABA$_A$R subtypes are highly expressed in the spinal cord dorsal horn (Paul et al., 2012). We sought to assess whether the ablation of this subtype from the spinal cord would

influence nociceptive responses in naïve mice. To this end, we employed the von Frey test of mechanical stimulation, Hargreaves' plantar test for heat sensitivity, pin prick test of noxious mechanical stimulation and cold allodynia tests, and analyzed the response thresholds in the $\alpha2^{fl/fl}$, hoxb8$\alpha2^{-/-}$ and $\alpha2^{R/R}$ mice, which carry a point-mutation of histidine to arginine residues (H→R) on the α2-benzodiazepine binding site, rendering them insensitive to most BDZ (Figure 2A-D). The latter mice were included as they were used in a subsequent test to demonstrate the contribution of spinal α2-$GABA_AR$ to BDZ-mediated antihyperalgesia. In all four tests, the three genotypes did not show any differences in the pain readouts.

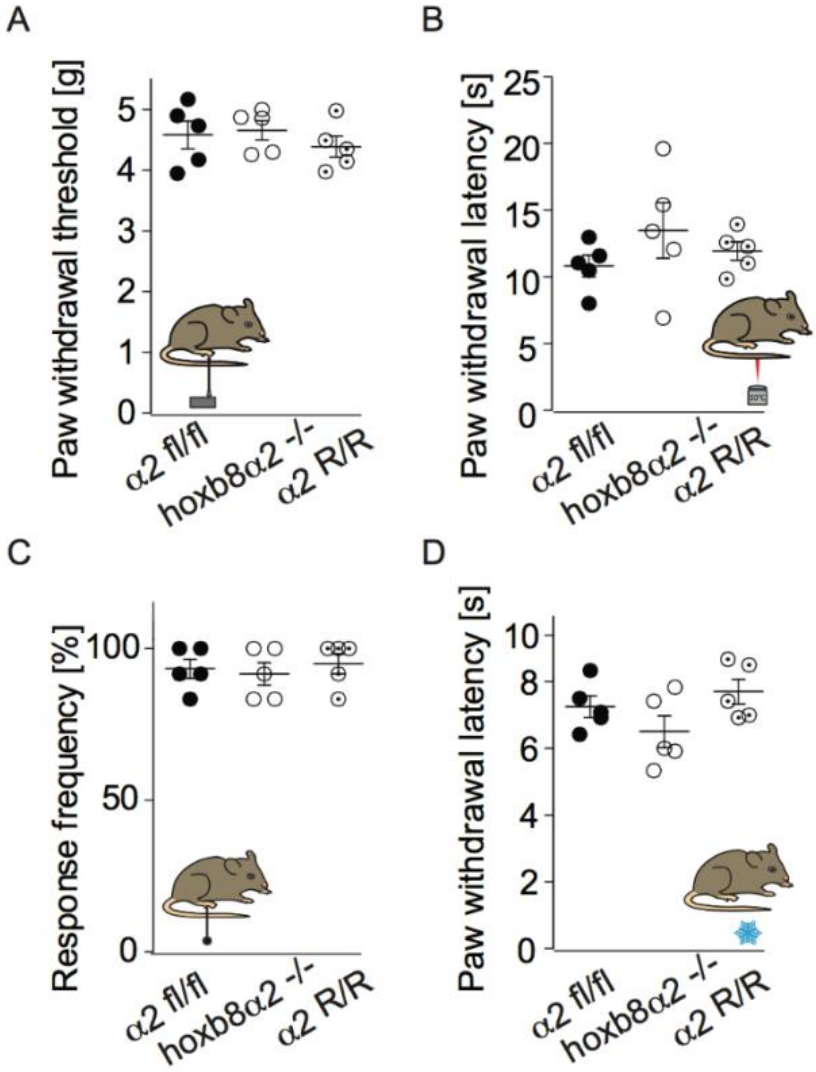

Figure 2. Lack of differences in acute nociception in hoxb8$\alpha2^{-/-}$ mice compared to control mice. Response thresholds of naïve $\alpha2^{fl/fl}$, hoxb8$\alpha2^{-/-}$ and $\alpha2^{R/R}$ mice. A, mechanical paw withdrawal thresholds for von Frey ($\alpha2^{fl/fl}$: 4.6±0.2 g; hoxb8$\alpha2^{-/-}$: 4.7±0.2 g; $\alpha2^{R/R}$: 4.4±0.2 g), thermal withdrawal latencies for Hargreaves' ($\alpha2^{fl/fl}$: 10.80±0.8 s; hoxb8$\alpha2^{-/-}$: 13.5±2.1 s; $\alpha2^{R/R}$: 11.9±0.7 s), paw response frequency for pin prick test ($\alpha2^{fl/fl}$: 93.3±3.1%; hoxb8 $\alpha2^{-/-}$: 91.7±3.7%; $\alpha2^{R/R}$: 95±3.3%), and cold allodynia testing ($\alpha2^{fl/fl}$: 7.4±0.3 s; hoxb8$\alpha2^{-/-}$:

6.5±0.5 s; $\alpha2^{R/R}$: 7.7±0.4 s). Each data point indicates individual mouse. Error bars indicate mean ± SEM, n=5 mice for all genotypes. $p > 0.05$, one-way ANOVA followed by Bonferroni *post hoc* test.

Characterization of light-evoked activity in dorsal horn inhibitory cells of vGAT::ChR2 mice

In order to assess the impact of spinal α2-$GABA_AR$ ablation on spinal inhibitory neurotransmission, we combined electrophysiological whole-cell patch-clamp recordings and optogenetics in spinal cord slices. To this end, we decided to cross the vGAT::ChR2-YFP allele (Zhao et al., 2011) into double transgenic $\alpha2^{fl/fl}$;hoxb8cre mice to allow activation of inhibitory neurons by exposure to blue light. Before doing experiments in hoxb8$\alpha2^{-/-}$;vGAT::ChR2 mice, we characterized photocurrents, light-induced action potential firing and light-induced synaptic transmission in the spinal cord slices of the vGAT::ChR2 transgenic mice. In this mouse line, channelrhodopsin 2 (ChR2) is fused to a fluorescent reporter (YFP) and expressed under the transcriptional control of the vesicular GABA transporter (vGAT) gene, which is expressed in all inhibitory neurons, including glycinergic neurons. YFP fluorescence in vGAT::ChR2 mice spinal cord slices was expressed across the entire spinal cord (Figure 3A, *bottom*). To record photocurrents, neurons in LII were held at a potential of -70 mV and the soma of the recorded neuron was exposed to blue light for 1 s or 4 ms (Figure 3A, *top*). About half of the recorded neurons responded to light stimulation with a photocurrent. One second blue light exposure induced a fast activating inward current that partially inactivated during prolonged light exposure and that rapidly returned to baseline upon off-set of light stimulation (Figure 3B, *top*). Shorter light exposure (4 ms) led to photocurrents of similar amplitude but of shorter duration (Figure 3C, *top*). The same light stimuli were then applied to the same neurons in current-clamp mode. One second light exposure led to tonic action potential firing, which is a characteristic of inhibitory neurons (Figure 3B, *bottom*), and to a single action potential in response to shorter (4 ms) light stimulation (Figure 3C, *bottom*). All light-evoked IPSC were completely blocked by a combination of strychnine and bicuculline (see Chapter 2, Part B).

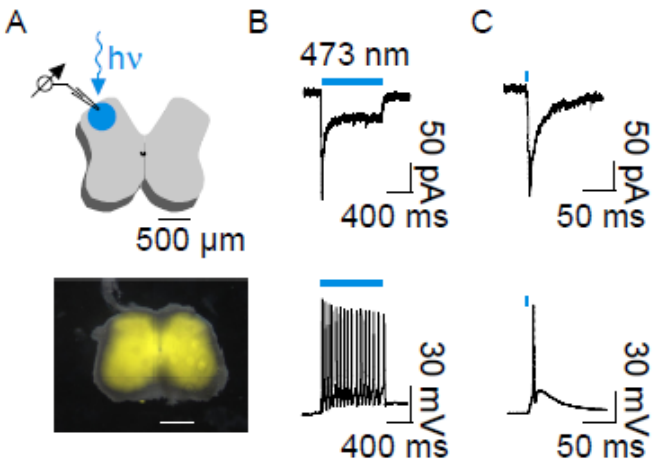

Figure 3. Optogenetic characterization of inhibitory dorsal horn neurons. A, *Top,* schematic depicting the light pulse (473, 4 ms) applied to the dorsal horn of acute spinal cord slices from vGAT::ChR2-YFP BAC transgenic mice. The recording pipette is represented on superficial dorsal horn. *Bottom,* Distribution of the ChR2-YFP fluorescence in a horizontal lumbar spinal cord slice of a vGAT::ChR2 mouse (scale bar 500 µm). B, *Top,* Partially desensitizing photocurrent recorded from a lamina II (LII) inhibitory interneuron evoked by a 1 s light exposure. *Bottom*, The same light exposure evoked a train of action potentials in current clamp mode. C, *Top,* Short photocurrent evoked by a 4 ms light stimulation. *Bottom*, Single action potential evoked by the same 4 ms light pulse, recorded in current clamp configuration.

Reduced synaptic currents but unchanged membrane currents evoked by exogenous application of GABA in the hoxb8α2$^{-/-}$ mice

We then continued with the analysis of hoxb8α2$^{-/-}$;vGAT::ChR2 transgenic mice and compared light evoked inhibitory neurotransmission in hoxb8α2$^{-/-}$;vGAT::ChR2 and α2$^{fl/fl}$;vGAT::ChR2 mice. To this end, we applied 4 ms light (blue bar, λ=473 nm, power density: 20.4 mW/mm^2) on acute spinal cord slices and first recorded light-evoked total IPSCs (i.e., mixed GABAergic and glycinergic currents). The amplitude values of the total IPSCs (mixed GABAergic and glycinergic) between α2$^{fl/fl}$ and hoxb8α2$^{-/-}$ mice were statistically not significant, however, there was a trend towards lower amplitudes in hoxb8α2$^{-/-}$ mice compared to α2$^{fl/fl}$ mice (α2$^{fl/fl}$: -1054 ± 200 pA, n=8 cells and hoxb8α2$^{-/-}$: -558 ± 154 pA n=10 cells, p=0.06, unpaired Student's t-test) (Figure 4A). We also analyzed possible changes in the amplitude of light-evoked glycinergic IPSCs in α2$^{fl/fl}$ and hoxb8α2$^{-/-}$ mice. To this end, we subtracted the amplitude values of light-evoked GABA-IPSCs (see Figure 4C) from the amplitudes of the total IPSCs. Differences in glycinergic IPSC amplitude between α2$^{fl/fl}$ and

hoxb8α2$^{-/-}$ were also not statistically significant (α2$^{fl/fl}$: -633±155 pA, n=8 cells and hoxb8α2$^{-/-}$: -374 ± 133 pA n=10 cells, p=0.22, unpaired Student's t-test) (Figure 4B). We recorded GABA-IPSCs from presumed excitatory photocurrent negative neurons in the presence of strychnine to block the glycinergic current component (Figure 4C). We found that light-evoked GABA-IPSCs were 50% smaller in amplitude in the hoxb8α2$^{-/-}$ mice (-151.7±30.4 pA, n=13 cells) compared to α2$^{fl/fl}$ mice (-353±65.2 pA, n=17 cells) (Figures 4C, D). Time constants of light-evoked IPSCs in hoxb8α2$^{-/-}$ mice were statistically not different compared to those from α2$^{fl/fl}$ mice (α2$^{fl/fl}$: 65.0±8.2 ms, n=17 cells; hoxb8α2$^{-/-}$: 83.4±9.0 ms, n=13 cells, p=0.14, unpaired Student's t-test, Figure 4E).

Although α2-GABA$_A$Rs are primarily located at synapses, the ablation of the α2 subunit might have an impact on the number of "reserve" receptor at extrasynaptic sites. To address this possibility, we recorded membrane currents evoked by extracellular (bath) application of GABA (50 µM) (Figure 4F). These currents reached similar amplitudes in hoxb8α2$^{-/-}$ mice and in α2$^{fl/fl}$ mice (-172.2±42.4 pA, n=7 cells, and -143.4±37.4 pA, n=7 cells, in hoxb8α2$^{-/-}$ and α2$^{fl/fl}$ mice, respectively) (Figure 4G).

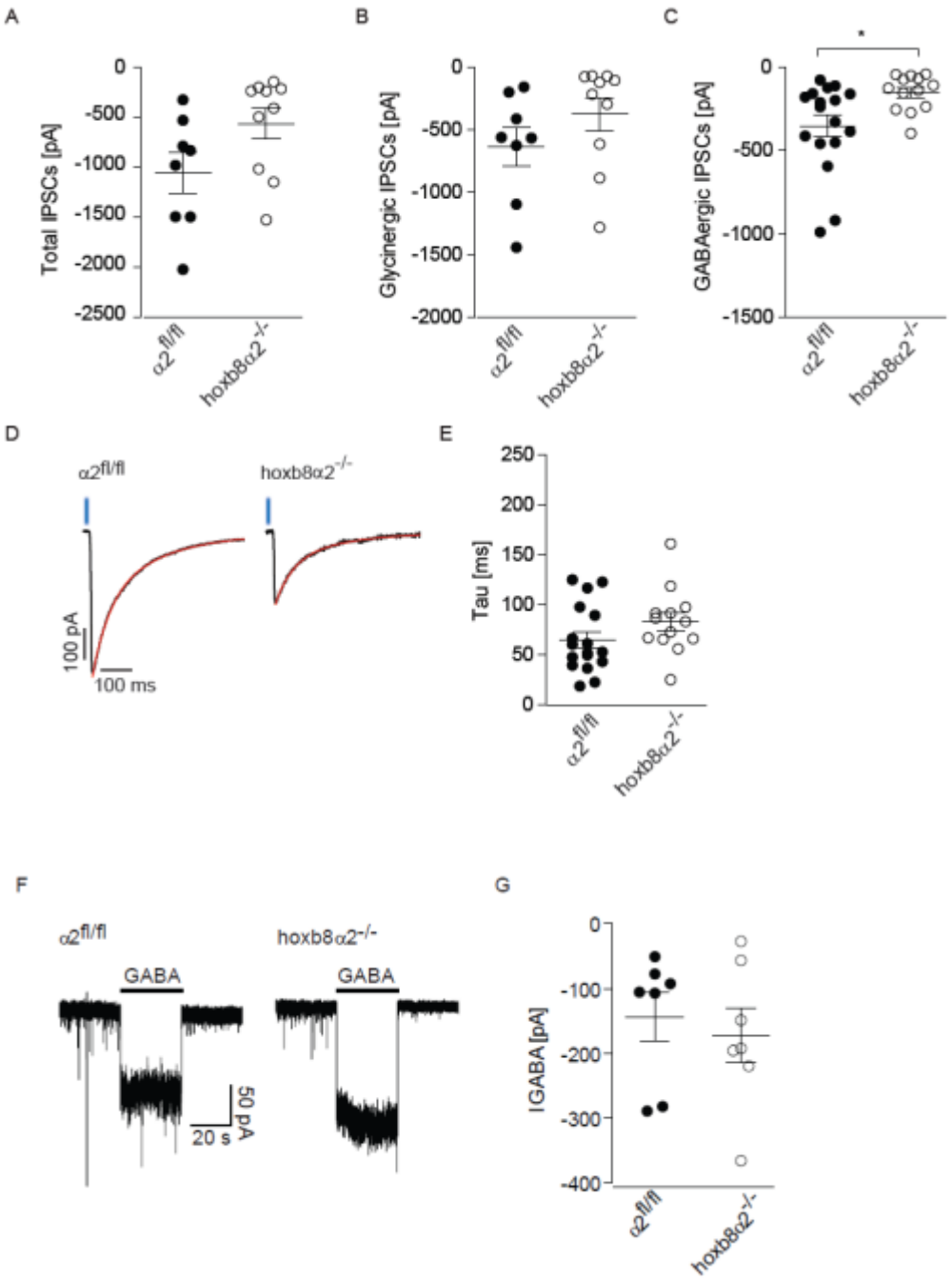

Figure 4. Reduced synaptic currents but unchanged membrane currents evoked by exogenous application of GABA in the hoxb8α2$^{-/-}$ mice. A, Graph showing no statistical significance in total light-evoked IPSC amplitudes between α2$^{fl/fl}$ and hoxb8α2$^{-/-}$ mice (α2$^{fl/fl}$: -1054±200 pA, n=8 cells from N=6 mice and hoxb8α2$^{-/-}$: -558±154 pA n=10 cells from N=9 mice, p=0.06, unpaired Student's t-test). B. Graph showing no statistical difference in glycinergic IPSC amplitude values between α2$^{fl/fl}$ and hoxb8α2$^{-/-}$ mice (α2$^{fl/fl}$: -633±155 pA, n=8 cells from N=6 mice and hoxb8α2$^{-/-}$: -374±133 pA, n=10 cells from N=9 mice, p=0.22, unpaired Student's t-test). C, Statistics showing a significant amplitude reduction of light-evoked GABA-IPSCs in hoxb8α2$^{-/-}$ mice compared to α2$^{fl/fl}$ mice (α2$^{fl/fl}$: -353±65.2, n=17 cells from N=14 mice, and hoxb8α2$^{-/-}$: -151.7±30.4 n=13 cells from N=12 mice, *p=0.02 unpaired Student's t-test). Error bars indicate mean±SEM. D, Example traces of light-evoked GABA-

IPSCs (4 ms light pulse) recorded in the presence of strychnine (0.5 µM), an antagonist of glycine receptors. Hoxb8α2$^{-/-}$ mice show reduced GABAergic IPSC amplitudes compared to α2$^{fl/fl}$. Decay kinetic (tau) values were obtained by using a double exponential fit, here shown in red. E, Scatter plot shows no significant change in baseline tau values between the two genotypes (α2$^{fl/fl}$: 65±8.2 ms; hoxb8α2$^{-/-}$: 83.4±9 ms, p=0.14, unpaired Student's t-test). F, Example traces of GABA-evoked membrane currents (50 µM GABA) in excitatory neurons of α2$^{fl/fl}$ and hoxb8α2$^{-/-}$ mice. G, No change in GABA-evoked membrane current amplitudes is observed between the two genotypes (α2$^{fl/fl}$: -143.4±37.4 pA and hoxb8α2$^{-/-}$: -172.2±42.4 pA, n=7 cells from N=5 mice, p=0.62, unpaired Student's t-test).

Extrasynaptic $GABA_A$Rs also underlie part of the tonic membrane currents present in a subpopulation of dorsal horn neurons (for review, see Farrant and Nusser, 2005). To test possible differences in such tonic membrane currents, we performed again whole-cell patch-clamp recordings again from presumed excitatory neurons and bath-applied bicuculline (20 µM) after 5 minutes of baseline current recording (Figure 5A *left panel*). Cells from hoxb8α2$^{-/-}$ mice had larger holding currents under baseline conditions compared to neurons from α2$^{fl/fl}$ mice (Figure 5B, *left* panel, α2$^{fl/fl}$: -27±2.0 pA, n=9 cells; hoxb8α2$^{-/-}$: -41.2±6.0 pA, n=7 cells). In addition, we found that the bicuculline sensitive component of these tonic currents was larger in hoxb8α2$^{-/-}$ mice than in α2$^{fl/fl}$ mice (Figure 5B, *right panel*, α2$^{fl/fl}$: -0.3±1.1 pA; hoxb8α2$^{-/-}$: -10.0±3.9 pA).

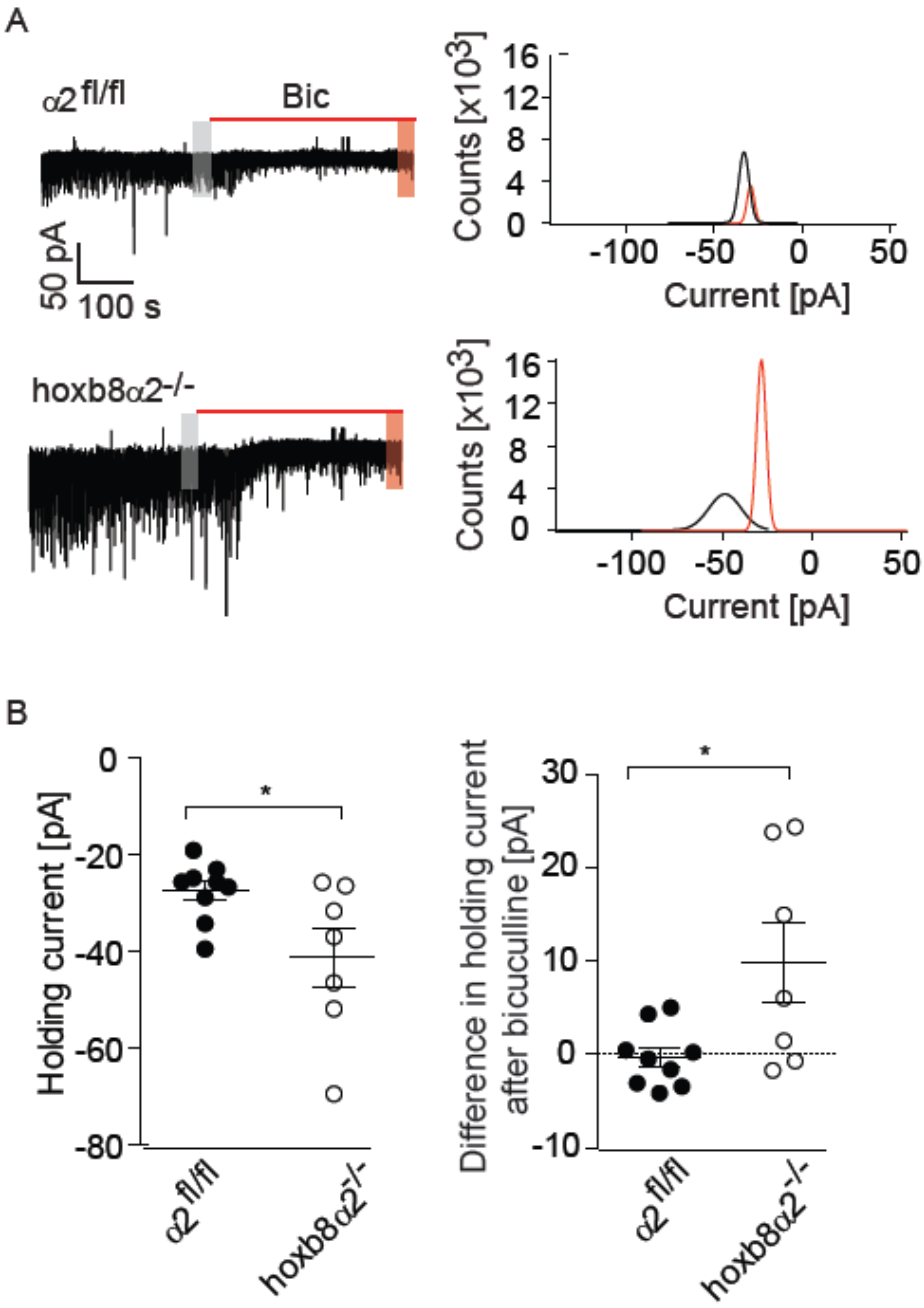

Figure 5. Increased tonic inhibition in hoxb8α2$^{-/-}$ compared to control animals. A, Example traces of tonic currents in α2$^{fl/fl}$ and hoxb8α2$^{-/-}$ mice before and after application of bicuculline (20 µM). Grey and red bars indicate the areas that were analyzed for the all-point histograms of control and bicuculline conditions, respectively. The all-point histograms follow a Gaussian distribution and depict the amplitude scattering in a 30s range analyzed from the current recorded in control and bicuculline conditions, respectively. After application of bicuculline, the amplitude range shifts to higher values and the noise (represented by the width of the curve) becomes smaller in hoxb8α2$^{-/-}$ compared to α2$^{fl/fl}$. B *Left,* Plot showing significantly higher holding currents in baseline conditions (before application of bicuculline) in hoxb8α2$^{-/-}$ mice (-41.2±6.0 pA, n=7 cells) compared to α2$^{fl/fl}$ mice (-27±2.0 pA, n=9 cells), *p=0.03, unpaired Student's t-test. *Right*, After application of bicuculline, hoxb8α2$^{-/-}$ mice show a larger shift in holding current amplitudes compared to α2$^{fl/fl}$ mice (α2$^{fl/fl}$: 0.3±1.1 pA, n=9

cells from N=7 mice and hoxb8α2$^{-/-}$: -10.0±3.9 pA, n=7 cells from N=4 mice, *p=0.02, unpaired Student's t-test. Error bars indicate mean±SEM. α2$^{fl/fl}$: hoxb8α2$^{-/-}$:

Hoxb8α2$^{-/-}$ mice show unaltered excitatory input from nociceptors compared to α2$^{fl/fl}$ mice

Since transmitter release from nociceptive fibers is under control of presynaptic $GABA_A$Rs that contain α2 subunits (Witschi et al., 2011), we investigated possible changes in the excitatory neurotransmission between primary afferent C-fibers and dorsal horn second order neurons. To allow selective activation of input from nociceptive primary sensory fibers we employed again optogenetics. Bilateral injections of CAG-AAV1 ChR2-mCherry virus were made into the sciatic nerve of naïve α2$^{fl/fl}$ and hoxb8α2$^{-/-}$ mice. These injections led to the infection of dorsal root ganglion cells of the lumbar segment L4 (Figure 6A). Analysis of the soma diameter of the infected DRG neurons indicated that the great majority of infected cells had a soma diameter of approximately 20 µm (Figure 6B, n=72 cells from N=3 mice) suggestive of nociceptive neurons. Seven days after virus injection, we prepared transverse spinal cord slices of the L4 segment for electrophysiological recordings from unidentified LII cells. After establishing whole-cell recordings we stimulated the dorsal horn with blue light (λ =473 nm, light exposure: 4ms, power density: 20.4 mW/mm^2) recorded light-evoked EPSCs (Figure 6C, *middle panel*). No statistically significant difference was observed between genotypes with regards to amplitude (α2$^{fl/fl}$: -108.2±34.7 pA; hoxb8α2$^{-/-}$: -117.8±41.3 pA, p=0.85 unpaired Student's t-test) and decay kinetics (α2$^{fl/fl}$: 7.6±1.6 ms; hoxb8α2$^{-/-}$: 8.5±0.9 ms, p=0.68 unpaired Student's t-test) or success rate (α2$^{fl/fl}$: 94.2±3.4%, hoxb8α2$^{-/-}$: 99±1.00%, p=0.20 unpaired Student's t-test). N=10 and 11 cells for α2$^{fl/fl}$ and hoxb8α2$^{-/-}$ mice, respectively (Figure 6C, *bottom*). A trend was seen for enhanced synaptic transmission between primary nociceptive fibers and second order neurons, which would be in line with reduced GABAergic inhibition of transmitter release from spinal nociceptor terminals.

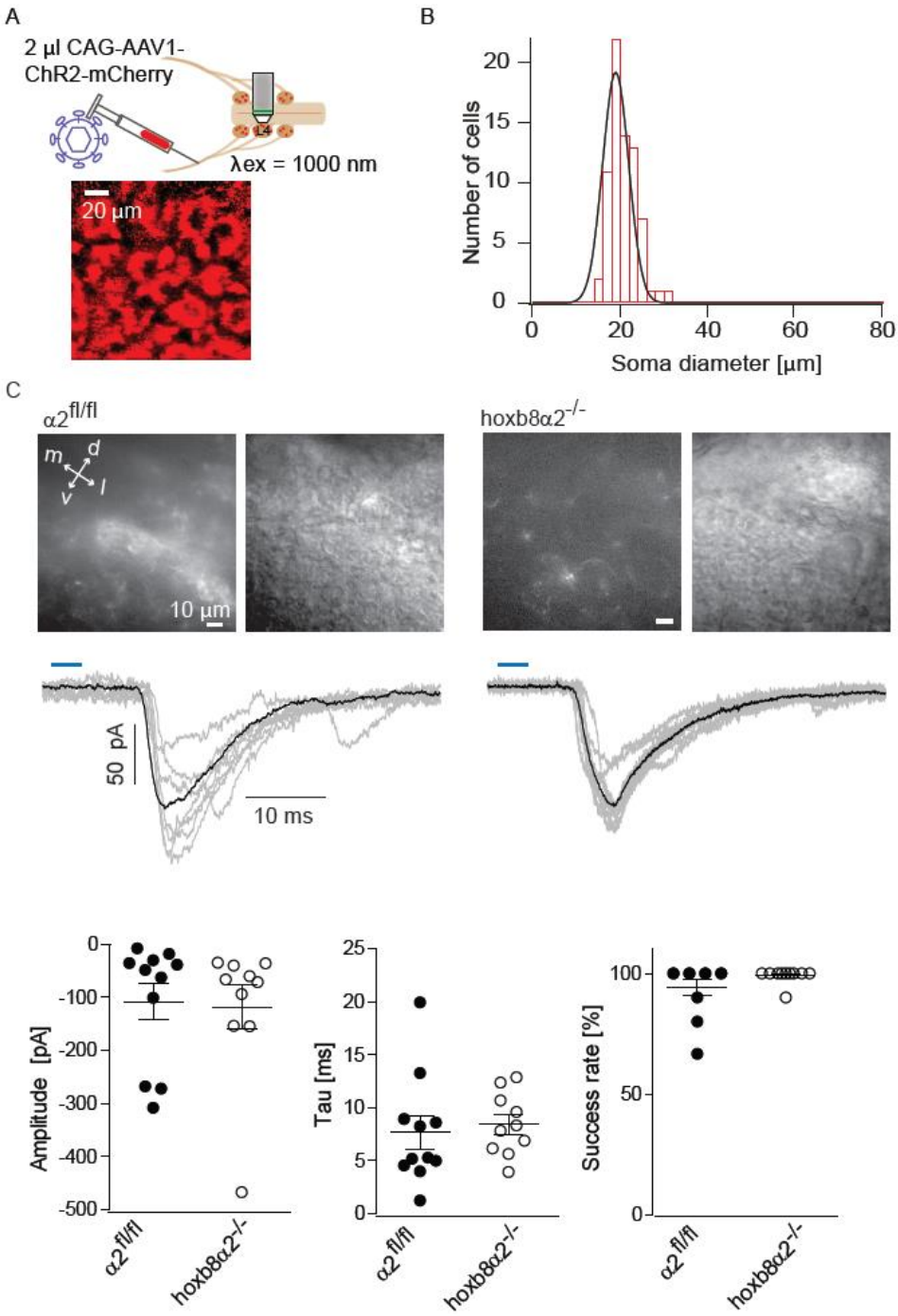

Figure 6. Excitatory input from primary nociceptive fibers onto dorsal horn second order neurons remains unaffected in the hoxb8α2$^{-/-}$ mice. A, Depiction of the CAG-AAV1 ChR2-mCherry injection into the sciatic nerve of α2$^{fl/fl}$ or hoxb8α2$^{-/-}$ mice. Z-projection two-photon image of virus-infected ganglion cells in DRGs of lumbar segment L4. B, Histogram showing the soma diameter ranges of the infected ganglion cells within the DRGs which could be fit by a Gaussian function. Average diameter: 20.9±0.4 µm; n=72 cells from N=3 animals. C, Fluorescence and IR images of LII (i.e. regions of interest) in acute spinal cord slices prepared from nerve-injected mice. The fluorescence image shows punctate mCherry expression on terminals of primary afferent fibers of the infected DRG cells. Example traces from the two genotypes showing the average (black) of 7 (α2$^{fl/fl}$)

and 10 (hoxb8α2$^{-/-}$) EPSCs (grey) after 4 ms blue light exposure of primary afferent terminals. D, Statistical comparisons of amplitude, success rate and tau show no differences between α2$^{fl/fl}$ and hoxb8α2$^{-/-}$ (α2$^{fl/fl}$: n=11 cells and hoxb8α2$^{-/-}$: n= 10 cells, p=0.9; 0.3, and 0.7 for amplitude, success rate and tau, respectively, unpaired Student's t-test). Error bars indicate mean±SEM.

Enhanced serotonergic input to the spinal dorsal horn of hoxb8α2$^{-/-}$ mice

Up to this point, the only finding that could potentially explain the absence of a nociceptive phenotype in hoxb8α2$^{-/-}$ mice is the increase in tonic GABAergic membrane currents. In order to extend our analyses to compensatory mechanisms in the glutamatergic system, we performed quantitative RT-PCR measurements to investigate possible differences in the expression of vesicular glutamate transporters in the DRGs of hoxb8α2$^{-/-}$ and α2$^{fl/fl}$ mice. In wild-type mice we found high expression of VgluT1 and VgluT2 mRNA. VgluT1 and VgluT2 are mainly expressed in non-nociceptive and nociceptive DRG neurons, respectively. Only very low levels of VgluT3 were detected. When we compared expression levels in hoxb8α2$^{-/-}$ and α2$^{fl/fl}$ mice, we detected a small but statistically significant decrease in mRNA copies of VgluT2 by 17% in the hoxb8α2$^{-/-}$ mice as compared to α2$^{fl/fl}$ mice (Figure 7A, *p=0.04, N=4 mice/genotype, mean±SEM). To assess possible related changes in protein expression, we did quantitative immunohistochemistry for the three VgluTs in spinal cord sections. We focused these analyses on the superficial and deep dorsal horn, the spinal termination area of primary nociceptors (Figures 7B, C). We found no differences in expression levels of VgluT2 but a small increase in VgluT3 expression, which is unlikely to be biologically relevant.

As a final step, we also quantified markers of serotonergic input and used antisera for serotonin and tryptophan hydroxylase 2 (TPH2) a marker enzyme for serotonergic terminals. In these experiments we found a highly significant increase immunoreactivity against both markers in hoxb8α2$^{-/-}$ mice compared to α2$^{fl/fl}$ (29%, 46%, and 28%, respectively) (Figure 7B, C*)*. Because serotonergic input exerts antinociceptive actions in the spinal cord, this up-regulation appears as a second possible compensatory mechanism possible explaining the absence of hyperalgesia in hoxb8a2$^{-/-}$mice.

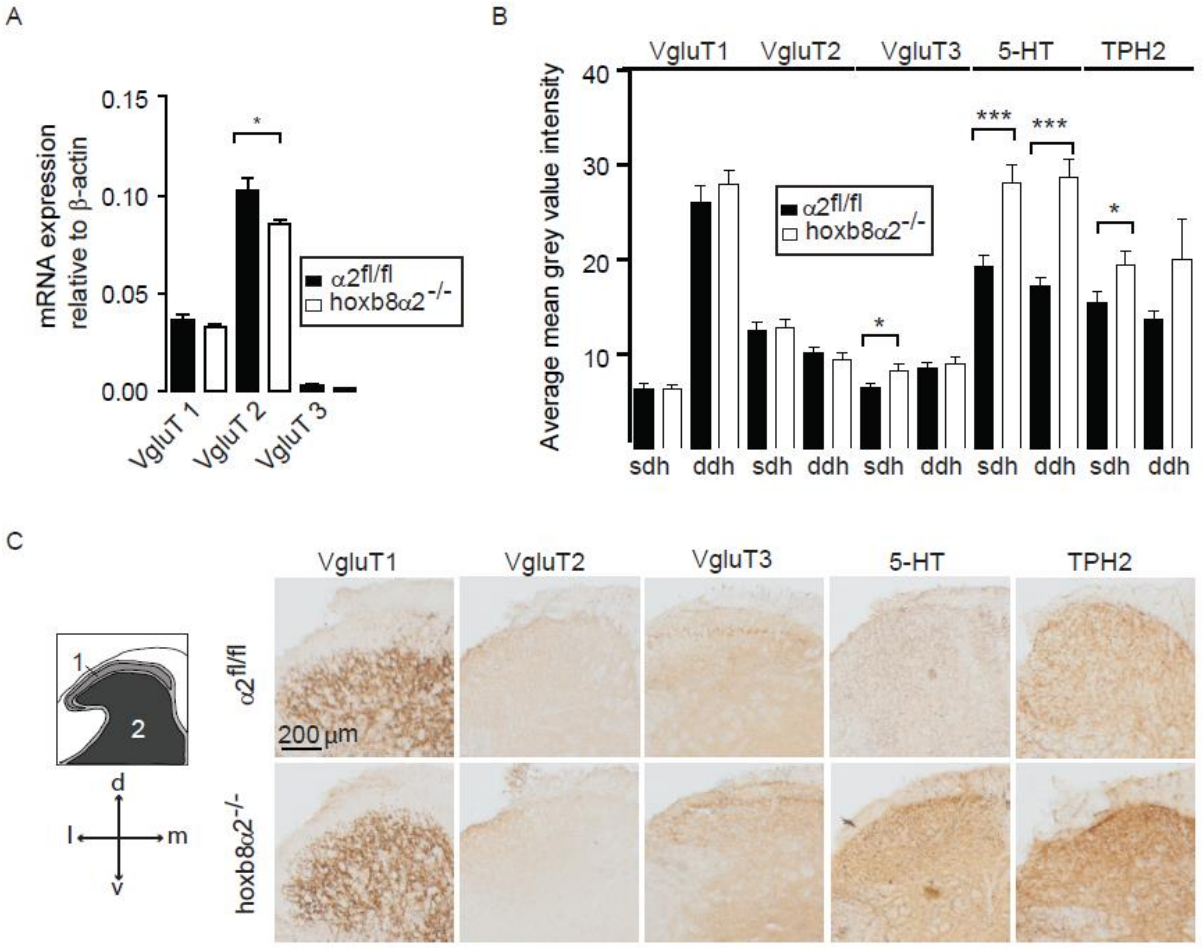

Figure 7. Reduced levels of VgluT2 mRNA in the dorsal root ganglia and enhanced levels of serotonin in the spinal cord of hoxb8α2$^{-/-}$ mice. A, mRNA copy numbers relative to β-actin of VgluT1-3 in the lumbar dorsal root ganglia of α2$^{fl/fl}$ and hoxb8α2$^{-/-}$ littermates. Significant reduction of VgluT2 mRNA in the DRGs of hoxb8α2$^{-/-}$ compared to α2$^{fl/fl}$ mice. VgluT1 (α2$^{fl/fl}$: 0.04±0.003; hoxb8α2$^{-/-}$: 0.03±0.002); VgluT2 (α2$^{fl/fl}$: 0.1±0.007; hoxb8α2$^{-/-}$: 0.08±0.002); VgluT3 (α2$^{fl/fl}$: 0.03±0.0005; hoxb8α2$^{-/-}$: 0.002±0.0002) from a total of N=4 mice/genotype, *p=0.04 unpaired Student's t-test. Error bars indicate mean±SEM. B. Quantification of immunoperoxidase intensities in stainings of VgluT1, VgluT2, VgluT3, 5-HT (N=4 mice) and TPH2 (N=2 mice) in α2$^{fl/fl}$ and hoxb8α2$^{-/-}$ mice from the superficial and deep dorsal horn (sdh, ddh). Histogram reveals significant increases in staining intensity against VgluT3 (sdh α2$^{fl/fl}$: 6.4±0.50; hoxb8α2$^{-/-}$: 8.3±0.62; *p=0.02), 5-HT (sdh α2$^{fl/fl}$: 19.2±1.2; hoxb8α2$^{-/-}$: 28.1±2.0 ***p<0.0001; ddh α2$^{fl/fl}$: 17.3±0.8; hoxb8α2$^{-/-}$: 28.6±2 ***p<0.0001), and TPH2 (sdh α2$^{fl/fl}$: 15.5±1.2; hoxb8α2$^{-/-}$: 19.5±1.4 *p=0.03) in hoxb8α2$^{-/-}$ mice compared to α2$^{fl/fl}$ mice. For the other comparisons p>0.05, unpaired Student's t-test. Error bars indicate mean±SEM. C, *(Left),* Schematic showing the spinal cord regions of interest that were considered for quantification of the immunoperoxidase intensity in stainings of VgluT1-3, 5-HT and TPH2 in Figure 7B (1, sdh; 2, ddh). *(Right),* Representative images showing one side of the superficial dorsal horn reveal increased levels of VgluT3, 5-HT and TPH2 in the dorsal horn of hoxb8α2$^{-/-}$ mice compared to α2$^{fl/fl}$ mice.

Potentiation of synaptic $GABA_AR$ currents and GABA-evoked membrane currents by HZ-166 is diminished in hoxb8$\alpha2^{-/-}$ mice

In a next set of experiments, we used the hoxb8$\alpha2^{-/-}$ mice to analyze their role in benzodiazepine mediated antihyperalgesia in more detail. For these experiments, we chose the less sedating benzodiazepine site agonist HZ-166 which has reduced agonistic activity at α1-$GABA_ARs$. Before doing in vivo experiments with HZ-166 we verified its in vitro pharmacological profile in HEK 293 cells transiently transfected with different combinations of $GABA_AR$ subunits (α1β2γ2, α2β3γ2, α3β3γ2 and α5β2γ2). In agreement with previous publications (Rivas et al.2009), both potency and efficacy of potentiation by HZ-166 were higher for α3-$GABA_ARs$ and α2-$GABA_ARs$ than for α1-$GABA_AR$ and α5-$GABA_AR$ subtypes (Figure 8).

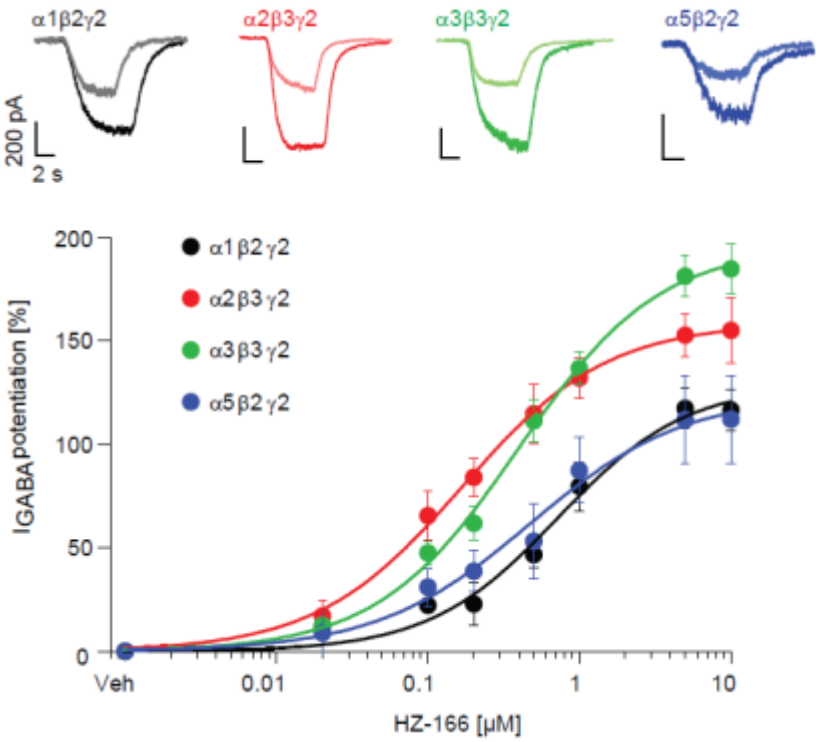

Figure 8. Potentiating effects of HZ-166 on four HZ-166-sensitive $GABA_AR$ subtypes. GABA-evoked membrane currents were measured in HEK 293 cells transiently transfected with recombinant α1β2γ2, α2β3γ2, α3β3γ2 and α5β2γ2 $GABA_ARs$. Top panels, traces show current responses evoked by GABA before (light trace) and during application of saturating concentrations of HZ-166 (10 μM, dark trace). Bottom graph representing dose-response curves of the four different $GABA_AR$ subtypes at increasing HZ-166 concentrations. GABA was applied at EC_{10} (1μM, 5μM, 8 μM, and 1μM for α1β2γ2, α2β3γ2, α3β3γ2 and α5β2γ2 $GABA_ARs$, respectively) for 6-10 s.

We then characterized the sensitivity of GABA-IPSCs to HZ-166 in slices taken from $\alpha2^{fl/fl}$ and hoxb8$\alpha2^{-/-}$ mice. We analyzed HZ-166 (10 µM) induced changes in the decay time constants (τ). After application of HZ-166, decay time constants of light-evoked GABAergic currents increased to 194.2±12% (n=17 cells) of control values in $\alpha2^{fl/fl}$ mice while in hoxb8$\alpha2^{-/-}$ mice they increased only to 157.1±12.3% (n=13 cells) (*p=0.04, unpaired Student's t-test) (Figure 9A). We also tested the sensitivity to HZ-166 of membrane currents evoked by exogenous GABA. We found that potentiation by HZ-166 was significantly reduced in hoxb8$\alpha2^{-/-}$ mice relative to $\alpha2^{fl/fl}$ mice ($\alpha2^{fl/fl}$: 88.2±16.2%, n=7 cells; hoxb8$\alpha2^{-/-}$: 45.7±8.3%, n=7 cells, *p=0.04, unpaired Student's t-test, Figure 9B).

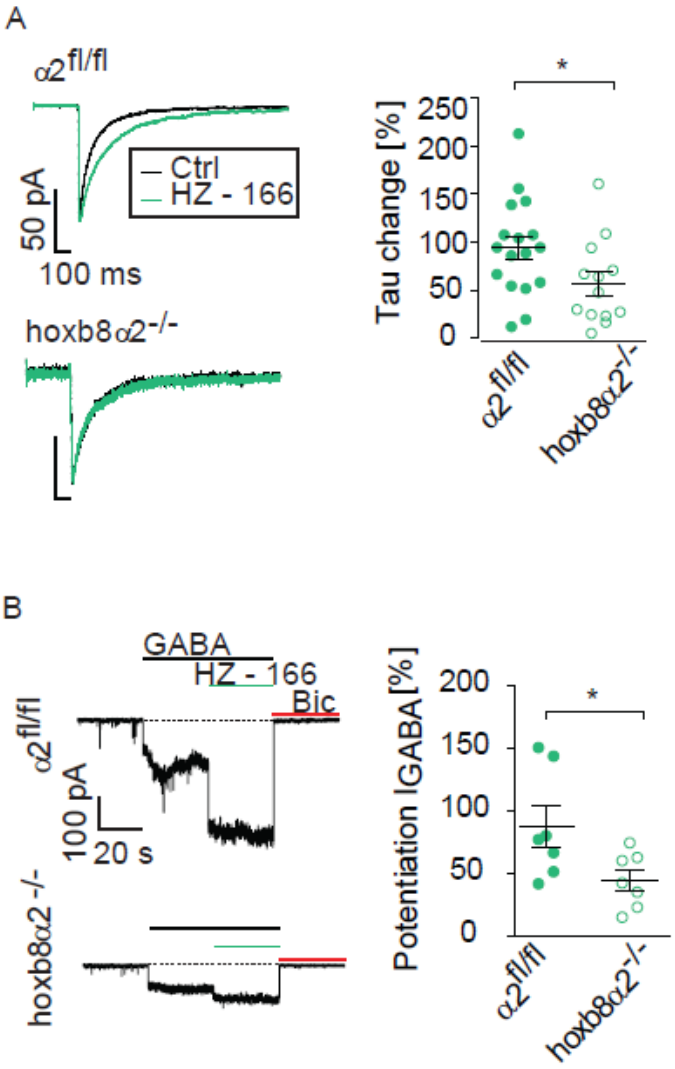

Figure 9. Diminished potentiation of GABAergic currents by HZ-166 in hoxb8$\alpha2^{-/-}$ mice. A, Example traces of light-evoked GABAergic currents recorded in the presence of strychnine in $\alpha2^{fl/fl}$ and hoxb8$\alpha2^{-/-}$ mice before (black) and after (green) application of 10 µM HZ-166. Potentiation of the GABAergic currents by HZ-166 is significantly reduced in hoxb8$\alpha2^{-/-}$ mice. Potentiation of GABAergic currents by HZ-166 in hoxb8$\alpha2^{-/-}$ mice is

significantly diminished relative to $\alpha2^{fl/fl}$ mice (n=17 and 13 for $\alpha2^{fl/fl}$ and hoxb8$\alpha2^{-/-}$ mice, respectively *p=0.04, unpaired Student's t-test). B, GABA-evoked membrane currents after application of HZ-166 in $\alpha2^{fl/fl}$ and hoxb8$\alpha2^{-/-}$ mice, respectively. In hoxb8$\alpha2^{-/-}$ mice, potentiation of GABA-evoked membrane currents by HZ-166 is significantly reduced compared to $\alpha2^{fl/fl}$ mice. All GABA-evoked currents are blocked by bicuculline (bic, 20 µM), the antagonist of $GABA_A$Rs (n=7 $\alpha2^{fl/fl}$ and hoxb8$\alpha2^{-/-}$, *p=0.04, unpaired Student's t-test).

We then performed again behavioral experiments to test whether the decreased sensitivity of GABA-IPSCs to HZ-166 translated into altered analgesic properties of HZ-166 in a rodent pain model. We used the formalin test, a model of inflammatory pain (Dubuisson and Dennis, 1977), in which 4% formalin is injected into one hind paw, and immediately afterwards nocifensive behavior (licking bouts directed to the injected paw) is quantified for 1 hour. We first checked if there were any differences in the number of formalin-evoked licking bouts between the genotypes. No such differences were found (Figure 10A). We then examined the analgesic effect of HZ-166 (16 mg kg^{-1}, i.p.) in the three genotypes. As expected, HZ-166 significantly reduced numbers of formalin-induced nocifensive reactions (assessed as time spent licking of the injected paw) in $\alpha2^{fl/fl}$ mice. By contrast, hoxb8$\alpha2^{-/-}$ mice and $\alpha2^{R/R}$, whose α2-$GABA_A$Rs are insensitive to HZ-166 mice (Paul et al., 2014) did not show significant reductions in nocifensive behaviors after HZ-166 (Figure 10B).

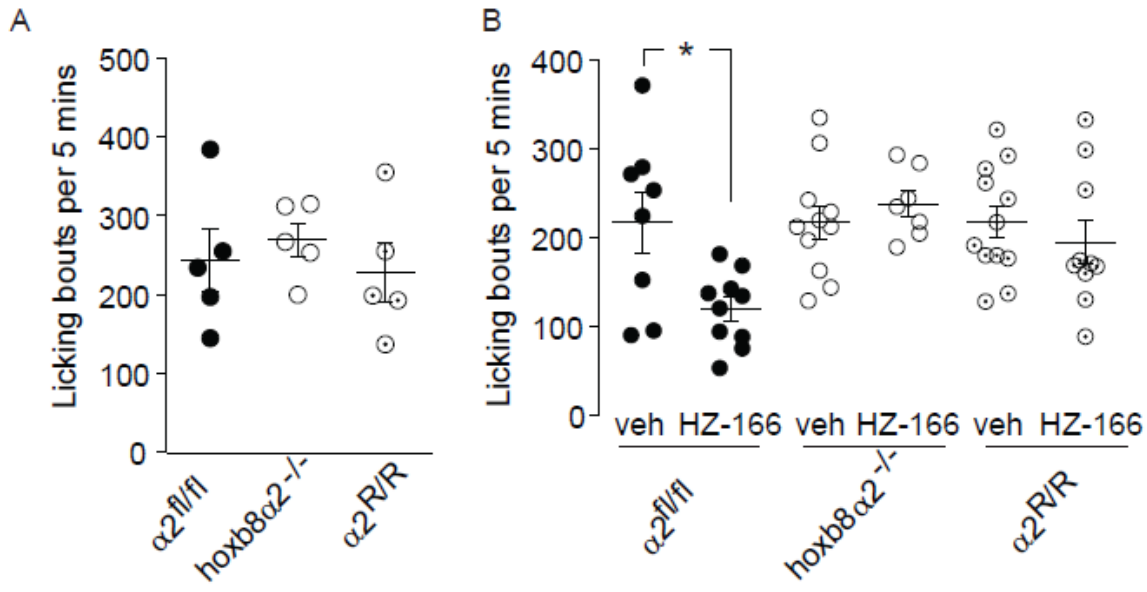

Figure 10. HZ-166-mediated antihyperalgesia is lost in α2 conditional knockout and global α2 point mutated mice. A, Plot depicting the sum of licking bouts directed to the ipsilateral hind paw in the formalin test quantified in 5 min intervals for 60 min in $\alpha2^{fl/fl}$, hoxb8$\alpha2^{-/-}$ and $\alpha2^{R/R}$ mice. No difference was observed ($\alpha2^{fl/fl}$: 243±39.9; hoxb8$\alpha2^{-/-}$: 269.4±21.2; $\alpha2^{R/R}$: 227.8±36.9), p=0.7, one-way ANOVA F(2,12)=0.4 (N=5 mice) for the interaction treatment x genotype, followed by Bonferroni *post hoc* test. B, Licking bouts per five minutes in mice

pretreated with HZ-166 one hour before formalin injection. Statistical analysis, circles indicate individual mice, and error bars indicate mean±SEM ($\alpha2^{fl/fl}$:119.2±13; hoxb8$\alpha2^{-/-}$: 237.9±14.; $\alpha2^{R/R}$:194.2±24.1), *$p < 0.05$, one-way ANOVA $F(5,52)=3.9$ (n=8, 10, 11, 7, 12 and 10 mice) for the interaction treatment × genotype, followed by Bonferroni *post hoc* test.

VI Discussion

Several lines of evidence indicate that α2-$GABA_A$Rs serve an important function in the control of spinal nociceptive circuits. Several studies have shown that specific activation (via positive allosteric modulation) of α2-$GABA_A$Rs reduces pain sensitivities in a number of rodent pain models (Knabl et al., 2009; Ralvenius et al., 2015). Based on these results one would expect that ablation of α2-$GABA_A$Rs from the spinal cord should lead to increased pain sensitivity or or even signs of spontaneous pain (Foster et al., 2015). However, a study showed that mice lacking α2-$GABA_A$Rs (hoxb8α2$^{-/-}$ mice) from the spinal cord showed no increased sensitivity to acute noxious mechanical and thermal stimuli (Paul et al., 2014). This could indicate the presence of potential compensatory mechanisms at the cellular and/or molecular level, which would be involved in countering the loss of inhibitory synaptic transmission. Revealing such mechanisms would be useful for novel drug-development strategies in countering chronic pain.

In the present study, we have examined the functional consequences of deletion of the $GABA_A$R α2 subunit from the spinal cord on the cellular and behavioral level. We first verified again that hoxb8α2$^{-/-}$ mice are indeed devoid of α2-$GABA_A$Rs in the spinal cord. We then confirmed in a variety of acute nociceptive tests (von Frey, pin prick, cold, heat, and formalin) that the mice do not exhibit elevated pain sensitivities. We then continued with an in-depth analysis of GABAergic neurotransmission in hoxb8α2$^{-/-}$ and corresponding wild-type (α2$^{fl/fl}$) mice. Our electrophysiological recordings revealed a reduction in the amplitudes of light-evoked GABA-IPSCs in hoxb8α2$^{-/-}$ mice with no change in decay kinetics. We found no changes in the amplitudes of currents evoked by superfusion with GABA and an *increase* rather than a decrease in the amplitudes of tonic GABAergic currents. One might hence argue that the absence of a pronociceptive phenotype in hoxb8α2$^{-/-}$ mice comes from preserved *tonic* GABAergic currents mediated by extrasynaptic $GABA_A$Rs, while synaptic $GABA_A$Rs would have no or only very little impact on spinal nociceptive control. Although this explanation cannot be fully ruled out at present, it seems unlikely to us as these tonic currents are very small and are present only in a subset of cells (Belelli et al., 2005). An alternative and in our opinion a more likely explanation for the absence of a pronociceptive

phenotype is the presence of some kind of compensatory mechanisms that would counteract diminished GABAergic inhibition at synapses by up-regulating another form of inhibition or by down-regulating excitation in nociceptive circuits. We found no evidence for an up-regulation of glycinergic inhibition, leaving us with the observed increase in the amplitude of tonic GABAergic currents as the only change in the GABAergic system that could potentially compensate for the loss of synaptic GABAergic inhibition.

Tonic GABAergic currents originate from the activation of extrasynaptic $GABA_ARs$ by ambient extracellular GABA. Since GABA concentrations are low outside synaptic clefts, $GABA_ARs$ mediating tonic GABAergic currents must have a high affinity for GABA. Previous work has shown that α4- and α5-$GABA_ARs$ fulfill these criteria (Delgado-Lezama et al., 2013; Fritschy and Panzanelli, 2014). Given the sparse expression of α4-$GABA_ARs$ in the spinal cord of wild-type mice (Paul et al., 2012), one could argue that increased tonic inhibition originated more likely from α5-$GABA_ARs$ than α4-$GABA_ARs$ (Perez-Sanchez et al., 2016). On the other hand, currents activated by exogenous GABA showed reduced sensitivity to HZ-166 in hoxb8$\alpha2^{-/-}$ mice suggesting an up-regulation of non α1, α2, α3, α5 $GABA_ARs$. Future experiments should aim to verify whether α4-$GABA_ARs$ were up-regulated upon spinal α2 ablation and hence contribute to the increased tonic inhibition in hoxb8$\alpha2^{-/-}$ mice. To this end, THIP (4,5,6,7-tetrahydroisoxazolo[5,4-c]pyridin-3-ol), a δ-preferring $GABA_AR$ agonist, may be useful to elucidate the role of α4-$GABA_ARs$, as they are known to associate with the δ subunit rather than the γ2 subunit (Storustovu and Ebert 2006; Bonin et al., 2011).

In addition to compensatory mechanisms originating from within the GABA of glycinergic system, we had also addressed potential changes in the glutamatergic system and had quantified excitatory synaptic input from primary nociceptors to the spinal dorsal horn. There was a trend towards more reliable synaptic transmission from primary nociceptors to second order LII neurons in hoxb8$\alpha2^{-/-}$ mice, consistent with diminished GABAergic inhibition of excitatory transmission.

We also investigated the mRNA levels of the vesicular glutamate transporters VgluT1-3 in the DRGs of hoxb8$\alpha2^{-/-}$ mice. In wild-type mice, VGluT1 is expressed mainly VgluTs are responsible for transporting the excitatory neurotransmitter glutamate into vesicles located within the terminal of primary afferent fibers (El Mestikawy et al., 2011). We found reduced

mRNA levels of VgluT2, but no changes VgluT1 and VgluT2. Although statistically significant, the change in VgluT2 mRNA expression was rather small and did not translate into altered VgluT2 protein expression in the dorsal horn, the site to which the VgluT protein expressed in DRG neurons is transported. It is therefore unlikely that the observed change in VgluT2 mRNA levels is of biological relevance.

As a final experiment, we had also investigated protein levels of serotonin (5-HT) and its producing enzyme TPH2 (tryptophan hydroxylase 2), by use of immunohistocytochemistry. 5-HT is synthesized in neurons of the nucleus raphe magnus, located in the hindbrain, which is the main source of spinal 5-HT release (Hornung, 2003). Spinally released serotonin can mediate both hyperalgesia and antinociception, depending on which subtype 5-HT receptors is activated (Yaksh and Wilson, 1979; Furst, 1999; Diniz et al., 2015). Activation of spinal 5-HT_3 receptors is antinociceptive (Fukushima et al., 2009; Kim et al., 2015). We demonstrated increased protein levels of serotonin and TPH2 in both the superficial and deep dorsal horn of the spinal cord in hoxb8$\alpha2^{-/-}$ mice. These results could suggest an increased serotonergic tone in the spinal cord of hoxb8$\alpha2^{-/-}$ mice as the most likely mechanism of compensation.

In the present study, we had also compared the effects of HZ-166 on GABAergic membrane currents in hoxb8$\alpha2^{-/-}$ and $\alpha2^{fl/fl}$ mice. Consistent with a major role of the $\alpha2$ subunit in the superficial dorsal horn, we found reduced potentiation by HZ-166 in neurons of hoxb8$\alpha2^{-/-}$ mice. The finding that potentiation was reduced but not completely lost is consistent with the presence of additional α subunits that can form benzodiazepine (HZ-166) sensitive $GABA_A$Rs. Despite this remaining potentiation by HZ-166 the analgesic effect of HZ-166 was virtually lost in hoxb8$\alpha2^{-/-}$ mice. A very similar phenotype has been found previously by Paul et al. (2014) in the zymosan A test, which is another inflammatory pain model. By contrast, analgesic effects in neuropathic mice were only partially reduced in hoxb8$\alpha2^{-/-}$ mice. This difference may indicate that different dorsal horn neuronal circuits control inflammatory and neuropathic pain.

In summary, this study confirmed the pivotal contribution of $\alpha2$-$GABA_A$Rs in the analgesic actions of $GABA_A$R modulators. A surprising finding was that mice lacking this receptor subtype did not show a pronociceptive phenotype. Our data suggest that an up-regulation of

serotonergic input to the spinal dorsal horn compensated for loss of pain control by synaptic $GABA_AR$s in these mice.

VII References

Basbaum AI, Bautista DM, Scherrer G, Julius D (2009) Cellular and molecular mechanisms of pain. Cell 139:267-284.

Belelli D, Peden D.R, Rosahl T.W, Wafford K.A, Lambert J.J (2005) Extrasynaptic $GABA_A$ receptors of thalamocortical neurons: a molecular target for hypnotics. The Journal of neuroscience 25:11513-11520.

Bohlhalter S, Weinmann O, Mohler H, Fritschy JM (1996) Laminar compartmentalization of $GABA_A$-receptor subtypes in the spinal cord: an immunohistochemical study. The Journal of neuroscience : the official journal of the Society for Neuroscience 16:283-297.

Bonin R.P, Labrakakis C, Eng D.G, Whissel P.D, De Koninck Y, Orser B.A (2011) Pharmacological enhancement of delta-subunit-containing $GABA_A$ R that generate a tonic inhibitory conductance in spinal neurons attenuates acute nociception in mice. Pain 6:1317-1326.

Brenner DS, Golden JP, Gereau RWt (2012) A novel behavioral assay for measuring cold sensation in mice. PloS one 7:e39765.

De Koninck Y (2007) Altered chloride homeostasis in neurological disorders: a new target. Current opinion in pharmacology 7:93-99.

Delgado-Lezama R, Loeza-Alcocer E, Andres C, Aguilar J, Guertin PA, Felix R (2013) Extrasynaptic GABA(A) receptors in the brainstem and spinal cord: structure and function. Current pharmaceutical design 19:4485-4497.

Diniz DA, Petrocchi JA, Navarro LC, Souza TC, Castor MG, Perez AC, Duarte ID, Romero TR (2015) Serotonin induces peripheral mechanical antihyperalgesic effects in mice. European journal of pharmacology 767:94-97.

Dubuisson D, Dennis S.G (1977) The formalin test: a quantitative study of the analgesic effects of morphine, meperidine, and brain stem stimulation in rats and cats. Pain 4:161-174.

Dugue GP, Brunel N, Hakim V, Schwartz E, Chat M, Levesque M, Courtemanche R,

El Mestikawy S, Wallen-Mackenzie A, Fortin GM, Descarries L, Trudeau LE (2011) From glutamate co-release to vesicular synergy: vesicular glutamate transporters. Nature reviews Neuroscience 12:204-216.

Farrant M, Nusser Z (2005). Variations on an inhibitory theme: plastic and tonic activation of $GABA_A$ receptors. Nature reviews. Neuroscience 6:215-229.

Foster E, Wildner H, Tudeau L, Haueter S, Ralvenius WT, Jegen M, Johannssen H, Hosli L, Haenraets K, Ghanem A, Conzelmann KK, Bosl M, Zeilhofer HU (2015) Targeted ablation, silencing, and activation establish glycinergic dorsal horn neurons as key components of a spinal gate for pain and itch. Neuron 85:1289-1304.

Fritschy JM, Panzanelli P (2014) $GABA_A$ receptors and plasticity of inhibitory neurotransmission in the central nervous system. The European journal of neuroscience 39:1845-1865.

Fukushima T, Ohtsubo T, Tsuda M, Yanagawa Y, Hori Y (2009) Facilitatory actions of serotonin type 3 receptors on GABAergic inhibitory synaptic transmission in the spinal superficial dorsal horn. Journal of neurophysiology 102:1459-1471.

Furst S (1999) Transmitters involved in antinociception in the spinal cord. Brain research bulletin 48:129-141.

Hornung JP (2003) The human raphe nuclei and the serotonergic system. Journal of chemical neuroanatomy 26:331-343.

Hösl K, Reinold H, Harvey RJ, Muller U, Narumiya S, Zeilhofer HU (2006) Spinal prostaglandin E receptors of the EP2 subtype and the glycine receptor alpha3 subunit, which mediate central inflammatory hyperalgesia, do not contribute to pain after

peripheral nerve injury or formalin injection. Pain 126:46-53.

Kim JM, Jeong SW, Yang J, Lee SH, Kim WM, Jeong S, Bae HB, Yoon MH, Choi JI (2015) Spinal 5-HT1A, not the 5-HT1B or 5-HT3 receptors, mediates descending serotonergic inhibition for late-phase mechanical allodynia of carrageenan-induced peripheral inflammation. Neuroscience letters 600:91-97.

Knabl J, Zeilhofer UB, Crestani F, Rudolph U, Zeilhofer HU (2009) Genuine antihyperalgesia by systemic diazepam revealed by experiments in $GABA_A$ receptor point-mutated mice. Pain 141:233-238.

Knabl J, Witschi R, Hosl K, Reinold H, Zeilhofer UB, Ahmadi S, Brockhaus J, Sergejeva M, Hess A, Brune K, Fritschy JM, Rudolph U, Mohler H, Zeilhofer HU (2008) Reversal of pathological pain through specific spinal $GABA_A$ receptor subtypes. Nature 451:330-334.

Kuner R (2010) Central mechanisms of pathological pain. Nature medicine 16:1258-1266.

Labrakakis C, Rudolph U, De Koninck Y (2014) The heterogeneity in $GABA_A$ receptor-mediated IPSC kinetics reflects heterogeneity of subunit composition among inhibitory and excitatory interneurons in spinal lamina II. Frontiers in cellular neuroscience 8:424.

Notter T, Panzanelli P, Pfister S, Mircsof D, Fritschy JM (2014) A protocol for concurrent high-quality immunohistochemical and biochemical analyses in adult mouse central nervous system. The European journal of neuroscience 39:165-175.

Olsen R.W, Sieghart W (2008) International Union of Pharmacology. LXX. Subtypes of gamma-aminobutyric acid (A) receptors: classification on the basis of subunit composition, pharmacology, and function. Update. Pharmacological reviews 60:243-260.

Paul J, Zeilhofer HU, Fritschy JM (2012) Selective distribution of GABA(A) receptor subtypes in mouse spinal dorsal horn neurons and primary afferents. The Journal of comparative neurology 520:3895-3911.

Paul J, Yévenes GE, Benke D, Di Lio A, Ralvenius WT, Witschi R, Scheurer L, Cook JM, Rudolph U, Fritschy JM, Zeilhofer HU (2014) Antihyperalgesia by alpha2-$GABA_A$ receptors occurs via a genuine spinal action and does not involve supraspinal sites. Neuropsychopharmacology : official publication of the American College of Neuropsychopharmacology 39:477-487.

Perez-Sanchez J, Lorenzo LE, Lecker I, Zurek AA, Labrakakis C, Bridgwater EM, Orser BA, De Koninck Y, Bonin RP (2016) alpha5$GABA_A$ Receptors Mediate Tonic Inhibition in the Spinal Cord Dorsal Horn and Contribute to the Resolution Of Hyperalgesia. Journal of neuroscience research.

Persohn E, Malherbe P, Richards JG (1991) In situ hybridization histochemistry reveals a diversity of $GABA_A$ receptor subunit mRNAs in neurons of the rat spinal cord and dorsal root ganglia. Neuroscience 42:497-507.

Ralvenius WT, Benke D, Acuna MA, Rudolph U, Zeilhofer HU (2015) Analgesia and unwanted benzodiazepine effects in point-mutated mice expressing only one benzodiazepine-sensitive $GABA_A$ receptor subtype. Nature communications 6:6803.

Rivas F.M, Stables J.P, Murphee L, Edwankar R.V, Edwankar C.R, Huang S, Jain H.D, Zhou H, Majumder S, Sankar S, Roth B.L, Ramerstorfer J, Furtmuller R, Sieghart W, Cook J.M (2009) Antiseizure activity of novel gamma-aminobutyric acid (A) receptor subtype-selective benzodiazepine analogues in mice and rat models. Journal of medicinal chemistry 52:1795-1798.

Sandkuhler J (2009) Models and mechanisms of hyperalgesia and allodynia. Physiological reviews 89:707-758.

Scroggs RS, Fox AP (1992) Calcium current variation between acutely isolated adult rat dorsal root ganglion neurons of different size. The Journal of physiology 445:639-658.

Snider WD, McMahon SB (1998) Tackling pain at the source: new ideas about nociceptors. Neuron 20:629-632.

Storustovu S.I and Ebert B (2006) Pharmacological characterization of agonists at delta-containing $GABA_A$ receptors:

Functional selectivity for extrasynaptic receptors is dependent on the absence of gamma2. The Journal of Pharmacolgy and experimental therapeutics 3:1351-1359.

Todd AJ, Spike RC (1993) The localization of classical transmitters and neuropeptides within neurons in laminae I-III of the mammalian spinal dorsal horn. Progress in neurobiology 41:609-645.

Witschi R, Johansson T, Morscher G, Scheurer L, Deschamps J, Zeilhofer HU (2010) Hoxb8-Cre mice: A tool for brain-sparing conditional gene deletion. Genesis 48:596-602.

Witschi R, Punnakkal P, Paul J, Walczak JS, Cervero F, Fritschy JM, Kuner R, Keist R, Rudolph U, Zeilhofer HU (2011) Presynaptic alpha2-$GABA_A$ receptors in primary afferent depolarization and spinal pain control. The Journal of neuroscience : the official journal of the Society for Neuroscience 31:8134-8142.

Yaksh TL, Wilson PR (1979) Spinal serotonin terminal system mediates antinociception. The Journal of pharmacology and experimental therapeutics 208:446-453.

Zeilhofer HU, Benke D, Yévenes GE (2012a) Chronic pain states: pharmacological strategies to restore diminished inhibitory spinal pain control. Annual review of pharmacology and toxicology 52:111-133.

Zeilhofer HU, Wildner H, Yévenes GE (2012b) Fast synaptic inhibition in spinal sensory processing and pain control. Physiological reviews 92:193-235.

Zhao S, Ting JT, Atallah HE, Qiu L, Tan J, Gloss B, Augustine GJ, Deisseroth K, Luo M, Graybiel AM, Feng G (2011) Cell type-specific channelrhodopsin-2 transgenic mice for optogenetic dissection of neural circuitry function. Nature methods 8:745-752.

Chapter 2

Optogenetic mapping of inhibitory neurotransmission in the murine spinal dorsal horn

Part A

Mapping local and supraspinal inhibitory inputs onto LII excitatory neurons of the spinal dorsal horn

[1,2]Laetitia Tudeau, [1]Helge C. Johannssen, [1,2]Hanns Ulrich Zeilhofer

[1] Institute of Pharmacology and Toxicology, University of Zurich, CH-8057 Zurich, Switzerland

[2] Institute of Pharmaceutical Sciences, ETH Zurich, CH-8093 Zurich, Switzerland

L.T performed the electrophysiological experiments and the virus injections in the brainstem
L.T analyzed and interpreted the experiments with the help of H.C.J and H.U.Z

I Abstract - Part A

The superficial dorsal horn (sdh, LI/II) is an important relay station for incoming nociceptive signals from the peripheral nervous system. In this region, inputs are modulated by a network of inhibitory and excitatory interneurons before being further relayed by projection neurons to supraspinal sites in the brainstem and the thalamus. Many studies have investigated synaptic transmission between nociceptive fibers and LII neurons, and techniques such as paired recording revealed tight connectivity between excitatory and inhibitory neurons in LII but also connectivity across laminae. More recently, advanced techniques have been developed that are able to map the spatial organization of excitatory and/or inhibitory synaptic transmission onto a specific neuron type. Previous studies have combined glutamate uncaging with laser scanning photostimulation (LSPS) and revealed the excitatory input zones onto neurons in LII, which extended across different laminae depending on the morphology of the postsynaptic neuron dendritic tree. In this current project, I first characterized light-evoked activity in vGAT::ChR2;GAD67^{eGFP} double transgenic mice. In these mice, the majority of inhibitory neuron somata can be easily identified by their green fluorescence. In transverse slices prepared from these mice, both superficial and deep dorsal horn GAD67^{eGFP} neurons fired action potentials reliably upon short (4 ms) stimulation with blue light. Laser scanning photostimulation was then used to determine the sites of origin of inhibitory input onto excitatory neurons of LII. Inhibitory input could be elicited both from white and grey matter stimulation although inputs from the grey matter dominated (79 %). Within the dorsal horn grey matter, input from the superficial dorsal horn was more abundant than input from the deep dorsal horn (46 versus 33%).

II Introduction

The spinal superficial dorsal horn laminae I and II (sdh, LI/ II) constitute the major termination site for nociceptive Aδ and C primary afferent fibers (Light and Perl, 1977). The incoming sensory stimuli are processed and modulated by a network of excitatory and inhibitory interneurons and ultimately converge onto projection neurons in LI that eventually transmit the final output to supraspinal CNS areas (Scheibel and Scheibel, 1968; Todd, 2010; Zeilhofer et al., 2012b). Maintaining a balance between excitation and inhibition is crucial for normal nociceptive processing, and down-regulation of the GABAergic and glycinergic network is thought to promote the development of chronic pain symptoms, such as allodynia and hyperalgesia (Sivilotti and Woolf, 1994; Zeilhofer and Zeilhofer, 2008; Zeilhofer et al., 2012a). The organization of primary afferent inputs to dorsal horn neurons has been extensively studied (Light and Perl, 1977; Woodbury and Koerber, 2003). It has been described that LII neurons mostly receive direct monosynaptic input from Aδ and C-fibers, in contrast to LIII neurons, which mostly receive direct inputs from Aβ-fibers (Lu and Perl, 2003; Torsney and MacDermott, 2006). The paired recording method demonstrated direct connections between LII inhibitory islet cells and excitatory neurons but also direct connections between LII and LI neurons (Lu and Perl, 2003, 2005). However, this technique is restricted to examining connections between neurons that are not far apart from each other essentially because a reduced field of view is necessary for precise visibility of the cells when penetrating whole-cell with the recording pipette. On the other hand, laser stimulation has permitted the study of the intrinsic connectivity between LII neurons but also translaminar connectivity between LII and LIII/IV interneurons (Kato et al., 2013). This technique is therefore well suited for studying spatial connectivity patterns in the spinal cord. Examining spatial organization of local and translaminar circuitry became possible with laser scanning photostimulation (LSPS) (Callaway and Katz, 1993; Katz and Dalva, 1994). LSPS employs scanning a region of interest with light while recording physiological responses from a defined neuron or set of neurons. It has been originally combined with caged neurotransmitters and nowadays can be also used in genetically modified animals which express light-sensitive actuators in subsets of neurons (such as vGAT::ChR2 mice). In the latter variant, LSPS ultimately activates a specific cell type and enables to record light-evoked

synaptic responses. For several spatial mapping approaches in acute spinal cord slices, UV light was used in LSPS experiments to uncage glutamate (Kato et al., 2007; Kato et al., 2009; Kato et al., 2013; Kosugi et al., 2013). Upon UV light stimulation, glutamate is uncaged and evokes firing in neurons located in close proximity to the glutamate release site. Ultimately, evoked synaptic responses can be recorded in postsynaptic neurons. Kato et al. (2013) have described a differential wiring of excitatory and inhibitory inputs to LII islet cells and mapped the organization of inputs to LIII-LIV neurons with this technique. The LSPS is an attractive tool to study inhibitory connectivity onto LII excitatory neurons in the dorsal horn.

We applied LSPS in combination with an "optogenetic" mouse line the vGAT::ChR2-YFP instead of glutamate uncaging. LSPS was applied to acute coronal spinal cord slices from BAC transgenic vGAT::ChR2 mice. In these mice, ChR2 expression is driven by the vGAT promoter, which leads to expression of ChR2 in all inhibitory neurons of the central nervous system (CNS). Upon photoactivation of dorsal horn inhibitory neurons, we were able to record light-induced IPSCs in postsynaptic LII excitatory neurons and map the inhibitory input zones onto these cells. In addition, we present some preliminary data on inputs to LII excitatory neurons that originate from the neurons in the rostral ventromedial medulla (RVM). Morphological reconstructions of postsynaptic neurons gave us additional insights on potential translaminar connectivity between LII and LIII neurons. This study provides information on the location of zones from which inhibitory input to excitatory LII neurons can be evoked.

III Aim of this chapter - Part A

So far, most studies of dorsal horn inhibitory circuits focused on LII inhibitory interneurons and on excitatory or inhibitory inputs to these cells and to cells in the deeper laminae (Kato et al., 2007; Kato et al., 2009; Kato et al., 2013; Kosugi et al., 2013). The precise origin of inhibitory inputs onto LII excitatory neurons in pain processing however remains poorly understood.

One aim of this chapter was to establish a method enabling us to examine the spatial organization of inhibitory synaptic inputs onto LII excitatory neurons. I started characterizing light-induced activity of GAD67^{eGFP};vGAT::ChR2 (referred to as GAD67^{eGFP}) and then mapped the distribution of local inhibitory synaptic transmission to lamina II (LII) excitatory spinal dorsal horn neurons by combining LSPS and whole-cell patch-clamp recordings. Finally, I reconstructed the dendritic tree of two excitatory postsynaptic neurons in order correlate sites of the origin of inhibitory input with the morphology of the recorded neuron.

IV Material and methods

Animals

Animal procedures were approved by the Cantonal Veterinary Office (License permissions 86/2013 and 031/2016). Experiments were either done in BAC transgenic vGAT::ChR2-YFP mice (Zhao et al., 2011) or in vGAT::ChR2-YFP;GAD67^{eGFP} double transgenic mice. Mice were three to four-week-old and of either sex.

Drugs and chemicals

All chemicals were purchased from Biotrend (Anawa, Switzerland).

Spinal cord slice preparation and electrophysiological recordings

Animals were decapitated and underwent laminectomy. Transverse 400 µm thick slices of the lumbar spinal cord slices were prepared in ice-cold solution with the following composition (Dugue et al., 2009) (in mM): 130 K-gluconate, 15 KCl, 0.05 EGTA, 20 HEPES and 25 glucose titrated to pH 7.4 with KOH and supplemented with 50 µM D-APV to prevent glutamate excitotoxicity. Slices were then kept 30 min for recovery in a solution containing (in mM) 225 D-Mannitol, 2.5 KCl, 1.25 NaH_2PO_4, 25 $NaHCO_3$, 0.8 $CaCl_2$ and 8 MgCl2 and 25 glucose (37°C, bubbled with 95% O_2, 5% CO_2). Finally, slices were transferred to an artificial cerebrospinal fluid (aCSF), also known as extracellular solution with the following composition (in mM): 120 NaCl, 2.5 KCl, 1.25 NaH_2PO4, 26 $NaHCO_3$, 5 HEPES, 1 $MgCl_2$, 2 $CaCl_2$ and 14.6 glucose. Slices were transferred to a recording chamber and continuously perfused with aCSF equilibrated with 95% O_2, 5% CO_2 at a flow rate of 1ml min^{-1}. Neurons in the sdh (LI, LII <150 µm from the dorsal margin) were visually identified with an iXON Ultra camera (Andor Technology, Belfast, UK) using the infrared gradient contrast equipment of the microscope (Zeiss Examiner. A1, Göttingen, Germany). Electrical recordings of the inhibitory neurons were done in current clamp mode with 0 pA holding current, and in voltage clamp mode at -60 mV holding membrane potential. In laser scanning photostimulation experiments (LSPS), whole-cell voltage-clamp recordings were performed at room temperature at a holding potential of -60 mV on presumed excitatory (ChR2$^-$) neurons. Patch pipettes were prepared from borosilicate glass capillaries and had an open tip resistance of 3-5 GΩ. Patch pipettes were filled with an

internal solution containing (in mM): 140 KCl, 4 $MgCl_2$ + 6 H_20, 10 HEPES, 10 EGTA, 2 MgATP, 0.5 NaGTP when recording inhibitory inward currents in voltage-clamp mode. Recording action potentials in the current-clamp mode as well as light-evoked photocurrents in voltage clamp mode required the following internal solution (mM): 130 K-D-gluconate, 20 KCl, 2 MgCl2+H2O, 0.05 EGTA, 2MgATP, 10 Na Hepes.

i. Characterization of light-evoked responses in GABAergic and presumed glycinergic neurons

Transverse spinal cord slices from $GAD67^{eGFP}$ mice were used for the experiments. The identification of $GAD67^{eGFP}$ cells was done through excitation of the tissue with the 490 nm excitation fluorescence wavelength (GFP reporter). Fluorescence was easy to detect in superficial dorsal horn $GAD67^{eGFP}$ neurons due to their strong expression of GFP in the soma. Deep dorsal horn inhibitory neurons which release both GABA and glycine (Todd, 1990) also express $GAD67^{eGFP}$ but at intensities too low to be reliably detected above the neuropil fluorescence background of the ChR2-YFP. Their inhibitory phenotype was identified by the presence of the photocurrent. Access resistance of the cell was continuously monitored by giving short hyperpolarizing steps (-5 mV) between the different light stimulations. Recordings were discarded if the access resistance changed > 20% between the beginning and the end of the experiment. Three consecutive light stimulations of 4 ms (473 nm) starting at 20.4 mW/mm^2 and decreasing step-wise to a final power density of 11.5 mW/mm^2, were applied to the cell soma. Light-evoked action potentials from either $GAD67^{eGFP}$ or presumed glycinergic cells in LII and III, respectively, were recorded. The firing success rate (i.e. sensitivity of the cells to different light intensities) was measured in each population of inhibitory neurons. Three action potentials out of three consecutive light stimulations (of equal intensity) were considered as 100% success rate. In voltage clamp experiments, light-evoked photocurrents from either $GAD67^{eGFP}$ or presumed glycinergic cells were recorded at 1 s and 4 ms light exposures with similar decreasing intensities as in current clamp experiments (i.e., 20.4 -11.5 mW/mm^2).

ii. Laser scanning photostimulation (LSPS)

The laser and optical fiber were obtained from RappOptogenetics (Hamburg, Germany). The laser beam was coupled to a single optic fiber directly coupled into an Axio Examiner.A1 fixed-staged microscope (Zeiss, Göttingen, Germany). Scanning was done by the UGA-40 GEO, which harbors a set of rotating mirrors allowing the laser beam to move in a pre-configured direction. The settings for the laser beam scanning directions were done by using the UGA-40 software (RappOptoelectronics, Hamburg, Germany). Ultimately, these parameters enabled to direct the laser beam to follow a 20 x 20 stimulation grid from left to right, and top to bottom. The dimensions of the stimulation grid for mapping the inhibitory synaptic responses were set to 800 µm x 800 µm (400 stimulation sites à 40 x 40 µm). Each area was illuminated for 4 ms and an interval of 96 ms with no light stimulation was implemented between stimulation of neighboring areas. Stimulation was done through a 10x water immersion objective. The shape and size of the stimulus were chosen to maximize sensitivity in the detection of synaptic inputs and hence avoid excluding regions of the dorsal horn that could have potential synapses with the recorded neuron. The light intensity reaching the tissue was 2.3 mW/mm^2. In most cases, five consecutive scans were applied on the tissue.

Transverse spinal slices from vGAT::ChR2 mice were used to record inhibitory input from excitatory interneurons of LI-LII. LII was recognized under the 10x water-immersion objective by its transparent appearance. Individual neurons were visualized with a 40x immersion objective. Excitatory neurons were identified by the absence of light-evoked photocurrent after a 1s light pulse directed onto their soma. Recording of synaptic responses to photostimulation was done in whole-cell mode. Light-evoked inhibitory currents were recorded at a holding potential of -60 mV. A high chloride-based internal solution (KCl, *see Spinal cord slice preparation and electrophysiological recordings*) lead to a chloride reversal potential close to zero and hence large inhibitory inward currents could be obtained. Access resistance of the cell was continuously monitored by giving short hyperpolarizing steps (-5 mV) between each laser photostimulation. Recordings were discarded if the access resistance changed > 20%. All electrical signals were sampled at 5 kHz and filtered at 2.9 kHz. Data was analyzed using IgorPro (WaveMetrics, Inc.,USA).

Data analysis

A macro (*see Appendix 1: Macro*) was built to analyze each trial (stimulation point) from individual scans in control and drug conditions (i.e. 1 scan, 400 trials). The threshold set for detecting light-evoked IPSC events was baseline ≥ 2*standard deviation of the noise obtained during an interval where no synaptic event was visible. The outcome of one scan delivered a 20 x 20 probability table, and a 20 x 20 heat map. The probability table provided values corresponding to the number of times an inhibitory input was detected by the macro after a total amount of scans. The threshold we considered for inhibitory inputs to be triggered was >1 event per trial. For each recorded cell, an infra-red (IR) image of the spinal dorsal horn was taken with the 10x objective and overlaid onto the 20 x 20 heat map. Therefore, 1) the 20 x 20 probability table could be divided into two halves: superficial and deep dorsal horn, 2) Each value of the table was assigned an identity: grey matter LI/LII (GM LI/LII), grey matter LIII-LV (GM LIII-LV), dorsal white matter (WM dorsal), lateral/medial white matter (WM lat/med). The sum of events was calculated for each recorded cell in control conditions in each of these four categories. In some cases, more than five scans were performed on the spinal dorsal horn.

Dendritic tree morphology

Recording pipettes were filled with an internal solution containing 0.5% biocytin (Sigma Aldrich) in order to visualize the dendritic tree of LII excitatory neurons. After the recordings, the pipette was carefully retracted from the recorded neuron. Slices were fixed in 4% PFA containing 15 % picric acid and subsequently stored in 10 % saccharose-0.05% NaN_3 in phosphate buffer saline (PBS) until further analysis. Slices were washed briefly in PBS and permeabilized extensively in 1% TritonX-100-10% normal NGS in PBS for up to 5 hours at room temperature. Subsequently, slices were incubated at 4°C for two days in Alexa Fluor 488-conjugated streptavidin (1:150; Dianova) to label the biocytin-filled neuron. All antibodies were diluted in 10% NGS-0.1% Triton X-100 in PBS. Sections were air-dried and mounted on gelatin coated glass slides (Thermos Scientific) in fluorescence mounting medium (Dako, Agilent Technologies). Fluorescent images were acquired on a Zeiss LSM710 Pascal confocal microscope using a 0.8 NA x 20 Plan apochromat objective and the ZEN 2012

software (CarlZeiss). A 20 plane Z-stacks (step size: 2.4 µm) was generated to obtain a 3D view of the dendritic tree extension.

Reconstruction of the dendritic tree was done with the *Simple Neurite Tracer* plug-in from Fiji (Image J). The reconstruction resulted in a z-stack that was then converted into a maximal intensity projection 2D image that was then overlaid to the corresponding heat map. This allowed the visualization of synaptic events onto the postsynaptic neuron.

V Results

Inhibitory neurons of both the superficial and the deep dorsal horn respond reliably at strong light intensities

In the first experiments, we performed targeted recordings in slices from GAD67^{eGFP};vGAT::ChR2-YFP (henceforth referred to as GAD67^{eGFP}) mice. GABAergic neurons of the superficial dorsal horn were reliably identified under the 40x objective due to the intense eGFP expression in their somata driven by the GAD67 promoter (Figure 1A). These inhibitory neurons of the deep dorsal horn also express GAD67^{eGFP} but their fluorescence was too weak to be detectable above the background of the neuropil ChR2-YFP fluoresence. Their inhibitory phenotype was identified by the presence of the photocurrent in cells of the deep dorsal horn (Figure 1B). We recorded light-evoked photocurrents in voltage-clamp mode after 1 s and 4 ms light pulses in both of these inhibitory cell subpopulations. Peak-to-baseline photocurrent amplitudes in the example traces shown in Figure 1C displayed no significant differences in amplitude between both cell types after 1 s (superficial dorsal horn inhibitory neuron: -114 pA; deep dorsal horn inhibitory neuron: -132 pA) and 4 ms (superficial dorsal horn inhibitory neuron: 123 pA; deep dorsal horn inhibitory neuron: 103 pA) light stimulations.

We then characterized the firing activity of both superficial and deep dorsal horn inhibitory neurons at different light intensities (20.4 - 11.5 mW/mm^2, Figure 1E). At the maximum intensity both superficial and deep dorsal horn inhibitory neurons fired action potentials upon 4 ms light pulse exposure (473 nm, 20.4 mW/mm^2, Figure 1D). Both superficial and deep dorsal horn inhibitory neurons also responded to light intensities ranging from 12.70 - 20.40 mW/mm^2 with reliable action potential firing. At lower light intensities, both inhibitory cell types were not able to sustain high fidelity firing in response to blue light (Figure 1E).

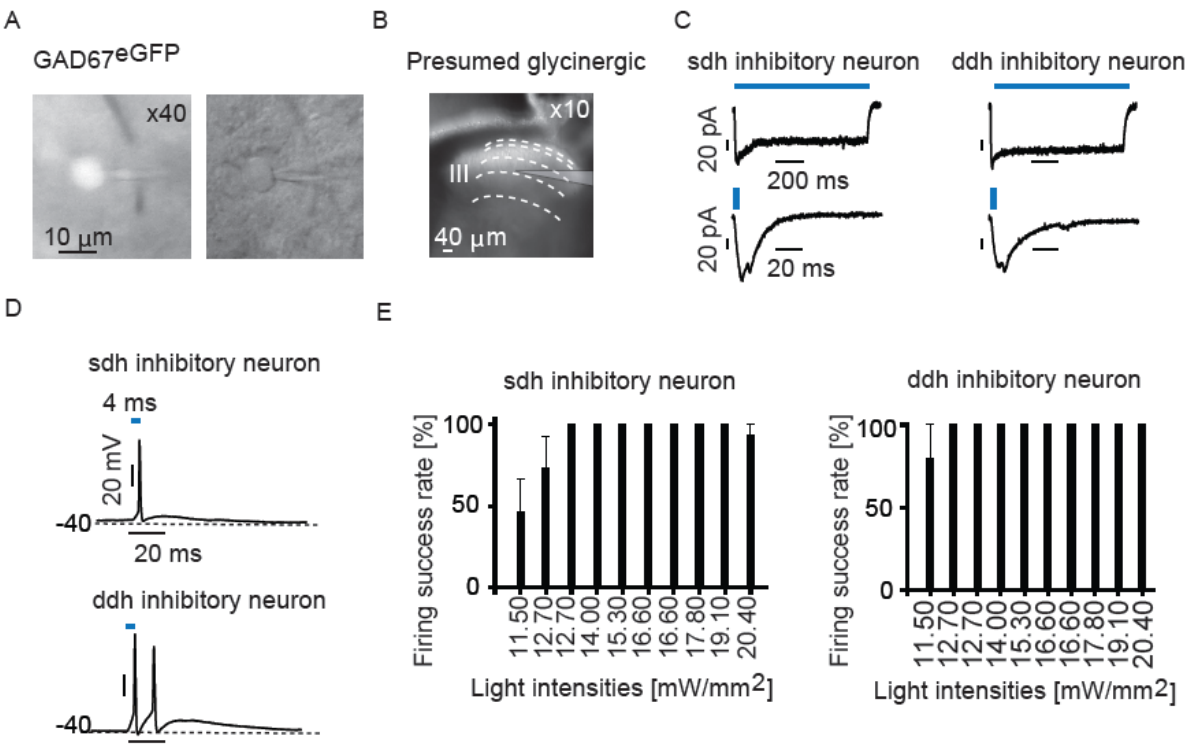

Figure 1. Characterization of light-evoked responses in inhibitory neurons. A, Fluorescence image of a GAD67^{eGFP} cell identified by the GFP reporter in the superficial dorsal horn lamina II (sdh, LII) under a 40x objective (*left)*. The same cell pictured in IR (*right*). The recording pipette is visible in both pictures and allowed us to record whole-cell activity from sdh inhibitory cells. B, IR image taken under the 10x objective that enabled us to target presumed glycinergic interneurons in the deep dorsal horn (ddh, LIII). The recording pipette is shown in grey. C, Example traces of voltage-clamp recordings in sdh and ddh inhibitory cells showing light-evoked photocurrents after 1s (blue bar, 473 nm, 716 mW/mm^2*)* and 4 ms light exposures (473 nm, 20.4 mW/mm^2*)*, respectively. D, Current clamp recordings representing light-evoked action potentials in a sdh and ddh inhibitory cell after a 4 ms light pulse (λ=473 nm, power density: 20.4 mW/mm^2). E. Firing success rate measured in sdh and ddh inhibitory cells after 4 ms light pulse stimulation. Light-intensity was decreased step wise from 20.4 - 11.5 mW/mm^2 (473 nm). For each light intensity step we triggered three light-stimulations.

Inhibitory inputs onto LII excitatory neurons originate from the grey and white matter

After characterizing the reliability of firing action potentials to given light stimulation intensities, we mapped the distribution of spinal inhibitory inputs onto LII excitatory neurons. To this end, we applied LSPS to acute slices of single transgenic vGAT::ChR2 mice (Figure 2A,B). While the blue light was stimulating the defined areas of the dorsal horn (squared shape, Figure 2B), we recorded light-evoked IPSCs from the postsynaptic neuron (Figure 2C). Light-evoked IPSCs could be reliably triggered by the light stimulus (inset, Figure 2C). Using this approach, we recorded light-evoked IPSCs from a total of 21 cells. From the probability

heat maps, we observed that all recorded neurons received inhibitory inputs from LI and LII, and 85% received inhibitory inputs also from the deep dorsal horn (LIII).

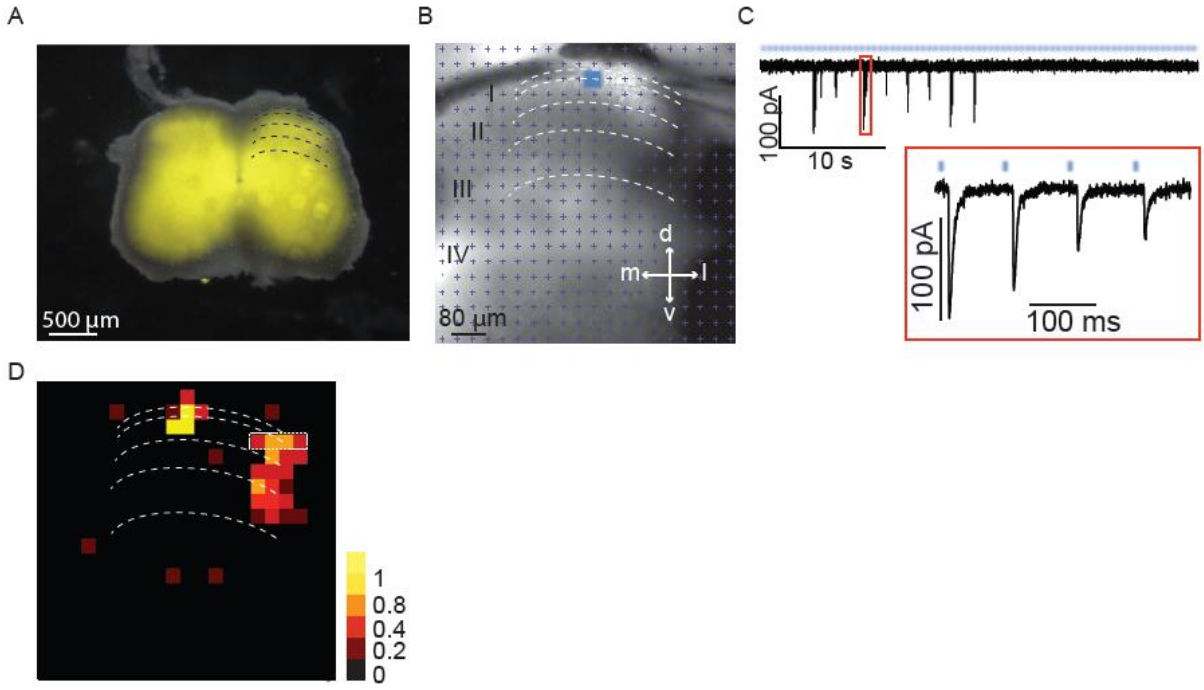

Figure 2. Laser scanning photostimulation setup. A, Acute transverse spinal cord slice taken from a vGAT::ChR2-YFP mouse under the 4x objective. ChR2-YFP is driven by the vGAT promoter and hence expressed in all inhibitory neurons. Expression of ChR2 is rendered visible by a YFP fusion protein coupled to the channel. Laminae I to IV are represented on the right dorsal horn (black dotted lines). B, IR image of the spinal dorsal horn taken with the 10x objective and a representative 20 x 20 stimulation grid overlaid to it (blue crosses). The light pulse (blue square, 40 x 40 µm) followed the grid and scanned the dorsal horn from left to right, top to bottom. C, Voltage-clamp recording trace after one scan of light-stimulation (blue dotted line, 400 light stimulations, 473 nm, 2.3 mW/mm^2). Inset shows five reliable light-evoked IPSCs upon 4 ms light exposure. D, 20 x 20 probability heat map obtained after five consecutive scans of the dorsal horn. Each trial constituting the heat map has identical coordinates to the stimulation points in B. These maps show the distribution of inhibitory input zones (represented as hot spots) in the dorsal horn. Hot spots that yield a light-evoked signal with a high probability are shown in yellow (colour scale, 1). Hot spots become darker with lower probability of neurotransmission (0, black).

We next investigated whether different populations of inhibitory neurons had a differential contribution to the total inhibitory neurotransmission in LII excitatory neurons. We performed LSPS in control (ctrl) and bicuculline (bic, 20 µM) conditions. Figure 3A (left column) shows two examples from two different cells. Top row shows an excitatory cell in LII (symbolized by a coloured spot) where most inputs originated from the lateral and dorsal

white and superficial dorsal grey matter (ctrl, Figure 3A, *top*). Laminar layers are represented by dotted white lines (LI-LIV). After application of bicuculline the probability of inhibitory transmission was reduced (Bic, Figure 3A, *top*). The bottom row, shows in control, clusters of inhibitory input in the lateral and dorsal white matter as well as in the superficial and deep dorsal horn grey matter. After bath-application of bicuculline, the probability of synaptic transmission was also reduced (Figure 3A, *bottom*).

In the probability heat maps, events appearing only once in a total of five scans (i.e., with a probability of 0.2) were considered as spontaneous rather than light-evoked signals. Such assumption was based on the fact that the probability of obtaining twice the same spontaneous event in all five scans was less than 5%. In 17 out of 21 cells, we assessed that the events were light-evoked and not spontaneous with more than 95% certainty.

Furthermore, we filled the postsynaptic neuron with biocytin to reconstruct the dendritic tree, and to compare its position with the inhibitory input zones of the postsynaptic neuron. We were able to reconstruct two cells (Figure 3B) in which the dorsoventrally dendritic fields extended to the deep dorsal horn (LV and LIII, respectively). These cells showed characteristics of vertical cells and were therefore classified as such. In both cells we observed inhibitory inputs on parts of the reconstructed cell but also in the deep dorsal horn and the dorsal white matter (Figure 3B). We indicated in a virtual right dorsal horn slice the somas of 19 excitatory cells that we were able to identify after the recordings. All somas were located in LII of the dorsal horn (Figure 3C).

To characterize the spatial distribution of inhibitory inputs we divided the probability heat maps from a total of 19 neurons into four regions: 1) dorsal white matter, 2) lateral/medial white matter, 3) grey matter (LI-LII, superficial dorsal horn), and grey matter (LIII-LV, deep dorsal horn). The results showed that 79% of the inputs arrived from stimulation of the grey matter and 21% from the white matter. The majority of inhibitory inputs occured in the superficial dorsal horn grey matter (46%, GM LI-LII) followed by the deep dorsal horn grey matter (33%, GM, LIII-LIV). The dorsal white matter contributed to 18% of the inputs in contrast to the lateral/medial white matter, which only contributed to 3% of the overall inhibitory neurotransmission.

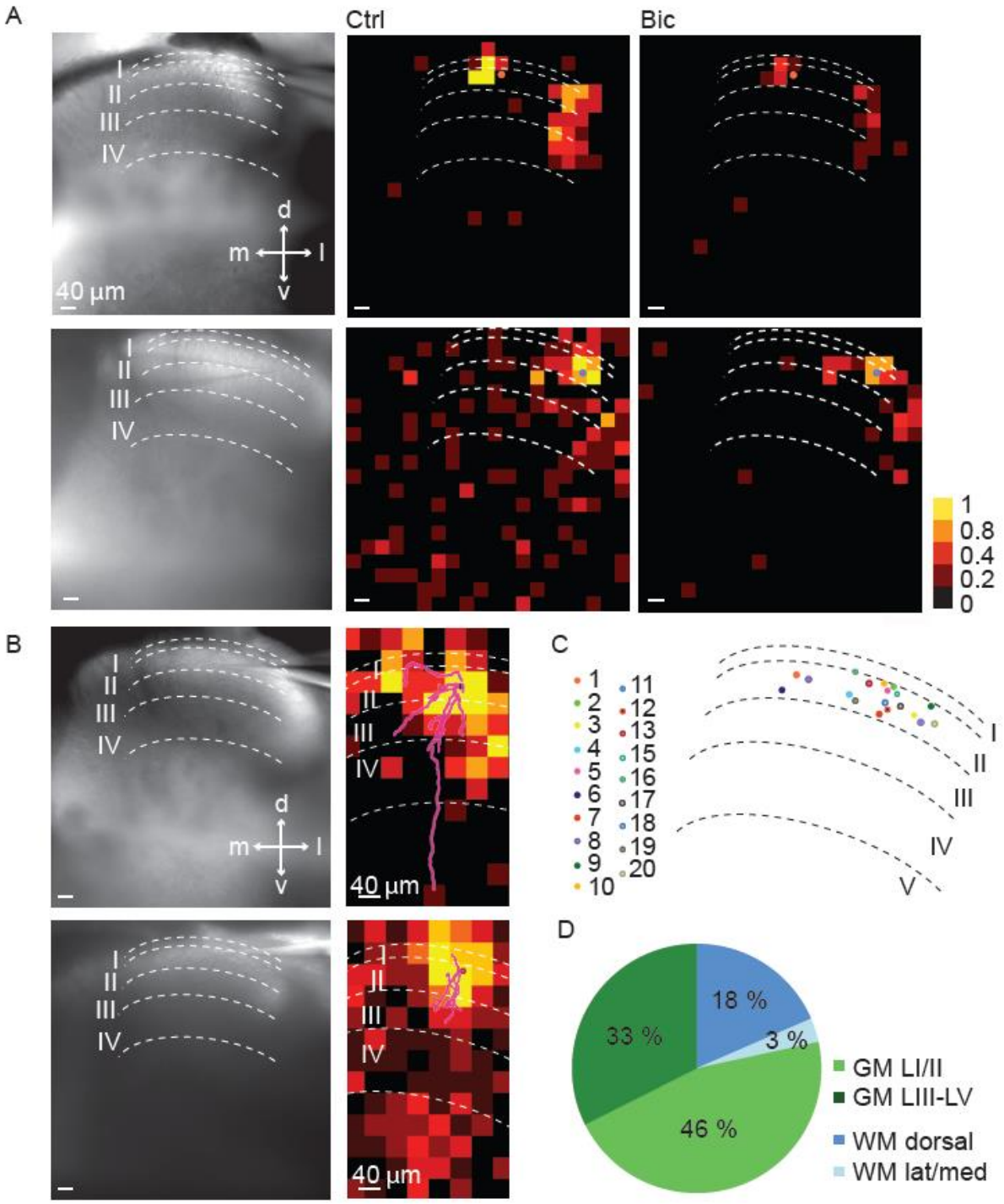

Figure 3. Localization of inhibitory inputs onto excitatory LII neurons. A, IR images of two different excitatory neurons in LII from which we recorded light-evoked synaptic events (*left column*). Laminae borders are represented in white dotted lines. Probability heat maps obtained after five consecutive scanning photostimulations in control (ctrl, *middle column*) and after bath-application of bicuculline (bic, 20 µM, *right column*) conditions. The synaptic input zones are represented by "hot spots" following a color scale (i.e., yellow strong probability of input, dark red low probability of input). Dots were added to the heat maps to symbolize the soma of the post-synaptic neurons from which the signals were recorded. B, *Left*, IR images of neurons from LII that were filled for dendritic tree reconstruction. *Right,* 2D dendritic tree reconstruction of two neurons

overlaid onto the probability heat maps obtained after LSPS. Somas were added and symbolized by a spot. C, Soma location of all neurons for which mapping of synaptic input zones was done in coronal slices (n = 19 cells), plotted on a drawing of the right dorsal horn. The borders of laminae I-V are shown in white (dotted lines). D, Prevalence of white matter (WM) and grey matter (GM) inhibitory inputs onto excitatory LII neurons (white matter dorsal horn, WM dorsal:18±3.43%; WM lat/med dorsal horn: 3±0.90%,; GM superficial dorsal horn, LI/LII:46±3.31% ; GM deep dorsal horn, LIII/LV: 33±3.64%). Values represent average±SEM.

The presence of descending inhibitory onto excitatory dorsal horn was verified in preliminary experiments where an AAV ChR2::mCherry virus was injected into the RVM of VgluT2::eGFP transgenic mice (Figure 4A). Targeted whole-cell recordings were performed on VgluT2::eGFP excitatory neurons of the sdh in coronal spinal cord slices. To characterize the neurotransmitter phenotype originating from the RVM, we used whole-field light stimulation (λ=473 nm, light exposure: 4 ms, field of view: 200-300 µm) on the sdh and recorded light-evoked postsynaptic currents. Our results showed a reduction in the postsynaptic current amplitude after application of bicuculline (Total IPSC: -446 pA; glycinergic IPSC: -446.5 pA, Figure 4B). Light-evoked signals disappeared after subsequently adding strychnine. The present results confirm the presence of both GABAergic and glycinergic inputs from the RVM onto excitatory LII neurons. However, it is not possible to distinguish whether GABA and glycine are co-released from the same axon terminals or whether they are released by GABAergic and glycinergic neurons, respectively.

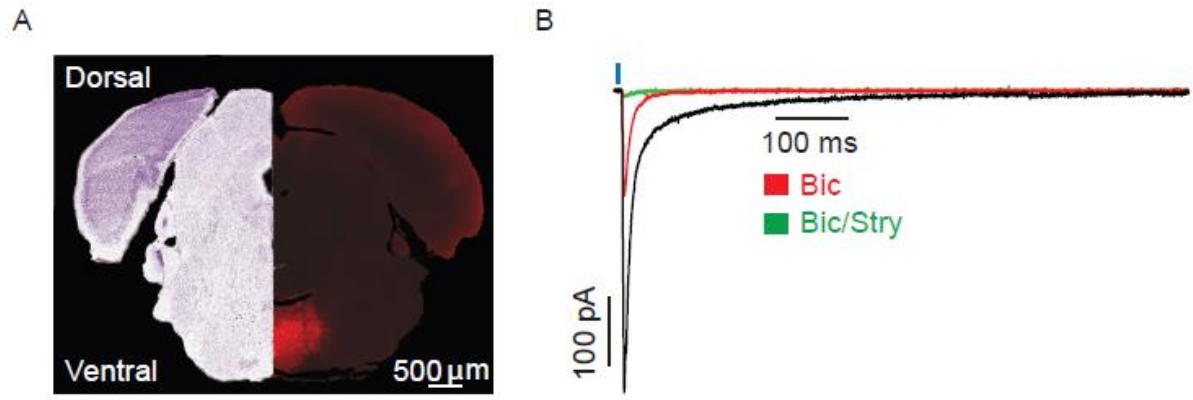

Figure 4. Mixed GABAergic/glycinergic inputs from the RVM modulate LII excitatory dorsal horn neurons. A, Coronal section taken with the confocal microscope from a VgluT2::eGFP transgenic mouse brain after injection of an AAV-encoding ChR2::mCherry virus into the RVM (red, site of injection). B, Light-evoked postsynaptic currents after 4 ms light stimulation (blue bar 473 nm, 2.7 mW, field of illumination 200-300 µm) in control (black), bicuculline (Bic 20 µM, red) and bicuculline and strychnine (Stry 0.5 µM, green) conditions.

Amplitude and latency properties of light-evoked IPSCs near the postsynaptic cell

We studied the amplitude and latency values of light-evoked IPSCs in the region surrounding the soma of the postsynaptic cell. Our analysis focused on nine trials of light-evoked IPSCs (Figure 5A, a-i). From a total of 20 cells, the average baseline-to-peak amplitude value of the light-evoked IPSCs from the nine trials was 221±18.17 pA (average±SEM). The individual average amplitude values from each trial are summarized in the 3 x 3 table (Figure 5C, *left*). In summary, the amplitude values of the IPSCs ranged beteween 110 and 291 pA. The amplitude values from IPSCs recorded dorsally relative to the soma were statistically not different to those recorded ventrally relative to soma (dorsal: 180±13.56 pA; ventral: 261±31.94 pA, p=0.20, Mann Whitney test). However, the amplitude values that were recorded from IPSCs medially located relative to soma were significantly larger than the amplitude values of IPSCs laterally located relative to soma (medial: 234±20.0 pA; lateral: 195±32.80 pA, ***p<0.0001, Mann Whitney test). Regarding latency values, latencies from IPSCs recorded dorsal to the soma were significantly longer compared to latency values that were recorded from IPSCs ventral relative to soma (dorsal: 10.30±0.49 ms; ventral: 8.33±0.37 ms, ***p<0.05 Mann Whitney test). However, we found no statistical difference between IPSCs latencies that originated either medially or laterally to the soma (medial: 9.28±0.45 ms; lateral: 10.75±0.70 ms, p=0.3, Mann Whitney test).

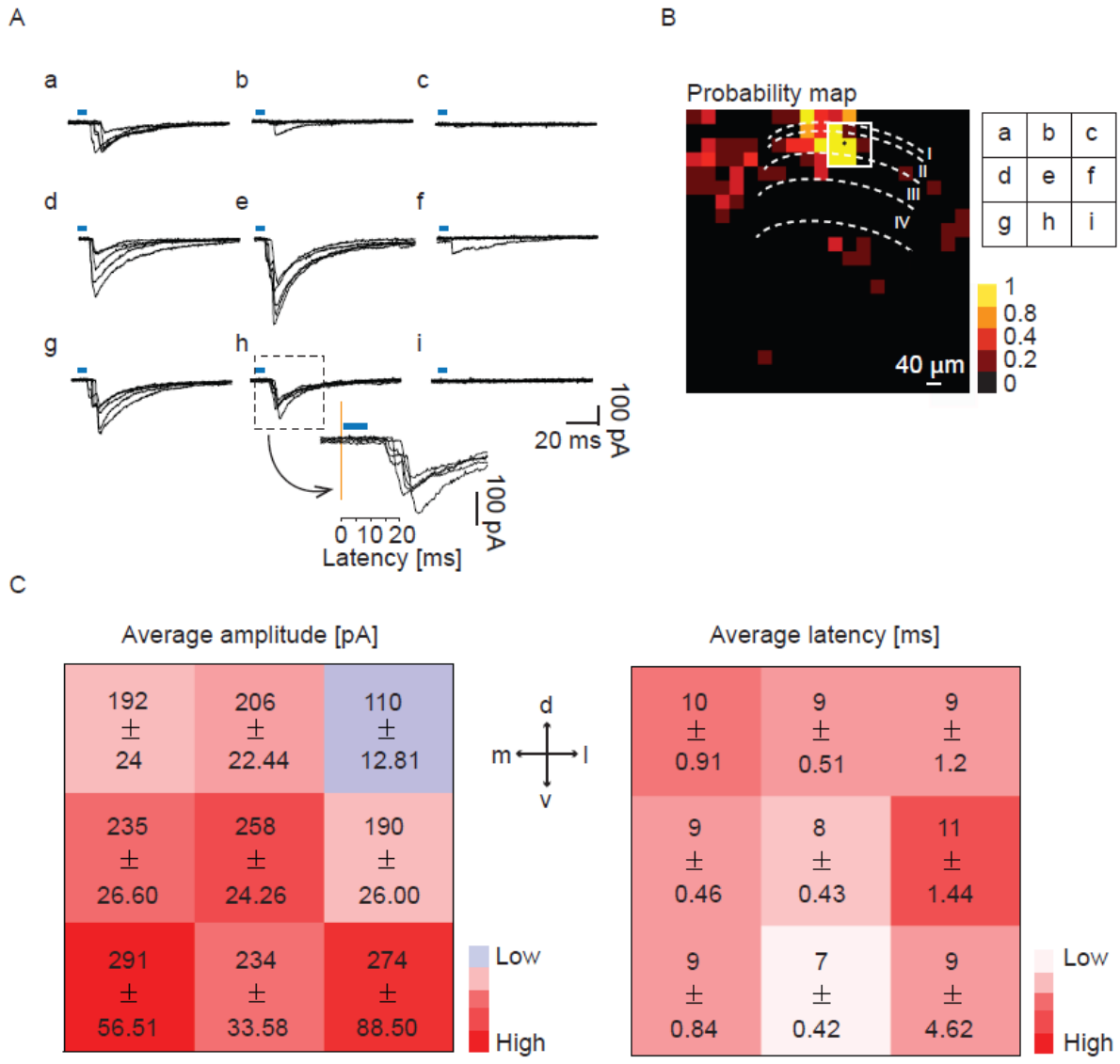

Figure 5. Amplitude and latency of light-evoked IPSCs surrounding the soma of the excitatory neuron. A, Example of superimposed light-evoked IPSCs from five stimulations (blue bar, 473 nm, 4ms, 2.3 mW/ mm^2) recorded from an excitatory cell located at the center of the white boxed region (3 x 3) in *B*. B, The white box was placed around the eight trials surrounding the soma (e) of the recorded neuron. C, Amplitude and latency averages of five light-stimulations per trial surrounding the soma (middle box) recorded from a total of n=20 cells. Amplitude of the events was measured from baseline to peak. a: 192±24 pA; b: 206±22.44 pA; c: 110.50±12.81 pA; d: 235±26.60 pA; e:258±24.26 pA; f: 190.60±26 pA; g: 291.16±56.51 pA; h: 234±33.58 pA; i: 274±88.5 pA. Values represent average±SEM. The latency was obtained by measuring the time between the onset of the stimulus and the inward current, respectively (refer to Figure 5A.h, inset orange dotted bar). a: 9.83±0.91 ms; b: 8.93±0.51 ms; c: 8.90±1.2 ms; d: 8.90±0.46; e: 7.73±0.43; f: 10.81±1.44; g: 8.98±0.84 ms; h: 7.49±0.42 ms; i: 9.06±4.62 ms. Values represent average±SEM. Amplitude and latency ranges are translated into a color code going from red (highest values) to blue/white (lower values).

VI Discussion

The purpose of the present study was to establish a protocol for LSPS in the spinal dorsal horn in order to locate the sources of synaptic inhibitory input onto excitatory LII neurons. We worked with acute spinal cord slices from BAC transgenic vGAT::ChR2 mice and thus relied on the activation of inhibitory GABAergic and glycinergic neurons to measure light-evoked IPSCs in excitatory neurons. We found it necessary to investigate possible discrepancies in firing activity or depolarization current amplitudes of the two neuronal subpopulations in response to the light paradigms that were used for the LSPS experiments (473 nm, light duration: 4 ms, power density: 20.4 mW/mm^2), and to assess whether the light-evoked responses preferentially originated from GABAergic or glycinergic neurons. We used $GAD67^{eGFP}$ mice for the characterization of GABAergic neurons. $GAD67^{eGFP}$ cells have a strong expression of GFP in the cell body, which made it easy to visualize under the epifluorescence microscope (Tamamaki et al., 2003). Presumed glycinergic neurons were recorded from the deep laminae. We found that inhibitory neurons of both the superficial and deep dorsal horn reliably fired action potentials upon the light stimulation (λ=473 nm, light exposure: 4 ms, power density: 20.4 mW/mm^2).

In our LSPS experiments, we successfully activated presynaptic inhibitory neurons and thereby mapped the inhibitory input zones onto excitatory LII neurons. Using this approach, we showed that excitatory LII neurons received almost 80% of inhibitory inputs from the grey matter and only 21% from the white matter. The latter inputs may arise from the stimulation of fibers descending to the dorsal horn from supraspinal areas, such as the brainstem (Vanegas and Schaible, 2004). It is indeed known that superficial dorsal horn neurons receive GABAergic and glycinergic inputs from neurons located in the RVM (Basbaum and Fields, 1984; Kato et al., 2006; Lau and Vaughan, 2014).

We suggest that in the LSPS experiments, terminals of descending fibers originating from inhibitory cells in the brainstem are depolarized due to the presence of vGAT::ChR2 that is expressed by all inhibitory neurons of the CNS (Zhao et al., 2011). Two cases could explain how excitatory neurons from the sdh receive inhibitory inputs from the white matter. In the first case, axon terminals of inhibitory neurons from the RVM cross the white-grey matter

border and target excitatory neurons in the spinal dorsal horn. In the second case, dorsal horn excitatory neurons have dendrites extending to the white matter onto which descending inhibitory axon terminals synapse. Radial cells could potentially be good candidates for crossing the grey-white matter border given the orientation of their dendritic tree, which also expands dorsally (Yasaka et al., 2007). Morphological reconstruction of the postsynaptic neuron could allow us to discriminate these two situations.

The original purpose of reconstructing the dendritic tree of the recorded cells with biocytin was to correlate the inhibitory input zones with the postsynaptic dendritic tree. Our two dendritic reconstructions showed that dendritic trees of LII excitatory neurons extended into LIII deeper laminae. Work from Kato et al., (2013) has reported excitatory synaptic inputs from sdh neurons onto LIII-LIV neurons. It is tempting to speculate that LIII/LIV dorsal horn neurons also receive inputs from sdh inhibitory neurons. Our preliminary results would therefore support the idea of translaminar communication, important in nociceptive processing, which would take place between ventrally extending dendritic trees from LII neurons and neurons in lamina III. The reconstruction that was obtained from the excitatory neurons strongly resembled the structure of vertical cells that were reported to account for one-third of all excitatory neurons in LII (Yasaka et al., 2010), and being non-GABAergic (Todd and McKenzie, 1989). The reconstructed dendritic trees predominantly extended in the ventral direction, which agrees with previous research that showed the same features among lamina II excitatory interneurons (Grudt and Perl, 2002; Punnakkal et al., 2014). We are aware, however, that having coronal spinal sections might severe dendritic structures extending in the rostro-caudal axis and hence reduce the number of cells identified as either radial or central cells, other morphological classes of excitatory dorsal horn neurons (Grudt and Perl, 2002; Maxwell et al., 2007; Yasaka et al., 2010).

We were interested in knowing the amplitude values surrounding the soma of the excitatory postsynaptic neurons, since the cell body was the only structure that we could locate with confidence on the probability heat maps. Our results showed high amplitude values (100-300 pA) for IPSCs evoked close to the soma. We are aware that amplitude values depend on several factors, such as the type of stimulation (electrical, light stimulation), the amount of synapses stimulated upon light exposure, and also the amount of postsynaptic receptors. One could speculate that the amplitude values measured from inhibitory inputs around the

soma might be larger than those originating from structures located distally to the cell body such as dendrites, due to a lower influence of dendritic filtering. Recording directly from dendrites could be an alternative to reduce the influence of dendritic filtering of the signal. This amplitude analysis should in addition be complemented with an improved reconstruction of the postysynaptic neuron in order to locate with precision the inhibitory inputs onto the structures of the postsynaptic cell.

In addition to amplitude, we also investigated the latency values from light-evoked IPSCs. Our analysis revealed latency values between 7-10 ms. We believe that the latency values we measured were slightly higher due to an additional 4 ms latency occuring between the TTL (transistor-transistor logic) trigger and the light transmission onset in our system, probably due to mechanical and electronical components of the light source used. Our latency values most likely reflect inhibitory monosynaptic connections, which are known to have short latencies (Rousseau et al., 2008; Jin et al., 2016).

In the present study, LSPS experiments in the spinal dorsal horn allowed us to visualize inhibitory input zones onto excitatory LII interneurons. We showed that most of the inhibitory inputs originated from the grey matter. However, a smaller percentage also arrived from the white matter. In the future, it would be desirable to complement LSPS experiments with complete reconstruction of the postsynaptic neurons. This would include reconstructions of the axon to learn which laminae are targeted by the recorded cell. In addition, the neuronal reconstruction would likely reveal sites on the postsynaptic neuron that preferentially receive inhibitory inputs. Furthermore, one should consider using parasagittal instead of coronal spinal cord slices, as this would be more likely to preserve the morphology of the recorded excitatory cells and the presynaptic inhibitory cells, both of which are mostly oriented in the rostro-caudal axis (Kato et al., 2007; Punnakkal et al., 2014).

Mapping the origin of inhibitory input onto excitatory neurons of LII together with the preliminary experiments focusing on descending inputs from the RVM, provide new insights into the origin intrinsic and supraspinal circuits, which are important in nociceptive pain processing. Furthermore, this set of data confirms that the excitability of excitatory neurons in LII is accurately controlled by a strong network of inhibitory input.

Appendix 1: Macro

```
#pragma rtGlobals=1 // Use modern global access method.
Macro FindEvents(filename,First4digits,secondNumber,NTraces)
String PMWavename, IgorWaveName, AmpspaceFileName,SpaceFileName, SpacePictureFileName,
FileName,AmpSpacePictureFileName,First4digits,secondNumber,AmpSpaceFileName2,AmpSpacePict
ureFileName2
Variable avg,SD,threshold,j,NumPoints, stop, k,yi, xi, NumofE,baseline,peak,n, lowlim, uplim, flag,
jlimit,field,NTraces, statlim
NewPath ExpData "Macintosh HD:Users:UserName:Desktop:Optogenetics:ScanData"
silent 1
Make /N=(20,20)/O space,ampspace,ampspaceN
Make /N=20 ye,xe
xe=NAN
ye=NAN
space=0
ampspace=0
n=1
AmpSpaceFileName=Filename+"ampspace"
AmpSpaceFileName2=Filename+"ampspaceN"
AmpSpacePictureFileName=FileName+"AmpspacePicture"
AmpSpacePictureFileName2=FileName+"AmpspacePictureN"
SpaceFileName=Filename+"space"
SpacePictureFileName=FileName+"Picture"
        Display /W=(5,44,215,235);AppendImage ampspace
                ModifyImage ampspace ctab= {-10e-11,0,YellowHot,1}
                ModifyGraph width=141.732,height=141.732
                SetAxis left 20,-1
                Setaxis bottom -1,20
                Display /W=(220,44,430,235);AppendImage ampspace
                ModifyImage ampspace ctab= {*,0,YellowHot,1}
                ModifyGraph width=141.732,height=141.732
                SetAxis left 20,-1
                Setaxis bottom -1,20
        Display /W=(435,44,645,235);AppendImage space
                ModifyImage space ctab= {0,2,YellowHot,0}
                ModifyGraph width=141.732,height=141.732
                SetAxis left 20,-1
                SetAxis bottom -1,20
Do
        Make /N=1200/O amp
        amp=NAN
        PMWavename=FileName+"_1_"+secondNumber+"_"+num2str(n+3-1)+"_1.ibw"
                IgorWaveName=First4digits+"_1_"+secondNumber+"_"+num2str(n+3-1)+"_1"
                print PMwavename
                LoadWave  /P=ExpData PMWavename
                Wavestats /Q $IgorWaveName
                $IgorWaveName-=V_avg
                Duplicate /O  $Igorwavename Trace
                Duplicate /O Trace DiffTrace
```

```
		Duplicate /O Trace IntTrace
		Differentiate Trace /D=DiffTrace
		WaveStats /Q DiffTrace
	Threshold=-2*V_sdev
	j=0.210
	k=0
	field=1
	stop=400
	do
	jlimit=0.2+(field*0.10118)
	flag=0
		do
			if (DiffTrace(j)<threshold)
			if (DiffTrace(j+0.0002)<threshold)
			if  (DiffTrace(j+2*0.0002)<threshold)
				ye(field-1)=trunc((field-1)/20)
				xe(field-1)=(field-1) -(ye(field-1)*20)
				yi=ye(field-1)
				xi=xe(field-1)
				space[xi](yi)+=1
				lowlim=0.2+((field)*0.10118)
				uplim=lowlim+0.10118
				statlim=lowlim+0.002
	Wavestats /Q/R=(lowlim,statlim) trace
	trace-=V_avg
	integrate trace /D=inttrace
	ampspace[xi](yi)+=(inttrace(uplim)-inttrace(lowlim))/5
	j=((trunc((j-0.2)/0.10118))+1)*0.10118+0.2
	field+=1
	flag=1
endif
endif
endif
j+=0.0002
while(j<=jlimit)
	if (flag==0)
	field+=1
endif
while(field<=400)
killwaves $IgorWaveName
n+=1
while (n<=NTraces)
Save/G/W/P=ExpData space as SpaceFileName
SavePICT/C=0/P=ExpData as SpacePictureFileName
Save/G/W/P=ExpData ampspace as AmpSpaceFileName
ModifyImage ampspace ctab= {-10e-11,0,YellowHot,1}
SavePICT/C=0/P=ExpData as AmpSpacePictureFileName
ModifyImage ampspace ctab= {*,0,YellowHot,1}
SavePICT/C=0/P=ExpData as AmpSpacePictureFileName2
EndMacro
```

Part B

Characterization of inhibitory neurotransmission onto excitatory dorsal horn interneurons after glycinergic neurons ablation in the spinal cord

Part B contains my contributions to a published study (Foster et al., 2015).
Some parts have been paraphrased from the original work.

Targeted ablation, silencing, and activation establish glycinergic dorsal horn neurons as key components of a spinal gate for pain and itch. Neuron, 2015

Foster E, Wildner H, **Tudeau L**, Haueter S, Ralvenius WT, Jegen M, Johannssen H, Hösli L, Haenraets K, Ghanem A, Conzelmann KK, Bösl M, Zeilhofer HU

I Abstract - Part B

The gate control theory of pain (Melzack and Wall, 1965) postulates that inhibitory interneurons in the superficial substantia gelatinosa act as “gate keepers”, either facilitating or stopping further transmission of nociceptive inputs to higher levels of the brain. Experimental evidence has demonstrated that dysfunction of inhibitory interneurons of the dorsal horn contributes to induction and maintenance of chronic pain states. In this project, we investigated the role of glycinergic interneurons in spinal nociceptive processing by ablating or silencing these neurons through intraspinal injection of adenoassociated virus vectors (AAV) harboring constructs for cre dependent expression of diphtheria toxin subunit A (DTA). My contribution was to quantify (i) the contribution of glycine to the inhibitory input onto excitatory LII neurons and (ii) the loss of glycinergic input upon local segmental ablation of glycinergic neurons. To enable reliable comparisons between slices taken from different animals, inhibitory neurotransmission was evoked employing optogenetics as this technique allows stimulation conditions to remain stable over time. We found that 70% of the gross inhibitory input onto LII excitatory neurons are mediated by glycine receptors. Further analyses reveal that most of the inhibitory input originates from mixed GABAergic/glycinergic neurons, which located in the deep dorsal horn. These results provide evidence for a major contribution of glycinergic neurons to inhibition of dorsal horn excitatory neurons.

II Introduction

The pivotal role of inhibitory synaptic transmission in spinal control of nociceptive signals was already proposed in the gate control theory of pain by Melzack and Wall (Melzack and Wall, 1965). In the original model, signals arriving from non-nociceptive (low-threshold myelinated sensory fibers) and nociceptive fibers (high-threshold unmyelinated sensory fibers) interact with local inhibitory interneurons to "open" or "close" the pain gate. This theory attributes a crucial role to inhibitory neurons in controlling the activity of spinal dorsal horn output neurons. Plenty of evidence suggests that the spinal dorsal horn serves as an important relay platform for synaptic processing in the pain pathway (Todd, 2010; Zeilhofer et al., 2012b). Maladaptive changes at this site, such as reduced inhibitory control over dorsal horn neuronal circuits lead to increased excitability and spontaneous activity of dorsal horn neurons, and hence contribute to a wide variety of pain pathologies manifested as allodynia (painful sensation to innocuous stimuli), and hyperalgesia (enhanced sensitivity to noxious stimuli) (Sorkin et al., 1998; Woolf and Salter, 2000; Drew et al., 2004; Sandkuhler, 2009; Kuner, 2010).

In the dorsal horn, inhibitory neurons represent about one-third of the total neuronal population. They use γ-aminobutyric acid (GABA) and glycine as fast inhibitory neurotransmitters (Zeilhofer et al., 2012b). Glycinergic neurons are mainly located in the deep dorsal horn (LIII-LV), the termination area of non-nociceptive afferent fibers (Todd and Spike, 1993). In addition to glycine, these neurons also release GABA. Purely GABAergic neurons are distributed in LII, the termination area of nociceptive sensory fibers (Zeilhofer et al., 2012b).

The circuitry of dorsal horn interneurons involved in spinal pain processing has not well been characterized, essentially due to the lack of techniques enabling the study of specific neuronal cell types together with their wiring to other cells. However, a plethora of techniques are currently used to improve the study of the dorsal horn neuronal circuitry. Such techniques include intersectional genetic strategies to specifically mark and ablate populations of inhibitory or excitatory neurons (Duan et al., 2014) or retrograde tracing to identify monosynaptically connected neurons (Wickersham et al., 2007). In this project, we studied the contribution of glycinergic inhibitory neurotransmission onto dorsal horn neurons in pain signaling. To answer this question, bacterial artificial chromosome (BAC) transgenic

mouse line that expresses the Cre recombinase selectively in glycinergic neurons was used and crossed with a BAC transgenic vGAT::ChR2-YFP mouse to enable photoactivation of dorsal horn inhibitory neurons. Intraspinal injections of AAV vectors harboring constructs for cre dependent expression of diphtheria toxin subunit A (DTA) were used to ablate glycinergic neurons and to study the subsequent changes in inhibitory synaptic transmission to excitatory neurons of the dorsal horn.

III Aim of this chapter - Part B

The aim of this project was to quantify (i) the contribution of glycine to the inhibitory input onto excitatory L II neurons and (ii) the loss of glycinergic input upon local segmental ablation of glycinergic neurons. The results of these experiments are part of a published study (Foster et al., 2015).

IV Material and methods

Animals

Animal procedures were in accordance with the University of Zurich Centre for Laboratory Animals guidelines and approved by the Cantonal Veterinary Office (License permission 64/2010, 75/2013, and 86/2013). GlyT2::Cre (Tg(Slc615-Cre)1Uze) mice were generated using BAC transgenesis (Zeilhofer et al., 2005), and crossed with vGAT::ChR2-YFP mice (Zhao et al., 2011) to obtain double transgenic mice (vGAT::ChR2; GlyT2::Cre). For the experiments, three to four week-old young adult vGAT::ChR2; GlyT2::Cre^- (henceforth referred to as Cre^-) and vGAT:.ChR2;GlyT2::Cre^+ (henceforth referred to as Cre^+) mice of either sex were used.

Drugs and chemicals

All chemicals were obtained from Tocris (Germany). (-)-Bicuculline methochloride (antagonist of $GABA_A$Rs), and strychnine hydrochloride (antagonist of glycinergic receptors) were dissolved in extracellular solution to a final concentration of 20 µM and 0.5 µM respectively.

Virus injection

AAV harboring a construct for cre dependent expression of DTA (AVV-flex-DTA) were cloned in-house and packaged at the Penn Vector core. At P(18), intraspinal injections were made in mice anesthetized with 2-5% isoflurane and immobilized on a stereotaxic frame (David Kopf Instruments, CA, USA) equipped with computer-controlled movable axes (Neurostar, Germany). Lumbar vertebrae L4 and L5 were exposed, and the vertebral column was fixed using a pair of spinal adaptors. Mice received two unilateral injections of AAV-flex-DTA together with AAV-mCherry (both 1 x 10^9 vector particles/injection) to visualize the site of injection. Injections were made at a rate of 30 nl/min with glass micropipettes (tip diameter, 30-40 µm) attached to a 10 µl Hamilton syringe, at a depth of 200-300 µm from the dorsal surface of the spinal cord. AAV-eGFP and AAV-mCherry were obtained from Penn Vector Core (Perelman School of Medicine, University of Pennsylvania) and the University of North Carolina (UNC) vector core, respectively.

Electrophysiology and optogenetic stimulation

Four to 8 days after AAV-flex-DTA injection, mice were decapitated in deep isoflurane anesthesia and transverse lumbar spinal cord slices were prepared. The cutting and recovery solutions were prepared as described previously (Dugue et al., 2009). 300 µm thick slices were cut in ice-cold solution of the following composition (in mM): 130 K-gluconate, 15 KCl, 0.05 EGTA, 20 HEPES and 25 glucose, titrated to pH 7.4 with KOH and supplemented with 50 µM D-APV to prevent glutamate excitotoxicity. For recovery, slices were kept for 30 minutes in a solution containing (in mM) 225 D-Mannitol, 2.5 KCl, 1.25 NaH_2PO_4, 25 $NaHCO_3$, 0.8 $CaCl_2$ and 8 MgCl2 and 25 glucose (35 °C, bubbled with 95% O_2, 5% CO_2). Finally, slices were transferred to aCSF solution with the following composition (in mM): 120 NaCl, 2.5 KCl, 1.25 NaH_2PO4, 26 $NaHCO_3$, 5 HEPES, 1 $MgCl_2$, 2 $CaCl_2$ and 14.6 glucose. Slices were transferred to a recording chamber and continuously perfused with aCSF equilibrated with 95% O_2, 5% CO_2 at a flow rate of 1ml min^{-1} at room temperature.

Our recordings were exclusively targeted to neurons located in the AAV1-flex-DTA infected red zone, visible when exciting the tissue at a 550 nm wavelength (i.e. RFP excitation wavelength) with the polychrome V system (Till Photonics Polychrome V, Germany). Whole-cell patch-clamp recordings were performed using the 40x objective at room temperature. We used borosilicate glass recording pipettes (resistance 4-5 MΩ) filled with internal solution containing (in mM): 120 CsCl, 2 $MgCl_2$ 6 H2O, 10 HEPES, 0.05 EGTA, 2 MgATP, 0.1 NaGTP, 5 QX-314 (295-310 mOsmol, pH 7.35, adjusted with CsOH) and used a HEKA EPC 9 amplifier controlled with Patchmaster (HEKA electronics) acquisition software. Cells were held at a potential of -70 mV. Light-evoked inhibitory postsynaptic currents (IPSCs) were elicited at a frequency of 5 stimulations min^{-1} by wide-field illumination of the dorsal horn. Illuminated area was ± 200-300 µm wide, light stimulation wavelength: 473 nm, light power: 2.7 mW, and light exposure: 4ms. After 10 min of stable baseline, slices were perfused with strychnine (stry, 0.5 µM) for 5 min. Bicuculline (bic, 20µM) was then subsequently added to strychnine for another 5 min. Drugs were then washed out for 15-25 min. All electrical signals were sampled at 20 kHz and filtered off-line at 2.9 kHz. Data was analyzed using IgorPro (WaveMetrics, Inc.,USA). Access resistance of the cell was continuously monitored by giving short hyperpolarizing steps (-5mV) between the synaptic stimulations. Recordings were discarded if the access resistance changed > 20%.

V Results

Decrease in light-evoked IPSC amplitudes after ablation of glycinergic dorsal horn neurons

We specifically and locally ablated spinal glycinergic neurons in vivo with intraspinal injection of AAV-flex-DTA, (Figures 1A and 1B) by using a FLEX system for irreversible Cre-dependent transgene activation, which provides reliable regulation of the toxin expression (Atasoy et al., 2008). After three AAV-flex-DTA unilateral injections at lumbar segments L3, L4, and L5, an eGFP reporter AAV added to the injection solution enabled us to visualize the spread of the AAV-flex-DTA injection in L3, L4, and L5. Infected $eGFP^+$ cells were confined to the injected side with a rostrocaudal spread of about -4 mm (Figure 1C). The loss of inhibitory neurons on the ipsilateral and contralateral sides at lumbar segments L3-L4-L5 was identified with Pax2, a marker for inhibitory neurons (Cheng et al., 2004; Huang et al., 2008). Our results indicate reduced levels of $Pax2^+$ neurons on the ipsilateral site of injection (Figure 1D, *left*) with no changes on the contralateral side (Figure 1D, *right*). Four days after intraspinal injection, the number of $Pax2^+$ spinal neurons was reduced by 46.5% ± 4.0% in Cre^+ mice relative to Cre^- mice (***p<0.001, one-way ANOVA, F(2,33)=59.1, followed by Bonferroni post hoc test) (Figure 1F). At day 26, the loss of inhibitory neurons was only slightly larger (59.9% ± 6.0%, p=0.15). Ablation was most pronounced in laminae III/VI, where 65.4% ± 1.1% (***p<0.0001, one-way ANOVA, F(2,33)=84.1, Bonferroni post hoc test) of all inhibitory neurons were lost by day 4 (Figure 1F).

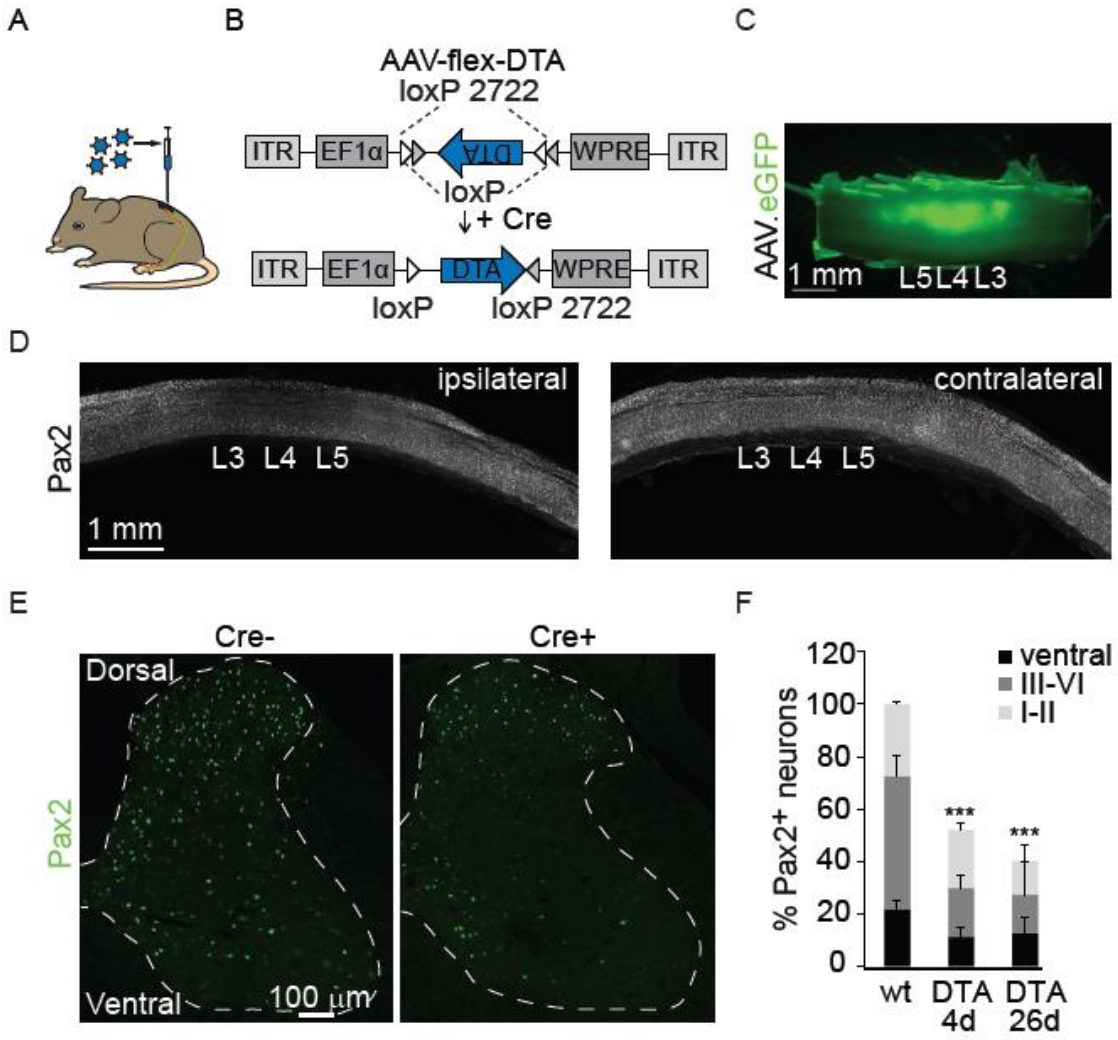

Figure 1. Specific loss of inhibitory interneurons after AAV-flex-DTA injection into the dorsal horn of Cre$^-$ and Cre$^+$ mice. A, AAV-flex-DTA was injected into the lumbar dorsal horn (L3-5) of Cre$^-$ and Cre$^+$ littermates. B, Expression of DTA is driven by the EF1a promoter (EF1a) and depends on Cre-mediated irreversible inversion of the DTA coding sequence. C, Green fluorescence (GFP) illustrates virus spread (AAV-eGFP) following three separate unilateral injections into the lumbar spinal cord at levels L3-L5. D, Sagittal sections of a spinal cord after injection of AAV-flex-DTA were stained against Pax2, a transcription factor expressed by more than 90% of adult spinal GAD67^{eGFP} and GlyT2::eGFP neurons. Sections show a marked reduction of Pax2$^+$ cells on the ipsilateral side (left) at lumbar segments L3 to L5 but not on the contralateral side (right). E, Confocal microscopy images, showing hemisections of the spinal cord (i.e., ipsilateral site to injection), reveal reduced Pax2 fluorescent signals (false-colored in green) Cre$^+$ (right) compared to Cre$^-$ mice (left). F, Quantification of Pax2$^+$ cells in LI-II, LIII-VI and the ventral horn of AAV-flex-DTA-injected Cre$^-$ mice (control) and AAV-flex-DTA-injected Cre$^+$ mice, respectively.

To characterize potential changes in inhibitory synaptic transmission onto LI/LII after ablation of glycinergic neurons, we combined electrophysiology and optogenetic techniques. We

recorded light-evoked IPSCs from LII dorsal horn neurons, which are located on the ipsilateral site of injection (region identified by mCherry expression, Figure 2A). After 4 ms light exposure, light-evoked IPSCs displayed significantly lower amplitudes in Cre$^+$ mice (0.62±0.10 nA) compared to Cre$^-$ mice (1.39±0.41 nA) (Figure 2B and 2C, for statistics see figure legend).

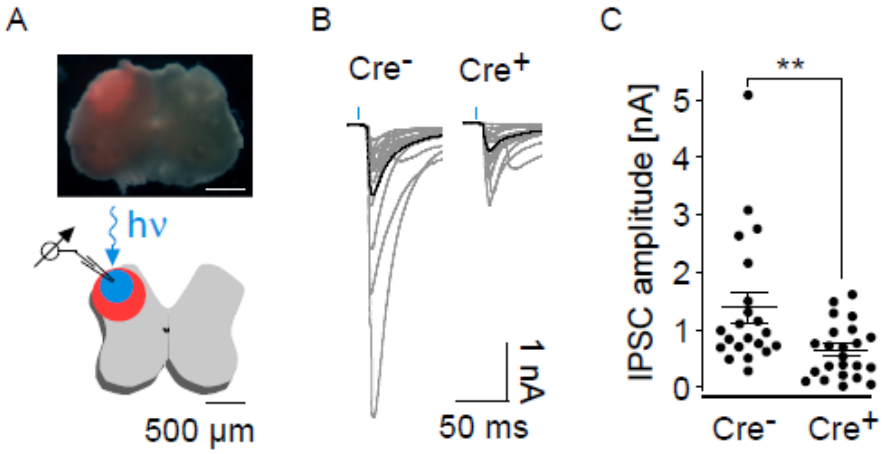

Figure 2. Reduced amplitudes of light-evoked IPSCs in AAV-flex-DTA ablation of glycinergic neurons leads to reduced light-evoked IPSCs in Cre$^+$ mice compared to Cre$^-$. A, *Top,* Distribution of mCherry expression in the spinal cord observed after unilateral injection of AAV-mCherry together with the AAV-flex-DTA virus in GlyT2::Cre;vGAT::ChR2 mice (scale bar 500 µm). *Bottom,* Schematic of the spinal cord illustrating the recording situation. A blue light (4 ms) pulse was applied in a region where mCherry expression (red) was visible, and recordings were performed from LII excitatory neurons. B, Average light-evoked IPSCs traces (black) from 21 neurons (Cre$^-$, *left*) and 23 neurons (Cre$^+$ mice, *right*). Average IPSCs from individual cells are represented in light grey. C, Plot representing average IPSC amplitudes of individual cells (dots) in Cre$^-$ and Cre$^+$ mice. **p < 0.01, unpaired Student's t-test. Error bars represent mean±SEM.

The glycinergic component strongly contributes to the IPSCs amplitude of Cre$^-$ and Cre$^+$ mice

We also investigated whether the remaining IPSCs originated from purely GABAergic neurons by determining the relative contribution of GABAergic and glycinergic components to IPSCs recorded from Cre$^-$ and Cre$^+$ mice. Our results showed that strychnine blocked 73.0±3.5% of the total IPSC amplitude in Cre$^-$ mice (n=12 cells), and 78.5±3.9% in Cre$^+$ mice (n=15 cells), indicating that on average more than 70% of the remaining IPSCs was glycinergic both for Cre$^-$ and Cre$^+$ mice (Figure 3C). The residual portion was blocked by bicuculline (Figure 3A).

The normalized traces of GABAergic and glycinergic IPSCs components displayed differences in decay kinetics, as shown in Figure 3B. As expected, glycinergic IPSCs showed a faster decay than GABAergic IPSCs.

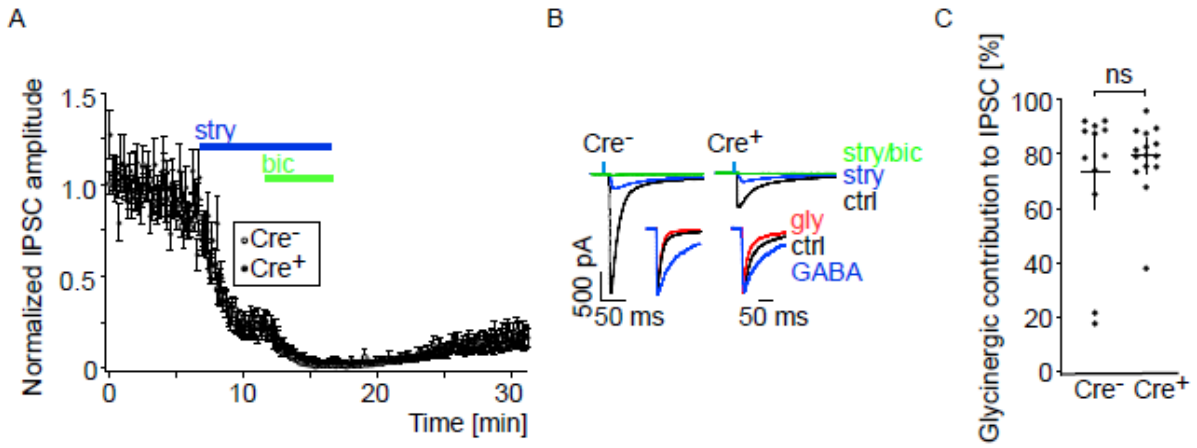

Figure 3. Unaffected glycinergic component of IPSC amplitudes between Cre⁻ and Cre⁺ after ablation of glycinergic neurons in the dorsal horn. A, Contribution of glycine and GABA to the IPSC amplitude in AAV-flex-DTA-injected Cre⁻ and Cre⁺ mice. Times course of the normalized light-evoked IPSCs from Cre⁻ and Cre⁺ mice after application of strychnine (stry, 0.5 µM), applied 6 min after recording, and a combination of strychnine plus bicuculline (bic, 20 µM) applied 12 min after recording. Normalized IPSCs amplitudes are significantly reduced, and decrease further after bath application of strychnine and bicuculline. During wash-out of the drugs, normalized IPSCs amplitudes slightly recovered. B, *Top,* Example traces showing averages of 10 consecutive light-evoked IPSCs after a 4 ms light pulse (blue bar, 4 ms) under control (ctrl) conditions, during application of strychnine and in the combined presence of strychnine and bicuculline. *Below,* Normalized traces (from Figure 3B, *top)* illustrating the different decay kinetics from the mixed IPSC (ctrl, black), GABAergic (blue), and glycinergic (gly, red) IPSC components. The glycinergic component was obtained by subtracting the GABAergic component from control IPSCs. C, Plot representing the glycinergic contribution to IPSC in individual cells. The contribution of the glycinergic components to IPSCs does not significantly change in Cre⁺ compared to Cre⁻ mice, n=12 and 15 cells from Cre⁻ (*left*) and Cre⁺ (*right*), respectively. p=0.49, unpaired Student t-test. Error bars represent mean±SEM.

VI Discussion

In this study, a viral vector-mediated neuron manipulation was used to determine the contribution of local glycinergic dorsal horn neurons to pain control. The results that are discussed in this section are restricted to the electrophysiology results, where inhibitory synaptic transmission was characterized in mice after AAV-flex-DTA mediated ablation of dorsal horn glycinergic neurons.

We chose an optogenetic approach to study the potential amplitude changes in inhibitory synaptic transmission after AAV-flex-DTA neuronal ablation. Double transgenic vGAT::ChR2-YFP;GlyT2::Cre mice were used to answer this question. Light stimulation of the spinal dorsal horn enabled us to stimulate a large fraction of inhibitory neurons located in the superficial and deep dorsal horn simultaneously. Therefore, light-evoked IPSCs that were recorded from presumed excitatory neurons in LII gave us a hint on the overall inhibitory synaptic transmission taking place after neuronal ablation.

The expression of vGAT::ChR2 was rendered visible in the spinal cord by the presence of YFP expressed as a fusion protein coupled to ChR2. The expression of vGAT::ChR2 was distributed across the spinal cord. In vGAT::ChR2 mice, ChR2 is expressed both in GABAergic and glycinergic neurons. Most vGAT::ChR2 neurons of the superficial dorsal horn are purely GABAergic, whereas vGAT::ChR2 neurons in LIII and deeper are most likely glycinergic neurons, which co-release GABA and glycine (Todd et al., 1990; Todd et al., 1996, Zeilhofer et al., 2012). One potential caveat of using vGAT::ChR2-YFP BAC transgenic mice, is different cells might express different levels of ChR2. Thus, some cells might need more light to depolarize and ultimately evoke somatic action potentials than others. This has been verified in experiments presented in Chapter 2, Figure 1.

Comparing light evoked IPSC amplitudes after AAV-flex-DTA injection in vGAT::ChR2;GlyT2::Cre^{+} and vGAT::ChR2;GlyT2::Cre^{-} mice revealed a significant reduction of inhibitory neurotransmission onto LII excitatory neurons in vGAT::ChR2;GlyT2::Cre^{+} mice. This result not only supports the fact that GlyT2::Cre^{+} neurons were successfully ablated by AAV-flex-DTA virus, but also confirms the presence of strong glycinergic inhibition in the sdh,

which is consistent with a dense expression of glycine receptors of the α3 subtype at this site (Harvey et al., 2004) and abundance of the GlyT2$^+$ neuropil in LII (Zeilhofer et al., 2005).

vGAT::ChR2 is expressed in GABAergic and mixed GABAergic/glycinergic neurons. It was therefore interesting to assess the contribution of the GABAergic and glycinergic components to the inhibitory currents remaining in GlyT2::Cre$^+$ mice after AAV-flex-DTA ablation. Given the resistance of purely GABAergic neurons to AAV-flex-DTA in GlyT2::Cre mice, it was expected that the relative contribution of GABA to the total IPSC amplitude would increase after AAV-flex-DTA mediated neuron ablation. The fact that this was not the case may suggest that excitatory neurons of the superficial dorsal horn receive most of their inhibitory input from the deep dorsal horn where most inhibitory neurons are mixed GABAergic/glycinergic. The remaining inhibition would then most likely come from deep dorsal horn inhibitory neurons located in segments not targeted by the virus injection. This result is fully consistent with the mapping data obtained in Chapter 2, Part A that showed connection formed between deep dorsal horn inhibitory neurons and superficial dorsal horn excitatory neurons.

References

Atasoy D, Aponte Y, Su HH, Sternson SM (2008) A FLEX switch targets Channelrhodopsin-2 to multiple cell types for imaging and long-range circuit mapping. The Journal of neuroscience : the official journal of the Society for Neuroscience 28:7025-7030.

Basbaum AI, Fields HL (1984) Endogenous pain control systems: brainstem spinal pathways and endorphin circuitry. Annual review of neuroscience 7:309-338.

Callaway EM, Katz LC (1993) Photostimulation using caged glutamate reveals functional circuitry in living brain slices. Proceedings of the National Academy of Sciences of the United States of America 90:7661-7665.

Cheng L, Arata A, Mizuguchi R, Qian Y, Karunaratne A, Gray PA, Arata S, Shirasawa S, Bouchard M, Luo P, Chen CL, Busslinger M, Goulding M, Onimaru H, Ma Q (2004) Tlx3 and Tlx1 are post-mitotic selector genes determining glutamatergic over GABAergic cell fates. Nature neuroscience 7:510-517.

Drew GM, Siddall PJ, Duggan AW (2004) Mechanical allodynia following contusion injury of the rat spinal cord is associated with loss of GABAergic inhibition in the dorsal horn. Pain 109:379-388.

Duan B, Cheng L, Bourane S, Britz O, Padilla C, Garcia-Campmany L, Krashes M, Knowlton W, Velasquez T, Ren X, Ross SE, Lowell BB, Wang Y, Goulding M, Ma Q (2014) Identification of spinal circuits transmitting and gating mechanical pain. Cell 159:1417-1432.

Dugue GP, Brunel N, Hakim V, Schwartz E, Chat M, Levesque M, Courtemanche R, Lena C, Dieudonne S (2009) Electrical coupling mediates tunable low-frequency oscillations and resonance in the cerebellar Golgi cell network. Neuron 61:126-139.

Foster E, Wildner H, Tudeau L, Haueter S, Ralvenius WT, Jegen M, Johannssen H, Hosli L, Haenraets K, Ghanem A, Conzelmann KK, Bosl M, Zeilhofer HU (2015) Targeted ablation, silencing, and activation establish glycinergic dorsal horn neurons as key components of a spinal gate for pain and itch. Neuron 85:1289-1304.

Grudt TJ, Perl ER (2002) Correlations between neuronal morphology and electrophysiological features in the rodent superficial dorsal horn. The Journal of physiology 540:189-207.

Huang M, Huang T, Xiang Y, Xie Z, Chen Y, Yan R, Xu J, Cheng L (2008) Ptf1a, Lbx1 and Pax2 coordinate glycinergic and peptidergic transmitter phenotypes in dorsal spinal inhibitory neurons. Developmental biology 322:394-405.

Jin X, Li S, Bondy B, Zhong W, Oginsky MF, Wu Y, Johnson CM, Zhang S, Cui N, Jiang C (2016) Identification of a Group of GABAergic Neurons in the Dorsomedial Area of the Locus Coeruleus. PloS one 11:e0146470.

Kato G, Kawasaki Y, Ji RR, Strassman AM (2007) Differential wiring of local excitatory and inhibitory synaptic inputs to islet cells in rat spinal lamina II demonstrated by laser scanning photostimulation. The Journal of physiology 580:815-833.

Kato G, Kosugi M, Mizuno M, Strassman AM (2013) Three-dimensional organization of local excitatory and inhibitory inputs to neurons in laminae III-IV of the spinal dorsal horn. The Journal of physiology 591:5645-5660.

Kato G, Yasaka T, Katafuchi T, Furue H, Mizuno M, Iwamoto Y, Yoshimura M (2006) Direct GABAergic and glycinergic inhibition of the

substantia gelatinosa from the rostral ventromedial medulla revealed by in vivo patch-clamp analysis in rats. The Journal of neuroscience : the official journal of the Society for Neuroscience 26:1787-1794.

Kato G, Kawasaki Y, Koga K, Uta D, Kosugi M, Yasaka T, Yoshimura M, Ji RR, Strassman AM (2009) Organization of intralaminar and translaminar neuronal connectivity in the superficial spinal dorsal horn. The Journal of neuroscience : the official journal of the Society for Neuroscience 29:5088-5099.

Katz LC, Dalva MB (1994) Scanning laser photostimulation: a new approach for analyzing brain circuits. Journal of neuroscience methods 54:205-218.

Kosugi M, Kato G, Lukashov S, Pendse G, Puskar Z, Kozsurek M, Strassman AM (2013) Subpopulation-specific patterns of intrinsic connectivity in mouse superficial dorsal horn as revealed by laser scanning photostimulation. The Journal of physiology 591:1935-1949.

Kuner R (2010) Central mechanisms of pathological pain. Nature medicine 16:1258-1266.

Lau BK, Vaughan CW (2014) Descending modulation of pain: the GABA disinhibition hypothesis of analgesia. Current opinion in neurobiology 29:159-164.

Light AR, Perl ER (1977) Differential termination of large-diameter and small-diameter primary afferent fibers in the spinal dorsal gray matter as indicated by labeling with horseradish peroxidase. Neuroscience letters 6:59-63.

Lu Y, Perl ER (2003) A specific inhibitory pathway between substantia gelatinosa neurons receiving direct C-fiber input. The Journal of neuroscience : the official journal of the Society for Neuroscience 23:8752-8758.

Lu Y, Perl ER (2005) Modular organization of excitatory circuits between neurons of the spinal superficial dorsal horn (laminae I and II). The Journal of neuroscience : the official journal of the Society for Neuroscience 25:3900-3907.

Maxwell DJ, Belle MD, Cheunsuang O, Stewart A, Morris R (2007) Morphology of inhibitory and excitatory interneurons in superficial laminae of the rat dorsal horn. The Journal of physiology 584:521-533.

Melzack R, Wall PD (1965) Pain mechanisms: a new theory. Science 150:971-979.

Punnakkal P, von Schoultz C, Haenraets K, Wildner H, Zeilhofer HU (2014) Morphological, biophysical and synaptic properties of glutamatergic neurons of the mouse spinal dorsal horn. The Journal of physiology 592:759-776.

Rousseau F, Aubrey KR, Supplisson S (2008) The glycine transporter GlyT2 controls the dynamics of synaptic vesicle refilling in inhibitory spinal cord neurons. The Journal of neuroscience : the official journal of the Society for Neuroscience 28:9755-9768.

Sandkuhler J (2009) Models and mechanisms of hyperalgesia and allodynia. Physiological reviews 89:707-758.

Scheibel ME, Scheibel AB (1968) Terminal axonal patterns in cat spinal cord. II. The dorsal horn. Brain research 9:32-58.

Sivilotti L, Woolf CJ (1994) The contribution of $GABA_A$ and glycine receptors to central sensitization: disinhibition and touch-evoked allodynia in the spinal cord. Journal of neurophysiology 72:169-179.

Sorkin LS, Puig S, Jones DL (1998) Spinal bicuculline produces hypersensitivity of dorsal horn neurons: effects of excitatory amino acid antagonists. Pain 77:181-190.

Tamamaki N, Yanagawa Y, Tomioka R, Miyazaki J, Obata K, Kaneko T (2003) Green

fluorescent protein expression and colocalization with calretinin, parvalbumin, and somatostatin in the GAD67-GFP knock-in mouse. The Journal of comparative neurology 467:60-79.

Todd AJ (1990) An electron microscope study of glycine-like immunoreactivity in laminae I-III of the spinal dorsal horn of the rat. Neuroscience 39:387-394.

Todd AJ (2010) Neuronal circuitry for pain processing in the dorsal horn. Nature reviews Neuroscience 11:823-836.

Todd AJ, McKenzie J (1989) GABA-immunoreactive neurons in the dorsal horn of the rat spinal cord. Neuroscience 31:799-806.

Todd AJ, Spike RC (1993) The localization of classical transmitters and neuropeptides within neurons in laminae I-III of the mammalian spinal dorsal horn. Progress in neurobiology 41:609-645.

Todd AJ, Watt C, Spike RC, Sieghart W (1996) Colocalization of GABA, glycine, and their receptors at synapses in the rat spinal cord. The Journal of neuroscience : the official journal of the Society for Neuroscience 16:974-982.

Torsney C, MacDermott AB (2006) Disinhibition opens the gate to pathological pain signaling in superficial neurokinin 1 receptor-expressing neurons in rat spinal cord. The Journal of neuroscience : the official journal of the Society for Neuroscience 26:1833-1843.

Vanegas H, Schaible HG (2004) Descending control of persistent pain: inhibitory or facilitatory? Brain research Brain research reviews 46:295-309.

Wickersham IR, Lyon DC, Barnard RJ, Mori T, Finke S, Conzelmann KK, Young JA, Callaway EM (2007) Monosynaptic restriction of transsynaptic tracing from single, genetically targeted neurons. Neuron 53:639-647.

Woodbury CJ, Koerber HR (2003) Widespread projections from myelinated nociceptors throughout the substantia gelatinosa provide novel insights into neonatal hypersensitivity. The Journal of neuroscience : the official journal of the Society for Neuroscience 23:601-610.

Woolf CJ, Salter MW (2000) Neuronal plasticity: increasing the gain in pain. Science 288:1765-1769.

Yasaka T, Kato G, Furue H, Rashid M.H, Sonohata M, Tamae A, Murata Y, Masuko S, Yoshimura M (2007) Cell-type-specific excitatory and inhibitory circuits involving primary afferents in the substantia gelatinosa of the rat spinal dorsal horn in vitro. The Journal of physiology 581:603-618.

Yasaka T, Tiong SY, Hughes DI, Riddell JS, Todd AJ (2010) Populations of inhibitory and excitatory interneurons in lamina II of the adult rat spinal dorsal horn revealed by a combined electrophysiological and anatomical approach. Pain 151:475-488.

Zeilhofer HU (2005) The glycinergic control of spinal pain processing. Cellular and molecular life sciences : CMLS 62:2027-2035.

Zeilhofer HU, Zeilhofer UB (2008) Spinal dis-inhibition in inflammatory pain. Neuroscience letters 437:170-174.

Zeilhofer HU, Wildner H, Yévenes GE (2012a) Fast synaptic inhibition in spinal sensory processing and pain control. Physiological reviews 92:193-235.

Zeilhofer HU, Benke D, Yévenes GE (2012b) Chronic pain states: pharmacological strategies to restore diminished inhibitory spinal pain control. Annual review of pharmacology and toxicology 52:111-133.

Zeilhofer HU, Studler B, Arabadzisz D, Schweizer C, Ahmadi S, Layh B, Bosl MR, Fritschy JM (2005) Glycinergic neurons expressing enhanced green fluorescent

protein in bacterial artificial chromosome transgenic mice. The Journal of comparative neurology 482:123-141.

Zhao S, Ting JT, Atallah HE, Qiu L, Tan J, Gloss B, Augustine GJ, Deisseroth K, Luo M, Graybiel AM, Feng G (2011) Cell type-specific channelrhodopsin-2 transgenic mice for optogenetic dissection of neural circuitry function. Nature methods 8:745-752.

General discussion and outlook

Correct functioning of spinal GABAergic and glycinergic neurons is important for maintaining a physiological level of inhibitory neurotransmission in the dorsal horn. It is firmly established that a reduction of the inhibitory drive (i.e., disinhibition) contributes to pathological pain states, which in mice translates into increased sensitivity to innocuous inputs (i.e., allodynia), and enhanced sensitivity to noxious stimuli (i.e., hyperalgesia) (Zeilhofer et al., 2012b). Thus, a functional inhibitory network is crucial for controlling the excitability of output neurons in the superficial dorsal horn (sdh), and strongly influences the final nociceptive output to the brain.

In **Chapter 1** of this thesis, I characterized inhibitory neurotransmission onto sdh excitatory neurons in mice lacking spinal α2-$GABA_A$Rs. Our electrophysiological study showed reduced synaptic inhibition in the hoxb8α2$^{-/-}$ animals compared to control animals. This result goes in line with a previous study in our group that provided evidence for reduced GABAergic inhibition in the hoxb8α2$^{-/-}$ animals compared to control animals (Paul et al., 2014) and therefore emphasizes on the role of α2-$GABA_A$Rs as important subtypes mediating GABAergic inhibition in the sdh. A former study revealed high expression of α2-$GABA_A$Rs in the sdh by using α subunit-specific antibodies (Paul et al., 2012). The high expression level of α2-$GABA_A$Rs in the sdh might also explain the reduction in synaptic transmission that we observed in the hoxb8α2$^{-/-}$ animals.

In addition to assessing inhibitory synaptic transmission using electrophysiological recordings, we conducted behavioral experiments comparing the baseline thresholds of α2$^{fl/fl}$ and hoxb8α2$^{-/-}$ mice to acute nociception. To our surprise, baseline pain sensitivities to acute pain tests were similar in both genotypes. The discrepancy between the synaptic and behavioral phenotype suggests the presence of compensatory mechanisms that could take place at a cellular or molecular level. Increased tonic inhibition in hoxb8α2$^{-/-}$ animals is one mechanism we thought might compensate for reduced synaptic inhibition. Tonic inhibition is mediated by extrasynaptic receptors in response to GABA present outside the synapse (Farrant and Nusser, 2005) and depends mainly on the expression of the α4-δ or α5 containing $GABA_A$Rs subtypes (Fritschy and Panzanelli, 2014). Evidence was provided that GABAergic tonic

inhibition was mediated by α4 or α5-$GABA_A$Rs in some neurons of LII (Takahashi et al., 2006). In fact, I provide evidence that in hoxb8α2$^{-/-}$ animals, tonic inhibition is significantly increased. It is tempting to hypothesize that increased tonic inhibition could originate from an up-regulation of extrasynaptic α5-$GABA_A$Rs subtypes displaying stronger affinities for GABA (Perez-Sanchez et al., 2016). Although it was reported that synaptic $GABA_A$Rs are directly recruited from the extrasynaptic pool (Gerrow and Triller, 2014), one could speculate that the few α5-$GABA_A$Rs that are found at the synaptic site (Gerrow and Triller, 2014), could serve as a reserve for extrasynaptic receptors and diffuse laterally to these sites when the activity of tonic inhibition has to be elicited (e.g. in hoxb8α2$^{-/-}$ mice). Lateral diffusion was indeed described as a mechanism promoting receptor dynamics and diffusion across the plasma membrane (Triller and Choquet, 2005). An up-regulation of extrasynaptic α5-$GABA_A$Rs may therefore have compensated the loss of synaptic α2-$GABA_A$Rs. However, in our behavioral experiments hoxb8α2$^{-/-}$ mice suffering from inflammatory pain showed no analgesia after treatment with HZ-166.

Alternatively, a possible contribution of α4/δ-$GABA_A$Rs should be considered. Under baseline conditions α4-$GABA_A$Rs were shown to be expressed in the sdh layers only at low levels (Paul et al., 2012). However, several reports suggest that α4-$GABA_A$Rs are up-regulated in pain states and that their targeting with the specific α4-$GABA_A$R subtype modulator 4,5,6,7-tetrahydroisoxazolo[5,4-c]pyridine-3-ol (THIP) produces analgesia. It is at least possible that a similar up-regulation of α4 subunit occurs in the spinal cord of hoxb8α2$^{-/-}$ mice. To distinguish between α4-$GABA_A$R and α5-$GABA_A$Rs future experiments might use subtype selective modulators such as THIP which selectively facilitates α4-$GABA_A$Rs and L-655,708 which selectively inhibits α5-$GABA_A$Rs.

We next investigated whether we would observe changes from the excitatory input of nociceptors. We hypothesized that reduced excitatory neurotransmission onto LII neurons might compensate for the loss of synaptic inhibition. We checked the mRNA expression levels of VgluTs in DRG neurons to indirectly test if there would be less glutamate release from terminals of small-diameter primary afferents. We found that hoxb8α2$^{-/-}$ mice had reduced VgluT2 mRNA levels in neurons of the DRGs. VgluT2 is expressed by unmyelinated peptidergic fibers (Todd et al., 2003), therefore we could expect reduced excitatory inputs onto dorsal horn neurons. However, our electrophysiological results showed no difference in the

amplitude or reliability of light-evoked EPSCs in hoxb8α2$^{-/-}$ mice compared to α2$^{fl/fl}$ mice, suggesting that the loss of synaptic inhibition had no impact on the excitatory drive originating from small-diameter primary afferents onto dorsal horn neurons. In addition, we investigated the protein expression levels of VgluT1, 2, and 3 in the spinal dorsal horn of α2$^{fl/fl}$ and hoxb8α2$^{-/-}$ mice. In the dorsal horn, the expression of VgluTs is mainly found on terminals of primary sensory fibers (Todd et al., 2003; Seal et al., 2009). We found a small yet significant increase of VgluT3 in the sdh, the main expression site of VgluT3 in the spinal cord (Seal et al., 2009).

Furthermore, we investigated expression levels of serotonin in the dorsal horn. It is well established that serotonin can modulate the nociceptive pathway by mediating either pronociceptive or antinociceptive effects, which will rely on the type of 5-HT receptors found on the postsynaptic neuron (Bowker et al., 1981; Liu et al., 2002; Fukushima et al., 2009; Kim et al., 2015). Our results showed increases in serotonin and TPH2 in the spinal cord of hoxb8α2$^{-/-}$ mice, suggesting that an increase of serotonin in hoxb8α2$^{-/-}$ mice could be another mechanism to counteract the behavioral consequences of reduced GABAergic synaptic inhibition (Antal et al., 1996). Whether this increased serotonergic input is the main compensatory mechanism should be assessable in experiments using 5,7 DHT, which leads to the degeneration of serotonergic and noradrenergic axon terminals (Gross et al., 1985). When applied together with desipramine the ablation becomes specific for serotonergic terminals (Todurga et al., 2016). It has been reported that intrathecal injection of 5,7-dihydroxytryptamine (5,7 DHT) given together with desipramine does not change nociceptive thresholds in naïve wild-type mice (Yanarates et al., 2010). It might be interesting to test its effect in hoxb8α2$^{-/-}$ mice.

In the first part of Chapter 2, I focused on locating the origin of inhibitory synaptic inputs onto dorsal horn neurons. From our mapping experiments, it became clear that most of the inhibitory input zones originated from the dorsal horn grey matter which was expected since most of the inhibitory neurons are located in the grey matter (Todd and Spike, 1993; Zeilhofer et al., 2012b). Surprisingly, some excitatory LII neurons also received inhibitory inputs from the white matter. One possible explanation would be that LII excitatory neurons have dendrites that extend into the spinal white matter. Although the morphology of cells in LII is very diverse, it is known that LII neurons exhibit a predominant rostro-caudal spread of

their dendrites (Grudt and Perl,2002). Therefore, to confirm a possible spread of the dendritic tree to the white matter additional mapping and reconstruction should be performed in parasagittal spinal cord slices (Kato et al., 2007). In addition, our preliminary experiments revealed inhibitory inputs from supraspinal territories from the RVM to LII excitatory neurons. This might reflect synapses between dendrites of LII neurons and axons of the descending fibers, thereby explaining the presence of inhibitory input zones in the white matter (Antal et al., 1996). Preliminary dendritic tree reconstructions performed on LII excitatory neurons revealed the presence of ventrally expanding dendrites to the deep dorsal horn. From previous work, this morphology would correspond to vertical cells (Grudt and Perl, 2002). Our results show that some LII excitatory neurons receive inhibitory inputs from the deep dorsal horn, which could indicate the presence of feed-forward inhibition from myelinated low-threshold primary afferent fibers (LTMRs) in LIII, known to terminate in this area (Braz et al., 2014), to excitatory interneurons in LII (Yasaka et al., 2014). Although axons of some LII excitatory neurons were found to project onto LI projection neurons (Lu and Perl, 2005; Maxwell et al., 2007; Yasaka et al., 2010), further reconstruction of the axon would be needed to confirm the presence of polysynaptic pathways linking LTMRs to lamina I via the recorded neuron in LII (Lu and Perl, 2005; Torsney and MacDermott, 2006; Lu et al., 2013).

One limitation of our mapping experiments is not being able to distinguish somatic or axon stimulation and stimulation of axon terminal. Using a blocker for action potential firing (TTX) could allow us to exclusively stimulate the synaptic terminals. Reinforcing the depolarization of the terminals by 4-AP might be needed to evoke reliable neurotransmitter release (DePuy et al., 2013; Wang et al., 2014). Mapping monosynaptic neurotransmission would improve our characterization of the inhibitory input zones onto LII excitatory neurons. Indeed, this would reveal direct synapses taking place onto structures of the postsynaptic neuron such as dendrites and thereby indicate the regions in which the dendrites of the postsynaptic neuron extend to (Kato et al., 2007; Kato et al., 2013). With this approach, we would gain even more detailed information in the circuitry between LII excitatory neurons and inhibitory dorsal horn neurons, relevant in nociceptive signaling.

In the **second part** of **Chapter 2**, I characterized inhibitory synaptic transmission onto excitatory neurons in which dorsal horn glycinergic neurons were ablated by AAV-flex-DTA virus. We specifically defined the role of glycinergic neurons in mediating inhibitory control of

excitatory spinal cord neurons using optogenetic tools and confirmed their critical role in nociceptive signaling (Foster et al., 2015). These results hereby provide a direct proof of what has been proposed by other groups (Todd and Sullivan, 1990; Todd, 1996; Keller et al., 2001). Therefore, pharmacological targeting of glycinergic receptors in the superficial dorsal horn to restore inhibitory activity would constitute an alternative approach to targeting $GABA_ARs$ (Acuña et al., 2016). An advantage of this approach is the restricted expression of glycinergic innervation in the hindbrain and spinal cord (Zeilhofer et al., 2005), therefore unwanted effects such as sedation or addiction, would be less likely when modulating glycinergic receptors (Acuña et al., 2016).

In summary, in the first part of my thesis I describe two possible homeostatic plastic changes, namely increased tonic inhibition and increased serotonergic neurotransmission, which may explain the absence of enhanced sensitivity to pain in mice lacking α2-$GABA_ARs$. I show that in mice with reduced synaptic inhibition, an underlying cause of chronic pain, the organism is able to counter-balance such loss by increasing GABAergic-mediated tonic inhibition and facilitating serotonergic spinal neurotransmission. Furthermore, I confirmed that pharmacologically targeting α2-$GABA_ARs$ with a novel benzodiazepine HZ-166 appears to be effective in reducing pain. In the second part of my thesis, I established a new strategy to optogenetically map the origin of the inhibitory input zones onto spinal cord excitatory neurons. Characterizing the origin of inhibitory input zones provides additional insights on the influence of dorsal horn inhibitory neurotransmission in nociceptive signaling. These results highlight the existence of a complex GABAergic and glycinergic inhibitory network involved in controlling the excitability of excitatory interneurons in LII of the dorsal horn.

References

Acuña MA, Yévenes GE, Ralvenius WT, Benke D, Di Lio A, Lara CO, Munoz B, Burgos CF, Moraga-Cid G, Corringer PJ, Zeilhofer HU (2016) Phosphorylation state-dependent modulation of spinal glycine receptors alleviates inflammatory pain. The Journal of clinical investigation 126:2547-2560.

Antal M, Petko M, Polgar E, Heizmann CW, Storm-Mathisen J (1996) Direct evidence of an extensive GABAergic innervation of the spinal dorsal horn by fibres descending from the rostral ventromedial medulla. Neuroscience 73:509-518.

Bowker RM, Westlund KN, Coulter JD (1981) Origins of serotonergic projections to the spinal cord in rat: an immunocytochemical-retrograde transport study. Brain research 226:187-199.

Braz J, Solorzano C, Wang X, Basbaum AI (2014) Transmitting pain and itch messages: a contemporary view of the spinal cord circuits that generate gate control. Neuron 82:522-536.

DePuy SD, Stornetta RL, Bochorishvili G, Deisseroth K, Witten I, Coates M, Guyenet PG (2013) Glutamatergic neurotransmission between the C1 neurons and the parasympathetic preganglionic neurons of the dorsal motor nucleus of the vagus. The Journal of neuroscience : the official journal of the Society for Neuroscience 33:1486-1497.

Farrant M, Nusser Z (2005) Variations on an inhibitory theme: phasic and tonic activation of GABA(A) receptors. Nature reviews Neuroscience 6:215-229.

Foster E, Wildner H, Tudeau L, Haueter S, Ralvenius WT, Jegen M, Johannssen H, Hosli L, Haenraets K, Ghanem A, Conzelmann KK, Bosl M, Zeilhofer HU (2015) Targeted ablation, silencing, and activation establish glycinergic dorsal horn neurons as key components of a spinal gate for pain and itch. Neuron 85:1289-1304.

Fritschy JM, Panzanelli P (2014) $GABA_A$ receptors and plasticity of inhibitory neurotransmission in the central nervous system. The European journal of neuroscience 39:1845-1865.

Fukushima T, Ohtsubo T, Tsuda M, Yanagawa Y, Hori Y (2009) Facilitatory actions of serotonin type 3 receptors on GABAergic inhibitory synaptic transmission in the spinal superficial dorsal horn. Journal of neurophysiology 102:1459-1471.

Gerrow K, Triller A (2014) $GABA_A$ receptor subunit composition and competition at synapses are tuned by GABAB receptor activity. Molecular and cellular neurosciences 60:97-107.

Gross G, Gothert M, Glapa U, Engel G, Schumann H.J (1985) Lesioning of serotoninergic and noradrenergic nerve fibers of the rat brain does not decrease binding of 3H-clonidine and 3H-rauwoliscine to cortical membranes. Naunyn Schmiedebergs Arch Pharmacol 328:229-235.

Grudt TJ, Perl ER (2002) Correlations between neuronal morphology and electrophysiological features in the rodent superficial dorsal horn. The Journal of physiology 540:189-207.

Kato G, Kawasaki Y, Ji RR, Strassman AM (2007) Differential wiring of local excitatory and inhibitory synaptic inputs to islet cells in rat spinal lamina II demonstrated by laser scanning photostimulation. The Journal of physiology 580:815-833.

Kato G, Kosugi M, Mizuno M, Strassman AM (2013) Three-dimensional organization of local excitatory and inhibitory inputs to neurons in laminae III-IV of the spinal dorsal horn. The Journal of physiology 591:5645-5660.

Keller AF, Coull JA, Chery N, Poisbeau P, De Koninck Y (2001) Region-specific developmental specialization of GABA-glycine cosynapses in laminas I-II of the rat spinal dorsal horn. The Journal of

neuroscience : the official journal of the Society for Neuroscience 21:7871-7880.

Kim JM, Jeong SW, Yang J, Lee SH, Kim WM, Jeong S, Bae HB, Yoon MH, Choi JI (2015) Spinal 5-HT1A, not the 5-HT1B or 5-HT3 receptors, mediates descending serotonergic inhibition for late-phase mechanical allodynia of carrageenan-induced peripheral inflammation. Neuroscience letters 600:91-97.

Liu ZY, Zhuang DB, Lunderberg T, Yu LC (2002) Involvement of 5-hydroxytryptamine(1A) receptors in the descending anti-nociceptive pathway from periaqueductal gray to the spinal dorsal horn in intact rats, rats with nerve injury and rats with inflammation. Neuroscience 112:399-407.

Lu Y, Perl ER (2005) Modular organization of excitatory circuits between neurons of the spinal superficial dorsal horn (laminae I and II). The Journal of neuroscience : the official journal of the Society for Neuroscience 25:3900-3907.

Lu Y, Dong H, Gao Y, Gong Y, Ren Y, Gu N, Zhou S, Xia N, Sun YY, Ji RR, Xiong L (2013) A feed-forward spinal cord glycinergic neural circuit gates mechanical allodynia. The Journal of clinical investigation 123:4050-4062.

Maxwell DJ, Belle MD, Cheunsuang O, Stewart A, Morris R (2007) Morphology of inhibitory and excitatory interneurons in superficial laminae of the rat dorsal horn. The Journal of physiology 584:521-533.

Paul J, Zeilhofer HU, Fritschy JM (2012) Selective distribution of $GABA_A$ receptor subtypes in mouse spinal dorsal horn neurons and primary afferents. The Journal of comparative neurology 520:3895-3911.

Paul J, Yévenes GE, Benke D, Di Lio A, Ralvenius WT, Witschi R, Scheurer L, Cook JM, Rudolph U, Fritschy JM, Zeilhofer HU (2014) Antihyperalgesia by alpha2-$GABA_A$ receptors occurs via a genuine spinal action and does not involve supraspinal sites. Neuropsychopharmacology : official publication of the American College of Neuropsychopharmacology 39:477-487.

Perez-Sanchez J, Lorenzo LE, Lecker I, Zurek AA, Labrakakis C, Bridgwater EM, Orser BA, De Koninck Y, Bonin RP (2016) alpha5$GABA_A$ Receptors Mediate Tonic Inhibition in the Spinal Cord Dorsal Horn and Contribute to the Resolution Of Hyperalgesia. Journal of neuroscience research.

Seal RP, Wang X, Guan Y, Raja SN, Woodbury CJ, Basbaum AI, Edwards RH (2009) Injury-induced mechanical hypersensitivity requires C-low threshold mechanoreceptors. Nature 462:651-655.

Takahashi A, Mashimo T, Uchida I (2006) GABAergic tonic inhibition of substantia gelatinosa neurons in mouse spinal cord. Neuroreport 17:1331-1335.

Todd AJ (1996) GABA and glycine in synaptic glomeruli of the rat spinal dorsal horn. The European journal of neuroscience 8:2492-2498.

Todd AJ, Sullivan AC (1990) Light microscope study of the coexistence of GABA-like and glycine-like immunoreactivities in the spinal cord of the rat. The Journal of comparative neurology 296:496-505.

Todd AJ, Spike RC (1993) The localization of classical transmitters and neuropeptides within neurons in laminae I-III of the mammalian spinal dorsal horn. Progress in neurobiology 41:609-645.

Todd AJ, Hughes DI, Polgar E, Nagy GG, Mackie M, Ottersen OP, Maxwell DJ (2003) The expression of vesicular glutamate transporters VGLUT1 and VGLUT2 in neurochemically defined axonal populations in the rat spinal cord with emphasis on the dorsal horn. The European journal of neuroscience 17:13-27.

Todurga Z.G, Gunduz O,Karadag C.H, Ulugol A (2016) Descending seotonergic and noradrenergic systems do not regulate the antipruritic effects of cannabinoids. Acta neuropsychiatrica 6:321-326.

Torsney C, MacDermott AB (2006) Disinhibition opens the gate to pathological pain signaling in superficial neurokinin 1 receptor-expressing neurons in rat spinal cord. The Journal of neuroscience : the official journal of the Society for Neuroscience 26:1833-1843.

Triller A, Choquet D (2005) Surface trafficking of receptors between synaptic and extrasynaptic membranes: and yet they do move! Trends in neurosciences 28:133-139.

Wang X, Hooks BM, Sun QQ (2014) Thorough GABAergic innervation of the entire axon initial segment revealed by an optogenetic 'laserspritzer'. The Journal of physiology 592:4257-4276.

Yanarates O, Dogrul A, Yildirim V, Sahin A, Sizlan A, Seyrek M, Akgul O, Kozak O, Kurt E, Aypar U (2010) Spinal 5-HT7 receptors play an important role in the antinociceptive and antihyperalgesic effects of tramadol and its metabolite, O-Desmethyltramadol, via activation of descending serotonergic pathways. Anesthesiology 112:696-710.

Yasaka T, Tiong SY, Hughes DI, Riddell JS, Todd AJ (2010) Populations of inhibitory and excitatory interneurons in lamina II of the adult rat spinal dorsal horn revealed by a combined electrophysiological and anatomical approach. Pain 151:475-488.

Yasaka T, Tiong SY, Polgar E, Watanabe M, Kumamoto E, Riddell JS, Todd AJ (2014) A putative relay circuit providing low-threshold mechanoreceptive input to lamina I projection neurons via vertical cells in lamina II of the rat dorsal horn. Molecular pain 10:3.

Zeilhofer HU, Wildner H, Yévenes GE (2012b) Fast synaptic inhibition in spinal sensory processing and pain control. Physiological reviews 92:193-235.

Zeilhofer HU, Studler B, Arabadzisz D, Schweizer C, Ahmadi S, Layh B, Bosl MR, Fritschy JM (2005) Glycinergic neurons expressing enhanced green fluorescent protein in bacterial artificial chromosome transgenic mice. The Journal of comparative neurology 482:123-141.

Acknowledgements

For his insightful and inspirational guidance as director of thesis:
Prof. Dr. Hanns Ulrich Zeilhofer

For their involvement as PhD committee members:
Prof. Dr. Martin Müller
Prof. Dr. David Wolfer

For his critical and helpful inputs as PhD supervisor:
Dr. Helge Johannssen

For his capacity to find solutions no matter what, where or when, my biophysicist friend:
Dr. Mario Acuña

For their generous assistance, my friends:
Dr. Robert Ganley
Dr. Mirko Santello

For offering remote support, my friends:
Dr. Olivier Roca-Lapirot
Prof. Dr. Gonzalo Yévenes

For fixing major computer issues encountered while writing up, my friends:
Franklin Wahl
Mariana Zaichuk (and Dmitriy Polishchuk)

For providing an incredibly pleasant environment to work in:
All the members of the Zeilhofer group, past and present, amongst which: Caro, Dietmar, Edmund, Elena, Gioele, Hendrik, Isa, Jennifer, Karen, Karthik, Katrin, Louis, Martina, Nandhini, Noémie, Rebecca, Thomas and William.

Beyond the thesis proper, colleagues, friends and family whose presence and action gave additional meaning to this work will recognize themselves.